A PRELIMINARY INVESTIGATION INTO THE APPLICATION OF ULTRASONIC TECHNIQUES TO MEMBRANE FILTRATION

RD Sanderson · Jianxin Li · DK Hallbauer · LJ Koen · V Yu Halbauer-Zadorozhanya · M Hurndall

WRC Report No. 930/1/03

Water Research Commission

A PRELIMINARY INVESTIGATION INTO THE APPLICATION OF ULTRASONIC TECHNIQUES TO MEMBRANE FILTRATION

Final report to the
Water Research Commission

By

RD Sanderson, Jianxin Li, DK Hallbauer, LJ Koen,
V Yu Halbauer-Zadorozhanya, M Hurndall

Institute for Polymer Science, Department of Chemistry,
University of Stellenbosch,
Private Bag X1, Matieland 7602

WRC Project No : 930/1/03
ISBN No : 1-86845-949-7

JANUARY 2003

Disclaimer

This report emanates from a project financed by the Water Research Commission (WRC) and is approved for publication. Approval does not signify that the contents necessarily reflect the views and policies of the WRC or the members of the project steering committee, nor does mention of trade names or commercial products constitute endorsement or recommendation for use.

Executive Summary

1 INTRODUCTION

Membrane fouling is the single most critical problem limiting the wider application of separation by membrane filtration. The flux decline that accompanies fouling affects the operational efficiency and economics of many membrane separation processes such as microfiltration (MF), ultrafiltration (UF), nanofiltration (NF), electrodialysis (ED), and reverse osmosis (RO). In efforts to develop methods by which to reduce or prevent fouling, much research has been conducted. The development of a non-invasive technique to monitor the presence and growth of a fouling layer in real time, under realistic operating conditions, is potentially of great importance - to optimize plant operation and minimize operating costs.

In this project an ultrasonic time-domain reflectometry (UTDR) technique was developed as a non-invasive technique to investigate fouling layer formation and growth on membrane surfaces in MF, UF, RO. The ultrasonic testing technique provides a method for the early detection and monitoring of fouling in progress.

This preliminary investigation has formed the basis for a second project (1166) on the visualisation of the effects of electro-magnetic turbulence defouling techniques in membrane units. This project is currently in progress.

2 OBJECTIVES

The original aims of the proposed project were:

- To understand and measure the effectiveness of electrical defouling in spiral wrap desalination elements.
- To extend this process where possible to ultrafiltration and microfiltration membranes.
- If possible, to extend the process to cross-flow capillary for tubular design.
- To see if the process has other possibilities.
- To ensure effective patenting of all innovations.

Early on in the project the above objectives were modified to encompass the following.

It was considered more advantageous to move to the modified objectives in order to utilise the potential of the technology.

The revised objectives of this study were to:

- Investigate the use of ultrasonic time-domain reflectometry (UTDR) as a possible visualization technique for the detection fouling on membrane surfaces.
- Design a suitable desalination cell for ultrasonic testing in RO modules.
- Design a flat-bed-type device for the detection and monitoring of membrane fouling in MF and UF.
- Evaluate the efficiency of various cleaning techniques by UTDR.
- Correlate the UTDR response with membrane performance and corroborate the results via morphological characterization of the fouling layer.

The original objectives had to be modified during project execution because of problems encountered with co-operation and commitment from a local membrane company who were to supply the Project Team with, and give the team access to, fouled spiral modules. The Steering Committee subsequently agreed that the Project Team should continue the fundamental work being done on flat sheet cells and to characterise the technique and to attempt to perfect it as far as possible by the end of the project

3 EXPERIMENTAL APPROACH

Rectangular flat-sheet cells, built from Perspex and aluminium, and tubular and capillary membrane cells, were designed and used in this study. Systems for UTDR measurements and ultrasonic cleaning were set up and used. A focal transducer was designed and built. Various liquid separation systems such as MF, UF and RO, were set up. Different types of foulants were used: paper mill effluent, calcium carbonate and calcium sulphate. Various cleaning techniques such as forward flushing, ultrasonic cleaning and ultrasound with flushing were used and evaluated by UTDR in this study.

4 RESULTS

4.1 Ultrasonic measurement of fouling and cleaning of MF membranes

The UTDR technique was first applied to the non-invasive, in-situ, continuous visualization of fouling and defouling in flat-sheet MF nylon membranes. Results showed that the UTDR technique could effectively detect fouling-layer initiation and growth on, and its removal from, the membrane in real-time. The acoustic signal response had a good correspondence with flux-decline behavior during fouling.

The UTDR technique was also capable of detecting subtle changes, such as the presence and/or absence of a cake layer on the membrane surface, and distinguishing between two modes of growth at axial velocities of 1.0 and 4.2 cm/s. More specifically, the formation of a second echo in the time domain demonstrated that the UTDR technique could be used to quantify the thickness of a fouling layer on a membrane surface.

The fact that the UTDR technique monitors changes on the membrane surface makes it very suitable to study membrane cleaning and to determine the effectiveness of various cleaning techniques. Results of cleaning experiments showed that ultrasound associated with crossflushing was the most effective cleaning method; it was better than either the flushing or ultrasonic cleaning (without flow) methods. Cleaning by the former method resulted in a 40 x increase in permeate flux.

Results of SEM analyses of fouled and cleaned membrane surfaces supported UTDR visualization.

4.2 Ultrasonic measurement of fouling and cleaning of UF membranes

The UTDR technique could effectively detect fouling-layer initiation and growth on, and its removal from, a UF membrane in real-time. The structure of an asymmetric composite PS membrane was detected by UTDR.

The UTDR technique was also capable of detecting subtle changes in cake layer formation on the membrane surface, and the stop and recommencement of ultrafiltration.

The formation of a second (fouling layer) echo signal in the time domain demonstrated that the UTDR technique could be used to quantify the thickness of a fouling layer on the membrane surface.

In cleaning experiments, results showed that ultrasound associated with forward flushing was an effective cleaning method. The fact that the UTDR technique monitors changes on a UF membrane surface makes it very suitable to study membrane cleaning.

Results of SEM analyses of fouled and cleaned membrane surfaces again supported UTDR visualization.

4.3 UTDR measurement of inorganic fouling and cleaning of RO membranes

The results of this study showed that an ultrasonic testing technique was able to visualize inorganic fouling of RO membranes non-destructively, in situ, and under actual operating conditions in a flat-sheet, high-pressure test cell.

The ultrasonic technique could monitor subtle changes on a membrane surface due to the growth of calcium carbonate fouling. More specifically, a fouling echo obtained in the time domain indicated the actual state of the fouling layer on the membrane surface.

An increase in the amplitude of the fouling echo resulted from the build-up of the fouling layer. Moreover, the movement of the fouling echo in the time-domain was seen, due to an increase in the thickness of the fouling layer. The ultrasonic testing technique was capable of distinguishing between dead-end and crossflow modes of fouling growth.

The fact that the UTDR technique can monitor the removal of a fouling layer and membrane cleaning makes it a very suitable tool to study the effectiveness of various cleaning techniques.

5 CONCLUSIONS

- The ultrasonic signals of fouling processes provide a good measurement of fouling-layer growth in membrane separation test cells.
- The ultrasonic technique effectively detected fouling-layer initiation, its growth on and removal from the membrane in real-time. Data also showed the formation and growth of a fouling layer echo as fouling proceeded. Therefore, the UTDR technique can be used to quantify the thickness of a fouling layer on the membrane surface.
- The UTDR technique was successfully applied to, and fouling monitored in: MF, UF and RO; and with feeds that included: paper industry effluent, kaolin, calcium sulphate and calcium carbonate.
- The UTDR technique can be used to monitor cleaning and evaluating the cleaning effectiveness of various cleaning methods. Results of cleaning experiments show that ultrasound associated with flushing is the most effective cleaning method of those tested.
- Results of SEM analyses of fouled and cleaned membrane surfaces supported UTDR visualization.

Numerous publications have emanated from this work and consideration is currently being given to patenting a surveillance apparatus for monitoring membrane fouling. These achievements will be expanded on in the following project #1166.

RECOMMENDATIONS

This preliminary investigation has formed the sound basis for a second project (#1166) on the visualisation of the effects of electro-magnetic turbulence defouling techniques in different membrane units. (This project is currently in progress.)
Membrane units should include the following: UF tubular and capillary membrane modules and also spiral-would modules.
Ultrasonic reflection modelling should also be developed, to understand the signal reflection of a fouling layer on the membrane surface.

oOo

Acknowledgements

The research in this report emanated from a project funded by the Water Research Commission:

A preliminary investigation into the application of ultrasonic techniques to membrane filtration

The Steering Committee responsible for this project consisted of the following members:

Dr G Offringa	Water Research Commission (Chairman)
Dr IM Msibi	Water Research Commission
Prof PP Coetzee	Rand Afrikaans University
Mr G Gericke	ESKOM TSI
Dr EP Jacobs	Institute for Polymer Science, University of Stellenbosch
Dr V Yu Hallbauer-Zadorozhnaya	University of Stellenbosch
Mr EH König	WINGOC
Mr SA Pieterse	City of Cape Town
Dr VL Pillay	ML Sultan Technikon
Mr M Pryor	Umgeni Water
Prof RD Sanderson	Institute for Polymer Science, University of Stellenbosch
Mr R Schwab	Department of Water & Forestry
Ms A Swartz	Mineral Water Development International Ltd

The financial support of the Water Research Commission and the contributions from the members of the steering committee are gratefully acknowledged.

The practical assistance of Mr D.J. Koen from the Institute for Polymer Science, University of Stellenbosch is also gratefully acknowledged.

TABLE OF CONTENTS

Section 2

Section 3

Section 4

Section 5

List of Tables

CP	Concentration polarazation
D	Coefficient of transmission
DOTM	Direct observation through membrane
ED	Electrodialysis
f	Frequency (Hz)
MF	Microfiltration
NF	Nanofiltration
Nylon	Dupont trade name for polyamide 6, 6
PA	Polyamide
PES	Polyethersulphone
PI	Polyimide
P_i	The sound pressures of the incident wave (N/m^2)
P_r	The sound pressures of the reflected wave (N/m^2)
PS	Polysulphone
P_t	The sound pressures of the transmitted wave (N/m^2)
R	Coefficient of reflection
RO	Reverse osmosis
T	Time of wave's arriving (s)
ΔS	Thickness of material (m)
UF	Ultrafiltration
UTDR	Ultrasonic time-domain reflectometry
V	Velocity of sound wave in a medium
W_1	Acoustic impedance of Material 1 (kg/m^2s)
W_2	Acoustic impedance of Material 2 (kg/m^2s)

Greek letters

ρ	Density of the material (kg/m^3)

1 Introduction

1.1. Background

A membrane may be defined as a permeable or semi-permeable phase forming a selective barrier between two fluids, which restricts the movement of one or more of the components of one or both fluids across the barrier [Howell et al., 1993; Mulder, 1991]. Membranes are often polymeric materials. While the term filtration conventionally refers to the separation of solid, immiscible particles from liquid or gaseous streams, the application of membrane filtration includes the separation of dissolved solutes from liquid streams and the separation of gas mixtures [Cheryan, 1998].

Historically, the first recorded study of membrane phenomena was conducted by Abbe' Jean Antoine Nollet in 1748 [Lonsdale, 1982]. He immersed wine contained in an animal bladder in pure water and observed that water permeated through the bladder into the wine.

Although the membrane phenomenon has been observed and studied for over 200 years, it was not until the early twentieth century that the first commercial membranes for practical applications (bacteriological laboratory use) were developed by Zsigmondy [Lonsdale, 1982] and manufactured by Sartorius in Germany. These were symmetric microfiltration (MF) membranes. A major breakthrough in industrial membrane applications was achieved for reverse osmosis (RO) desalination of seawater by the development of asymmetric cellulose acetate (CA) membranes, by the phase inversion process, in the early 1960s [Loeb and Sourirajan, 1962]. Shortly thereafter, Michaels managed to make an asymmetric polyionic membrane for ultrafiltration (UF) [Micheals, 1968]. These membranes consisted of a very thin dense top layer (< 0.5 μm) supported by a porous sublayer (50-200 μm). These asymmetric membranes exhibited higher permeation and perm-selectivity.

In the 1950-80s, many original membrane technologies such as gas separation, haemodialysis, electrodialysis (ED), membrane distillation, nanofiltration (NF) and

pervaporation, and liquid membranes, were developed for commercial applications [Mulder, 1991; Noble and Stern, 1995; Jönsson, 1990].

Membrane technology for separations is a rapidly emerging technology due to its continuous operation, low energy consumption, easy adaptability, versatility and the requirement for only relatively mild operating conditions in comparison with conventional separation processes such as distillation, evaporation and crystallization. Membranes are now being used to effect a variety of separations: particles from solution, salts from water, toxins from blood, and one gas from a gas mixture, and so on. Two other technologically important applications of membranes are membrane electrodes and controlled release [Lonsdale, 1982].

However, fouling problems are still one of the most important reasons for the relatively slow acceptance of membrane technology. Fouling is generally defined as the deposition of retained particles, colloids, emulsions, suspensions, macromolecules, salts, etc. on or in a membrane [Mulder, 1991]. Fouling manifests itself as a decline in permeate flux with time of operation. It significantly affects operational efficiency and economics in numerous membrane separations, including MF, UF, NF, RO and ED.

It is known that pretreatment of feed water can be helpful in minimizing this fouling [Maartens, et al., 1999; Abdel-Jawad et al., 1997; Chakravorty et al., 1997; Dudley and Darton, 1997]. At the same time, membrane fouling can be minimized by the membrane geometry and stacking structure [Schwinge and Fane, 2001], surface feed flow velocities, turbulent pulses, sponge balls [Burch, 2001], backwashes [Redkar and Davis, 1994], air splurges [Laorie et al., 1997], ultrasound [Chai et al., 1999], electro and electromagnetic influences (certain effluents mainly) [Huotari, 1999, Baker et al., 1997], chemical and biological cleaning protocols. Synthetic membrane fouling is a very complicated phenomenon due to the wide variety of foulants encountered in practice.

A significant amount of research has been conducted to better understand the dynamics of the fouling process so that preventative methods can be developed. A more effective method for monitoring fouling initiation, as well as a means of

measuring fouling layer growth, is necessary for a better understanding of this complex problem. Changes in flux flow as well as pressure-induced changes are presently the two important indicators of fouling, and are often not enough to monitor fouling. Other techniques tried are the plugging index (PI), the fouling index (FI), the modified fouling index (MFI) [Mulder, 1991; Schippers, 1980]. There is still no well-developed technique to monitor fouling. The development of a non-invasive technique to monitor the presence and growth of a fouling layer on a membrane surface under realistic operating conditions in real time is thus of great importance.

1.2 Objectives

The original aims of the proposed project were:

- To understand and measure the effectiveness of electrical defouling in spiral wrap desalination elements.
- To extend this process where possible to ultrafiltration and microfiltration membranes.
- If possible, to extend the process to cross-flow capillary for tubular design.
- To see if the process has other possibilities.
- To ensure effective patenting of all innovations.

Early on in the project the above objectives were modified to encompass the following.
It was considered most advantageous to move to the modified objectives in order to utilise the potential of the technology.

The overall (modified) objective of the research was to describe the development of ultrasonic-time-domain-reflectometry and its use as a real-time visualisation technique for concentration polarisation and fouling layer monitoring on flat-sheet MF, UF and RO membranes, to compare these results with those obtained from the traditional methods of fouling indicators, such as permeate flux changes, and to 'visualise' the membrane surface covered by the fouling layer (visualisation of the membrane surface).

The revised objectives of this study were to:

- Investigate the use of ultrasonic time-domain reflectometry (UTDR) as a possible visualisation technique for the detection fouling on membrane surfaces.
- Design a suitable desalination cell for ultrasonic testing in RO modules.
- Design a flat-bed-type device for the detection and monitoring of membrane fouling in MF and UF.
- Evaluate the efficiency of various cleaning techniques by UTDR.
- Correlate the UTDR response with membrane performance and corroborate the results via morphological characterization of the fouling layer.

The original objectives had to be modified during project execution because of problems encountered with co-operation and commitment from a local membrane company who were to supply the Project Team with, and give the team access to, fouled spiral modules. The Steering Committee subsequently agreed that the Project Team should continue the fundamental work being done on flat sheet cells and to characterise the technique and to attempt to perfect it as far as possible by the end of the project

An ultrasonic time-domain reflectometry (UTDR) technique was developed as a non-invasive technique to investigate fouling layer formation and growth on membrane surfaces in MF, UF, RO and in modules of various configurations. The ultrasonic testing technique provides a method for the early detection and monitoring of fouling in progress.

This preliminary investigation has formed the basis for a second project (1166) on the visualisation of the effects of electro-magnetic turbulence defouling techniques in membrane units. This project is currently in progress.

1.3. Methodology

Rectangular flat sheet cells, built from Perspex and aluminium, and tubular and capillary membrane cells, were designed and used in this study. Systems for UTDR

measurements and ultrasonic cleaning were set up and used. A focal transducer was designed and built. Various liquid separation systems such as MF, UF and RO, were set up. Different types of foulants were used: paper mill effluent, calcium carbonate and calcium sulphate. Various cleaning techniques such as forward flushing, ultrasonic cleaning and ultrasound with flushing were used and evaluated by UTDR in this study.

1.4. Layout of report

This report is presented in six chapters. Chapter 2 presents an overview of prior research carried out in the field of membrane fouling and the detection of fouling, and includes all relevant non-invasive visualisation techniques. It also provides a thorough overview on the ultrasonic techniques. Chapters 3 and 4 describe the experimental approaches used in this research, as well as the experimental strategy that evolved for the development of UTDR in monitoring membrane fouling in flat MF and UF membranes. Chapter 5 describes the ultrasonic measurement of calcium carbonate deposition on and its removal from RO membranes. In Chapter 6, major conclusions from the results obtained and recommendations for the future research are made.

2 Historical and theoretical background

2.1. Membrane fouling

2.1.1. Fouling phenomenon

In membrane-based liquid separation processes, one or more components in the feed solution are preferentially retained at the membrane surface. Generally, the convective transport of these components to the surface is greater than the diffusive and convective transport away from the membrane. This leads to the accumulation of the rejected components near the surface, and is referred to as concentration polarization (CP). The CP in membrane separations is an undesirable phenomenon due to its adverse effects on membrane performance. The effects of CP include: a decline in permeate flux due to a reduced driving force for separation, a decline in product quality due to the increased diffusion of undesirable components through the membrane, and the increased risk of deposition of these components on the membrane surface.

The deposition of the rejected components on a membrane surface is referred to as "membrane fouling", and is universally accepted as the most critical problem in several membrane processes including microfiltration (MF), ultrafiltratoin (UF), nanofiltration (NF), reverse osmosis (RO), and electrodialysis (ED) [Belfort, 1984; Rautenbach and Albrecht, 1989; Mulder, 1991; Davis, 1992]. An extensive body of literature exists on the various aspects of membrane fouling due to the importance if this problem. Some excellent reviews on various aspects of membrane fouling are given by Potts et al. [1981], Belfort and Altena [1983], Fane and Fell [1987], Belfort [1989], Nilsson [1990], Marshall et al. [1993], Belfort et al. [1994], and Mulder [1995].

2.1.2. Membrane fouling studies

Experimental investigations

Since the pig-bladder experiments of Abbe Jean Antoine Nollet in 1784, membranes have been utilised in numerous liquid separation applications. Membrane fouling has been observed in nearly all of these applications [Strathmann, 1981; Lonsdale, 1982].

The experimental investigations of membrane fouling can be classified into three broad categories – inorganic fouling, colloidal fouling, and fouling due to dissolved organics and biological constituents in the feed.

Inorganic fouling occurs in separations where the solubility of a dissolved salt is exceeded. It is typically encountered in RO and ED but has also been observed in MF and UF. Colloidal fouling is a very common phenomenon in almost all membrane processes, and occurs when colloidal organic constituents in the feed are deposited on the membrane surface due to hydrodynamic and physical-chemical characteristics of the separation system. Biological and organic fouling is observed in separations where the feed solution exhibits substantial biological growth and dissolved organic content.

Theoretical investigations

Membrane fouling is widely acknowledged to be the most important economic determinant of most membrane processes. A number of mathematical models for concentration polarisation (CP) and fouling have been developed to understand this complicated phenomenon. The following mathematical models are available:

1. Empirical models [Sheppard et al, 1972]
2. Gel polarisation models [Michaels, 1968; Belfort and Altena, 1983; Kimura and Nakao, 1975]
3. Particle trajectory models [Hung and Tien, 1976; Bacchin et al., 1995]
4. Differential rate models [Carter and Hoyland, 1976]
5. Resistance models [Belfort and Marx, 1979; Schippers et al. 1981; Fane and Fell, 1987]
6. Surface reaction models [Okazaki and Kimura, 1984a; Gilron and Hasson, 1987; Borden et al., 1987]

Although a significant amount of research has been conducted to better the understanding of the dynamics of membrane separations, the real mechanism of separation remains incompletely understood. This is because the phenomenon of fouling is a very complicated phenomenon due to the wide variety of foulants encountered in practice. In addition, the fouling build-up on the membrane surface is not only related to the process parameters (feed concentration, cross-flow velocity and

pressure difference), but is also related to the foulant characteristics (shape, size, surface charge, compressibility and chemical composition) [Wakeman, 1991].

2.2 Measurement and control of fouling

2.2.1. Predictive methods

The efficiency and reliability of a membrane separation facility can be greatly enhanced if an analytical procedure is available for the quantitative prediction of the fouling tendency of a given feed solution. Many other parameters such as the plugging index (PI), the fouling index (FI), the modified fouling index or the membrane filtration index (MFI) etc. have been advanced to describe fouling [Mulder, 1991; Schippers, 1980]. Fouling is, however, too complex to be described by a single parameter.

2.2.2. After-the-fact analysis

Over the last ten years, numerous scientific and technological methods have been used to study fouling deposition and characteristion in effort to determine the possible mechanisms. Membranes fouled in the field are subjected to post-mortem analyses to investigate the causes of fouling. Typical analytical techniques utilised in the "autopsy" of fouled modules are scanning electron microscopy (SEM), x-ray fluorescence (XRF), x-ray diffractometry (XRD), inductively-coupled plasma (ICP) spectrometry, ion chromatography (IC), enery-dispersive x-ray spectroscopy (EDS), atomic absorption spectroscopy (AAS), prompt ion x-ray excitation (PIXE) and biocide sensitivity tests [Butt et al, 1995; Dudley and Darton, 1996].

Although these analytical methods can supply some information on the fouling mechanism, they have provided little information regarding the actual and dynamic build-up of foulant on a membrane surface.

2.2.3. Visualisation techniques

Membrane fouling has been the subject of a large number of indirect and direct real-time measurements, with greater emphasis on the former. Traditionally, real-time fouling investigations have involved the analysis of flux decline data for inference of

fouling. Other methods of fouling analysis include the monitoring of permeate concentration change, increase in the pressure drop along the membrane, and sudden change in retentate concentration.

To overcome the limitations of the above-mentioned methods in providing direct information about CP and fouling, a number of non-invasive techniques have been developed over the last ten years. McDonogh et al. [1995] reported two non-invasive techniques for the study of concentration polarisation during filtration of bovine serum albumen (BSA) and dextran blue. A radio isotope technique was used to measure the adsorption of species in the polarised layer. Mackley and Sherman [1992] conducted an in-situ direct observation of particle deposition during filtration of sub-millimetre particles. Using a 15 x magnification video camera, they were able to record the growth of cake and particle motions on the cake surface. Wakeman [1994] used a high-speed camera and a high magnification zoom lens to record the development of the cake layer at the centre axis of the membrane. Altman and Ripperger [1997] used a laser triangulometer in situ to measure the cake layer height under various filtration conditions.

These studies provided valuable information on polarization profiles and cake thickness, but little information on the phenomenon occurring at the membrane-solution interface as particles were deposited. Li et al. [1998] reported observations of particle deposition on membrane surfaces using in-situ, non-invasive continuous direct observation through a membrane (DOTM). The image observed by the microscope was recorded and viewed via a video camera attached to a super-VHS video recorder and monitor. The filtration tests were conducted in the imposed flux mode, so that the flux could be controlled at below, or above, the "critical flux." The "critical flux" is the flux rate (dependant on the crossflow velocity) which controls particle deposition on the membrane surface. Below the critical flux, particle deposition is negligible and above the critical flux, particle layers form rather quickly on the membrane surface. The results demonstrated that DOTM is a powerful technique with which the fundamentals of particle deposition and the interaction between particles and the membrane can be studied.

It is known that ultrasonic measurement is extensively used in high-resolution flaw detection, thin-material thickness gauging, medical research, and materials characterization to measure sound velocity and attenuation etc. [Lynnworth, 1989; Mason and Lorimer, 1988; Ensminger, 1998]. Recently, substantial progress has been made in the application of ultrasonic TDR to membranes and fouling research. Kools et al. [1998] had some success in employing ultrasound for the real-time visualization of thickness changes during the evaporative casting of polymeric films, while Peterson et al. [1998] employed ultrasound for real-time measurement of compressive strain during membrane compaction.

Mairal et al. [1999] described the first, and so far the only, systematic attempt to adapt and employ ultrasonic-time-domain-reflectometry (UTDR) for the non-invasive measurement of membrane fouling in real-time. UTDR is a versatile measurement technique that is used in a wide variety of industrial, medical and military applications. The technique uses ultrasound waves to measure the location of a moving or stationary interface and can provide information on the physical characteristics of the media through which the waves travel. UTDR thus appears to be ideally suited for the real-time monitoring of membrane fouling, as well as other phenomena of interest, such as membrane compaction. Although Mairal was not able to see or measure a fouling layer, his results showed a decline in the membrane signal amplitude as a fouling layer started to develop and grow on the membrane.

During this project, Koen [2000] reported results describing the use of UTDR for the investigation of membrane fouling and cleaning in flat-sheet RO membrane modules. These results showed that an echo of a fouling layer appeared and grew on the membrane surface, and disappeared as defouling with cleaning proceeded. Li and Sanderson [2002] described the use of non-invasive, in-situ, ultrasonic TDR to visualize fouling on a membrane surface in a crossflow microfiltration module during the filtration of paper mill effluent. Results showed that the UTDR technique could detect fouling layer initiation and its growth in real-time according to changes in ultrasonic signal amplitude. The UTDR technique was also capable of quantifying the thickness of a fouling layer due to the formation of a fouling echo signal. The UTDR technique was more sensitive to changes occurring on the membrane surface than was evident from the flux-decline behavior of the membrane.

Further research in this area was deemed most necessary. Later in this project, UTDR was used for the improved visualization of membrane fouling and the capabilities of the UTDR technique and its applicability in different membrane separation systems were further evaluated.

2.2.4. Technology dealing with fouling

It is known that the pretreatment of feed water can be helpful to minimize fouling [Maartens et al., 1999; Abdel-Jawad et al., 1997; Chakravorty and Layson, 1997; Dudlay and Darton, 1997]. Membrane fouling can also be minimized by changing the membrane geometry and stacking structure, using surface feed flow velocities and turbulent pulses and using sponge balls, backwashing, sparging, ultrasound, electro and electromagnetic influences (for certain effluents), chemical and biological cleaning protocols [Burch, 2001; Laborie et al., 1997; Kennedy et al., 1998; Redkar and Davis, 1995; Muralidhara, 1994; Huotari et al., 1999; Chai et al., 1999; Baker et al., 1997].

Cleaning ability of ultrasound

Several patents deal with the application of ultrasound in water treatment. Hurvey (1965) used an acoustic liquid whistle or transducer to produce cavitation on membranes. It is believed that the formation of air bubbles during cavitation suppresses fouling. When a cavitating air bubble is oscillating near a solid surface, it generates micro-jets of very high velocities that can effectively decrease the boundary layer thickness. In effect, mass transfer is enhanced.

Schimichi (1995) proposed the application of ultrasound in a purification process where water was passed through an ion-exchange resin bed. Li et al (1995) investigated the effect of ultrasound on the diffusion of electrolytes through a cellophane membrane and found that the diffusion velocity of electrolyte through the membrane was greater when ultrasound was applied.

Band [1997] studied the influence of specially mounted ultrasound signals on water desalination through special polymeric ion-exchange hollow fibres. Both Na^+ and H^+

ion exchange were enhanced under ultrasound. Chai et al [1999] used ultrasound to clean polymeric UF and MF membranes that were fouled with peptone. Ultrasound with a frequency of 45 kHz and an output power of 27.3 kW/m^2 was used.

In all these studies, ultrasound with low frequencies (kHz) and high power outputs was used. Frequencies in the order of 40 – 50 kHz showed the best cleaning abilities. In contrast to this, the visualisation technique needs good spatial resolution, and thus a shorter wavelength is required. Ultrasound with higher frequencies (more than 1 MHz) is therefore needed. At this high frequency the ultrasound has no cleaning ability (ultrasound of frequency 5 – 7.5 MHz is used for visualisation in the human body) and is therefore suitable to study concentration polarisation and fouling.

2.3. Ultrasonic testing techniques

2.3.1 Ultrasonics

Vibration waves of a frequency above the hearing range of the normal human ear are referred to as ultrasonics, and the term therefore includes all those waves with a frequency of more than about 20 000 cycles/sec. Frequencies of 20 000 to 100 000 cycles/sec are used for sound ranging, submarine signaling and communication. Those of 100 000 to 10 000 000 cycles/sec are used in testing materials for flaws etc.

The quartz crystal has the property of expanding and sending out an ultrasonic wave when a voltage, generated by a pulsar-receiver, is applied to it. It can also produce an electrical signal when it is mechanically vibrated. The transducer sends out this high frequency signal into the medium that needs to be investigated.

Any material that has elasticity can propagate ultrasonic waves. The propagation takes the form of a displacement of successive elements of the medium. If the substance is elastic, there is a restoring force that tends to bring each element of the material back to its original position. Since all such media also possess inertia, the particle continues to move after it returns to the position from which it started and finally reaches another different position, past the original one. From this second point it returns to its starting position, about which it continues to oscillate with constantly diminishing amplitude. The elements of the material will therefore execute different movements or

orbits as the waves pass through them. It is the differences in these movements that characterise basic types of ultrasonic waves; but no matter what the wave type, the general properties of ultrasonics remain.

As the wave travels through the material, successive elements in it experience these displacements, each such element in the wave path moving a little later than its neighbour. In other words, the phase of the wave or vibration changes along the path of wave transmission. This displacement can be plotted, and the graph is descriptive of the wave.

Types of waves

An ultrasonic wave being transmitted through a substance may be of several types. Each type causes a specific movement in the elements of the medium. The paths that these elements follow as they move in response to the wave are called their orbits. These orbits may be essentially parallel to the line of propagation, in which case the wave is *longitudinal*. On the other hand, they may be executed normal to the direction of propagation. Such waves are called *transverse* or *shear* waves.

Reflection and transmission of waves

The ultrasonic signal is reflected by a change in acoustic impedance, which happens when it reaches a layer with different acoustic impedance than the medium it is travelling through. When this happens, part of the energy travels forward as one wave through the second medium, while the rest of the signal is reflected back into the first medium, usually with a phase change. These reflections can be seen on an oscilloscope and be interpreted. Consider such an example where a plane acoustic wave is transmitted from one medium to another (Fig. 2-1) [Ford, 1970]. The material acoustic impedance $W = V \rho$. Fig. 2-2 shows wave reflection and transmission at a boundary between steel and water.

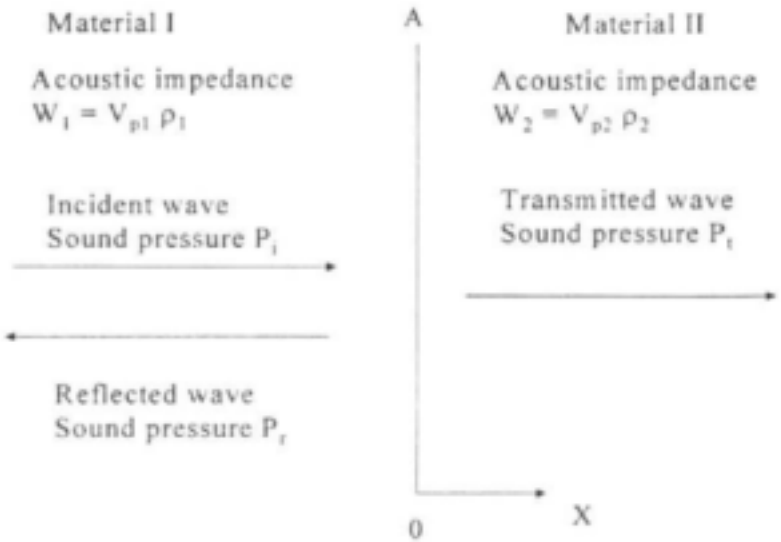

Fig. 2-1. Wave reflection and transmission at a boundary between two materials.

Consider such an example where a plane acoustic wave is transmitted from one medium to another as in Figure 2.1 [Ford, 1970]. Assume a plane wave in material I travelling in the positive x direction at right angles to the plane of the boundary, the material acoustic impedance W can be described as:

$$W = V_p \rho \tag{2.1}$$

where V_p is the sound velocity (m/s); ρ is the material density (kg/m^3).

The amplitude of the reflected wave is thus related to the incident one as [Ford, 1970]

$$R = \frac{\rho_2 V_2 - \rho_1 V_1}{\rho_2 V_2 + \rho_1 V_1} = \frac{W_2 - W_1}{W_2 + W_1} \tag{2.2}$$

and the amplitude of the transmitted wave related to the incident wave as

$$D = \frac{2\rho_2 V_2}{\rho_2 V_2 + \rho_1 V_1} = \frac{2W_2}{W_2 + W_1} \tag{2.3}$$

R and *D* are also called the coefficients of reflection and transmission, respectively, of the sound pressure (both are dimensionless numerical values).

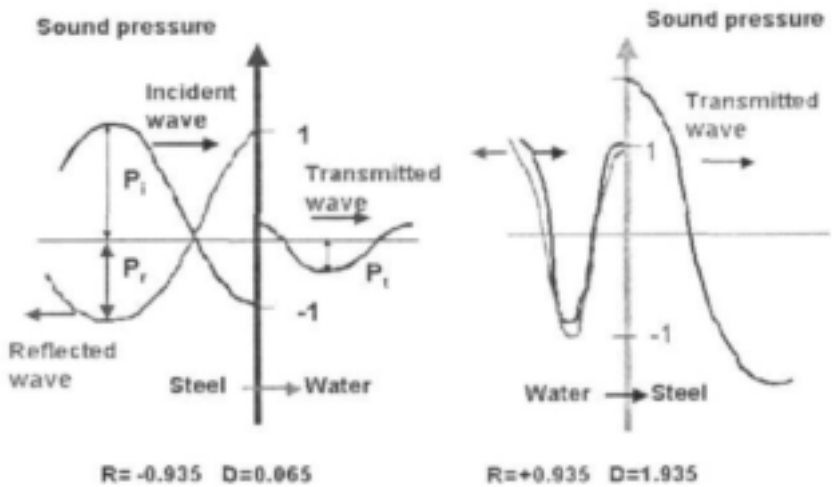

Figure 2.2: Sound wave reflections at the interface between steel and water [Krautkrämer, 1969].

As an example *C* and *D* on the interface steel/water can be calculated. Acoustic impedances of steel and water for longitudinal waves are [Krautkrämer, 1969]

$$W_1 \text{ (steel)} = 45 \times 10^6 \text{ kg/m}^2\text{s} \quad \text{and} \quad W_2 \text{ (water)} = 1.5 \times 10^6 \text{ kg/m}^2\text{s}$$

Thus

$$C = \frac{1.5 - 45}{1.5 + 45} = -0.935, \qquad D = \frac{2 \times 1.5}{1.5 + 45} = 0.065$$

Expressed as percentages the reflected wave has – 93.5 % of the sound pressure of the incident wave and the transmitted wave 6.5 %. The negative sign indicates the reversal of the phase relative to the incident wave that is the incident wave passes from a material of higher velocity into a low-velocity later [Krautkrämer, 1969].

If, in the reverse case, the wave coming from water strikes steel, an exchange of W_1 and W_2 furnishes

$$C = +0.935, \qquad D = 1.935.$$

Since C is positive, incident and reflected waves are in phase. The transmitted wave has 193.5 % of the sound pressure (see Figure 2.2).

2.3.2. UTDR technique in process monitoring

Ultrasonic echo ranging (the basis for the pulse-echo technique) is used by bats to locate obstacles and prey. The idea of humans using the reflection of a short ultrasonic pulse for the detection of objects was first reported by Sokolov [1929] for use in flaw detection. The pulse-echo technique has since been utilised in a wide range of applications. Some of the well-known applications of this technique are liquid-level detection, counting or signalling on production lines, solid density measurements, edge or width control, thickness monitoring in metal or polymer coatings, and detection of corrosion in metal pipes [Frederick, 1965; Lynnworth, 1989]. In addition, it is also used in ranging and position detection in military, industrial, and bioengineering applications [Lynnworth, 1989]. New developments have been reported for the application of this technique to medical diagnostics and film thickness measurement in semiconductor fabrication [Lynnworth, 1989] and to the measurement of membrane fouling and compaction [Bond et al., 1995; Mairal et al., 1999 and 2000].

UTDR is essentially an adaptation of the pulse-echo technique for membrane-science applications. It is designed to measure the location and acoustic impedance contrast, or relative "stiffness" of an interface. The acoustic impedance of a medium is given by the quantity ρv, where ρ is the density of the medium and v is the speed of sound in it. The technique is based on the simple principle that the distance d travelled by sound over time t in any medium is given by

$$d = v \times t \qquad (2\text{-}4)$$

The intensity of sound reflected from a surface depends on the topography and the stiffness of the surface; the stiffer and smoother the surface, the more intense the echo. Thus, if a sound source is directed towards a target surface, the position and amplitude of the peak in the time-domain representing the echo from the target would depend on the distance of the target from the source and its stiffness and topography.

2.3.3 Critique of the pulse-echo ultrasonic measurement literature

The UTDR technique incorporates features of the pulse-echo method and the reflection coefficient measurement. It is a very powerful and sensitive technique, supported by a large body of literature on wave scattering. The variety of applications successfully employing existing wave-scattering theories provides a strong basis for the development of the UTDR technique and a supporting scattering theory for fouling. Indeed, the technique has already shown substantial promise for such applications [Bond et al., 1995; Mairal et al., 1999 and 2000; Koen, 2000; Li et al., 2002]. Development and utilisation of UTDR will not only generate useful insights into fouling mechanisms and membranes performance, but can also provide a unique tool to assess and, where necessary, improve existing fouling models.

2.4. Ultrasonic equipment

2.4.1. Ultrasonic set-up

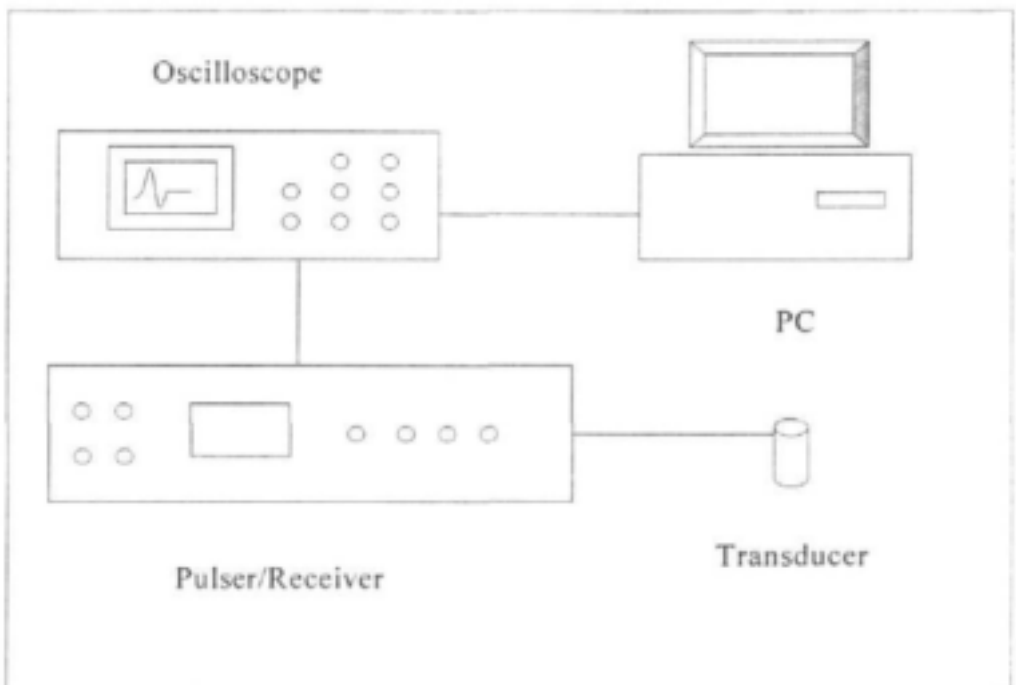

Fig. 2-3 Ultrasonic set-up for UTDR pulse-echo operation

Fig. 2-3 is a simplified drawing of all the hardware in the ultrasonic set-up. A pulsar/receiver generates the voltage signal that triggers the transducer to send out an ultrasonic wave. The oscilloscope that is connected to the pulsar/receiver captures and displays the data as amplitude changes on its front panel. These data can be stored on a computer's hard drive.

2.4.2. Pulsar/Receiver

A Panametrics Model 5058PR High Voltage Pulsar-Receiver was used in this study. It was designed especially for ultrasonic test and measurement applications that require a high material penetration capability. The pulsar section of the Model 5058PR can deliver up to 900 volts in an impulse-type excitation pulse to appropriate low frequency transducers. The receiver section provides 60 dB radio frequency (RF) gain, with an additional 30 dB available from an integral auxiliary preamplifier. A full

range of front panel controls permits either discrete, calibrated settings or continuous adjustments for all important instrument functions. Pulse voltage is continuously adjustable in four values from 100 to 900 volts with a front panel meter displaying the available voltage to the transducer. Receiver gain is selectable as 40 or 60 dB, while receiver attenuation is adjustable from 0 to 80 dB in 1dB steps with a ±1 dB vernier for precise setting. The Model 5058PR includes an internal preamplifier that can be used to create an additional 30 dB gain. Echo pulses can be selected as either normal or inverted 180° for peak detection applications.

The 5058PR can be internally triggered at any of seven pre-amplifier radio-frequency (PRF) rates from 20 Hz to 2 KHz, or externally triggered at any frequency up to 2KHz. Pulse damping is continuously adjustable over a range of 50 to 333 ohms, or in stepped values of 50, 100, 200, or 500 ohms. All transducer and RF output connectors are front-panel mounted for easy access.
Some features of the equipment are the following:

- High voltage pulsar, switched settings or continuously adjustable to 900 volts
- High gain, low noise broadband (10 MHz) receiver
- Pulse-echo and through transmission modes

2.4.3. Oscilloscope

The choice of the correct oscilloscope is very important, as real-time signal changes are displayed on it. The oscilloscope should have a digitising capability for real-time processing and display of the ultrasonic signals as well as appropriate time-domain resolution and sensitivity for accurate measurement of fouling layer growth. Fig. 2-4 shows the Hewlett Packard Oscilloscope Model 54602B used. Fig. 2-5 shows the pulsar/receiver – oscilloscope set-up for pulse-echo operation.

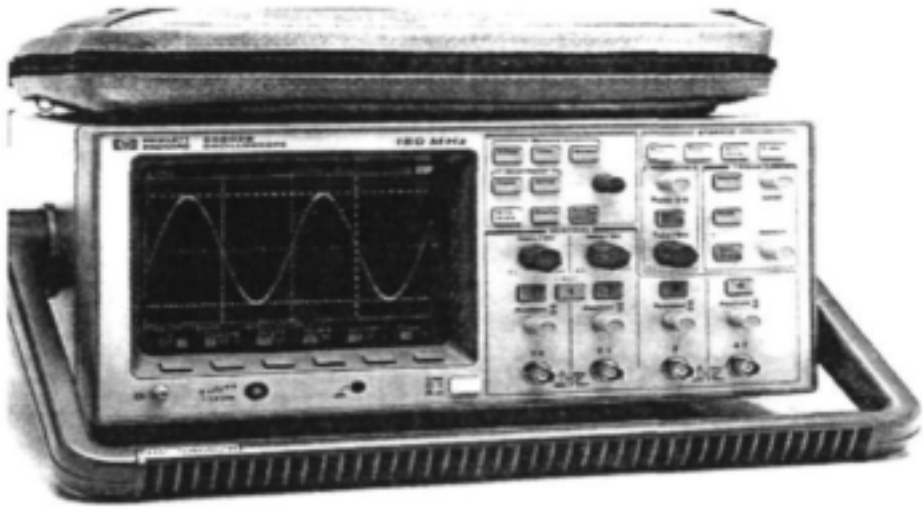

Fig. 2-4. Hewlett Packard Oscilloscope Model 54602B

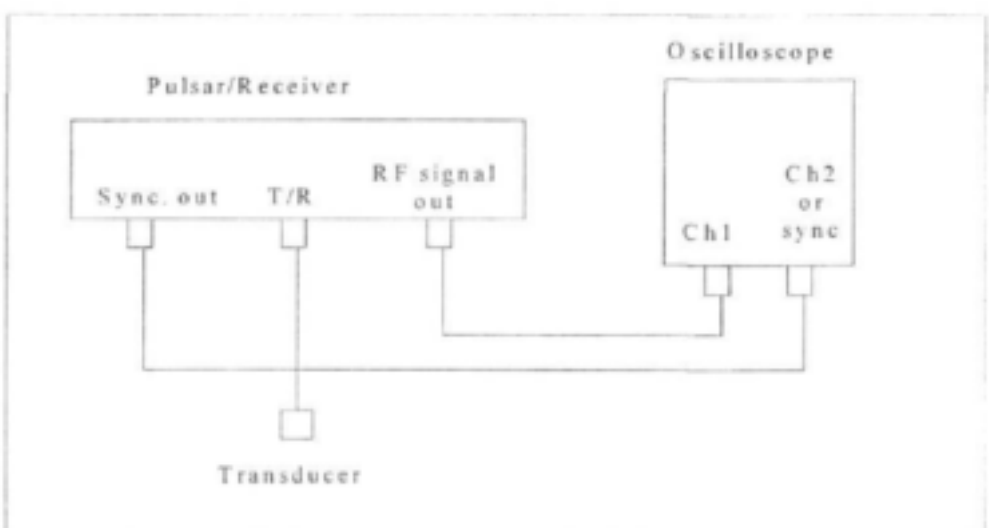

Fig. 2-5. Pulsar/Receiver – oscilloscope set-up for pulse-echo operation.

2.4.4. *Transducers*

The transducer is one of the most critical components of any ultrasonic test system. As a result a good deal of attention should be paid to selecting the proper transducer for the application. Of equal importance is the performance of the system as a whole. Variation in instrument characteristics and settings as well as material properties and coupling conditions play a major role in system performance.

Most often the transducer is chosen to enhance either the sensitivity or the resolution of the system. A system with good sensitivity has the ability to detect small variations at a given depth in the test material. A system with good resolution has the ability to produce simultaneous and distinct indications from reflectors lying at nearly the same depth and position with respect to the sound beam. In applications where good resolution is of primary importance it is common to select a highly dampened transducer. A high degree of damping will help to shorten interface ringdown or recovery time and allows the system to resolve closely positioned reflectors.

The specific transducer configuration also has an impact on system performance. Consideration should be given to the use of focused transducers, transducers with wear surfaces that are appropriate to the test material, and the choice of the appropriate frequency and element diameter.

In this study Panametrics Videoscan transducers were used. Videoscan transducers are untuned transducers, which provide heavily damped broadband performance. They are the best choice in many applications where good axial or distance resolution is necessary or in tests that require improved signal-to-noise in attenuating or scattering materials.

2.4.5. Theoretical resolution

The theoretical resolution of a specific frequency transducer can be calculated if the speed of the sound wave in the medium that is under investigation is known [Koen, 2000]. The wavelength can be calculated with Eq. 2-2 where

$$\psi = v/f, \tag{2-5}$$

with ψ = wavelength (m)

v = speed of soundwave (m/s)

f = frequency (Hz, or cycle/s)

The smallest detail that the transducer will pick up is that which is 0.25 of the sound wave's wavelength (explained in Fig. 2-6). The theoretical resolution can thus be calculated with Eq. 2-3 where

Resolution = 0.25ψ (2-6)

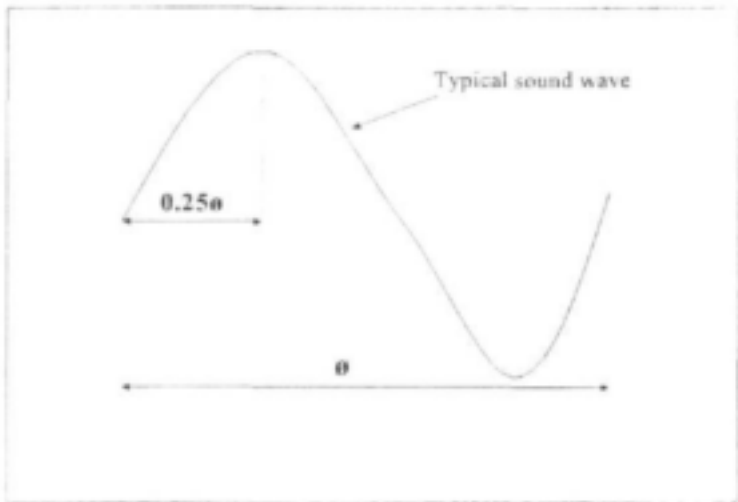

Fig. 2-6. Typical sound wave.

The possible theoretical resolution (in water) of the range of transducers that were used during this study is tabulated in Table 2-1.

Table 2-1

The theoretical resolution of the range of transducers used

Transducer (type)	Frequency (MHz)	Resolution (μm)
V106-RB	2.25	159
V182-RB	3.5	102
V109-RB	5	72
V120-RB	7.45	48
V111-RB	10	36

3 Ultrasonic measurements of fouling and cleaning of flat-sheet MF membranes

3.1. Introduction

Crossflow microfiltration is an increasingly important technique for processing particulate suspensions in areas such as biotechnology, water and wastewater treatment food and mineral processing [Cheryan, 1998; Tanny et al., 1982; Treffry-Goatley et al., 1987; Ginn and Cobb, 1997]. It is generally recognised that one of the major problems restricting the more widespread use of microfiltration systems is the significant flux decline as a result of particle deposition and the build-up of a filter cake on the surface of the septum or membrane.

Most crossflow-microfiltration studies have been typically limited to measurements of filtrate flux alone because cake thickness information was unavailable. Over the last ten years, many scientific and technological methods were used to study cake deposition and characterisation, in efforts to elucidate the possible mechanisms of fouling. The numerous experimental methods used for cake layer thickness measurement can be broadly classified into two categories: destructive and non-destructive measuring methods. Destructive measuring methods include cake weighting [Al-Malack and Anderson, 1996], freeze slicing [Schmidt and Löffeler, 1990] and reconstruction of the cake layer [Vyas et al., 2000]. Although these destructive measuring methods can measure cake thickness and porosity, they have provided little information regarding the actual and dynamic build-up of the cake on the membrane surface.

There have been numerous attempts to non-destructively measure, or monitor, cake thickness as a function of time. The following techniques/methods have been used: nuclear magnetic resonance spectroscopy (NMR) [Wandelt et al., 1992; La Heij, 1996], CATSCAN [Tiller, 1995], optical laser beam [Altmann and Ripperger, 1997], optical methods [Hamachi and Mietton-Peuchot 1999; Tung et al., 2001; Mores and Davis, 2001; Lu et al., 2001; McDonogh, 1995], photography [Mackley and Sherman, 1992; Wakeman, 1994; direct observation of particle deposition (DOTM) [Li and

Fane, et al., 1998], X-ray [Bierck, 1998; Bierck and Dick, 1990] and ultrasonic imaging and reflectometry [Hutchins and Mair, 1989; Haerle and Haber, 1993; Mairal and Greenberg, 1999 and 2000, Li and Sanderson, 2002]. Among them, the ultrasonic testing technique [Li and Sanderson, 2002] appears to be a very useful techniques for measuring cake layer deposition, growth and removal.

Hutchins and Mair [1989] developed an ultrasound imaging technique by utilizing transducers configured in a pulse-echo mode to monitor cake thickness during a ceramics slip-casting process. Haerle and Haber [1993] further expanded the work developed by Hutchins and Mair [1989] to examine the effect of frequency - 1 MHz was found to give the best peak resolution.

This section describes the use of an ultrasonic time-domain reflectometry (UTDR) technique to monitor the fouling and cleaning of microfiltration (MF) membranes in-situ and non-invasively. The study was carried out with paper mill effluent (the average particle size 0.947 μm) from a wastewater treatment plant. The UTDR technique can measure the cake thickness build-up as a function of time. The preliminary study showed the ultrasonic signals obtained.

3.2. Experimental

3.2.1. Experimental design - MF system and UTDR testing

The major considerations in choosing an appropriate MF system include industrial relevance and wastewater disposal problems. In this study, investigations were carried out into a MF system with effluent from a wastewater treatment plant of Mondi Kraft Mills, Mondi Ltd, South Africa. The wastewater treatment plant comprised the following processes: pre-treatment, dissolved air flotation (DAF), MF and UF. Samples were taken from the DAF product. The characteristics of the effluent are summarized in Table 3-1.

Nylon MF membranes (disc ϕ 290 mm) made by Pall Ltd, England, with a nominal pore size of 0.2 μm, were used in all of the fouling experiments.

The flat-sheet MF experimental setup, shown in Fig. 3-1, allows for the accurate control of inlet pressure, retentate flow rate and temperature. In each MF experiment, continuous stirring in the feed tank was provided for. Permeate flux was measured by a balance, connected to a PC. During the experiments the retentate and permeate were recycled to the feed tank and permeate was also recycled to the feed tank after flux measurements (zero recovery). Fig. 3-1 is also a schematic representation of UTDR measuring. The ultrasonic measurement system consisted of a 10 MHz ultrasonic transducer (Panametrics V111), a pulsar-receiver (Panametrics 5058PR) and a digital oscilloscope (HP Model 54602B) with sweep speeds from 5s/div to 2ns/div and 1mv/div sensitivity. The oscilloscope connected to the pulsar-receiver captured and displayed the data as amplitude changes on its front panel. Each set of ultrasonic data generated consisted of 500 data points, which can be stored on a computer's hard drive. Salad oil was used to couple the transducer to the top plate surface.

Table 3-1

Characteristics of paper mill effluent (DAF product)

(units in mg/l unless otherwise indicated)

Items	Value	Items	Value
pH	4.96	Potassium as K	30
Conductivity, μS/cm	5550	Sulphur as S	1075
Aluminum as Al	16	Bicarbonate as HCO_3	98
Boron as B	2	Nitrate as NO_3	<50
Calcium as Ca	353	Chloride as Cl	<10
Iron as Fe	3	Alkalinity as $CaCO_3$	27.2
Magnesium as Mg	27	Turbidity	64 NTU
Sodium as Na	908	Suspended solids (SS)	6636

*the data from Mondi Piet Retief, Mondi Ltd, South Africa.

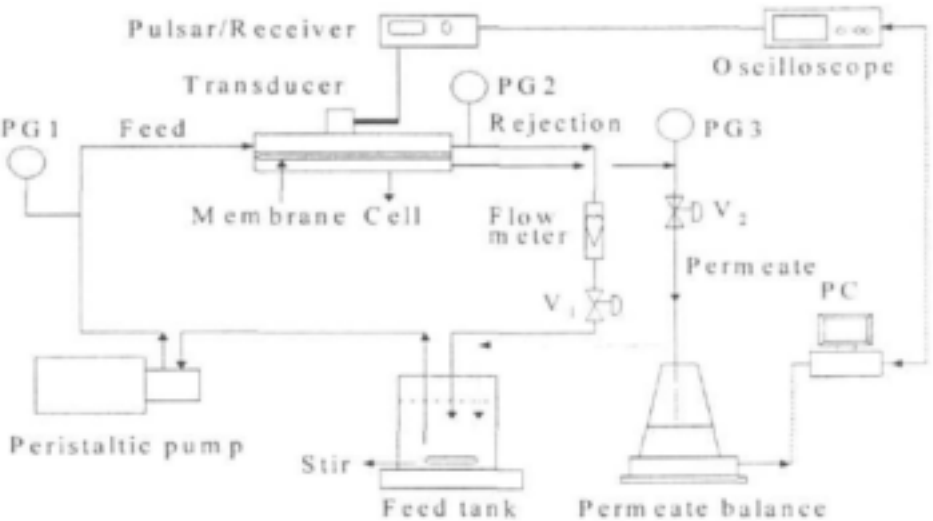

Fig. 3-1. Schematic representation of MF separation system and UTDR measuring.

3.2.2. Test cell

The characteristic properties of the material selected for construction of the test cell are very important, as the ultrasonic signal must be able to penetrate the material. Fig. 3-2 is a schematic representation of the test cell in the MF separation system. The cell was made from poly-methyl methacrylate (Perspex). The dimensions of the cell were 200 mm × 90 mm × 40 mm, with an effective membrane surface area of 20 cm^2. The thickness of the top plate was 20 mm. A porous sintered steel plate 100 mm × 30 mm ×2.5 mm was used as support for the membrane, while a spacer was also necessary due to the geometric dynamics of the cell.

The topside of the top part of the cell had a 90 mm × 45mm × 16mm recess. It was filled with food-grade salad oil, which was used as coupling agent between the transducer and the cell. The membrane with a support-plate/spacer combination was positioned on the bottom plate (see Fig. 3-3) and the unit was sealed with a dual o-ring combination. The complete module assembly was clamped together with twelve 6 mm-diameter bolts. A rectangular channel 100 mm × 40 mm × 5 mm formed the actual flow channel.

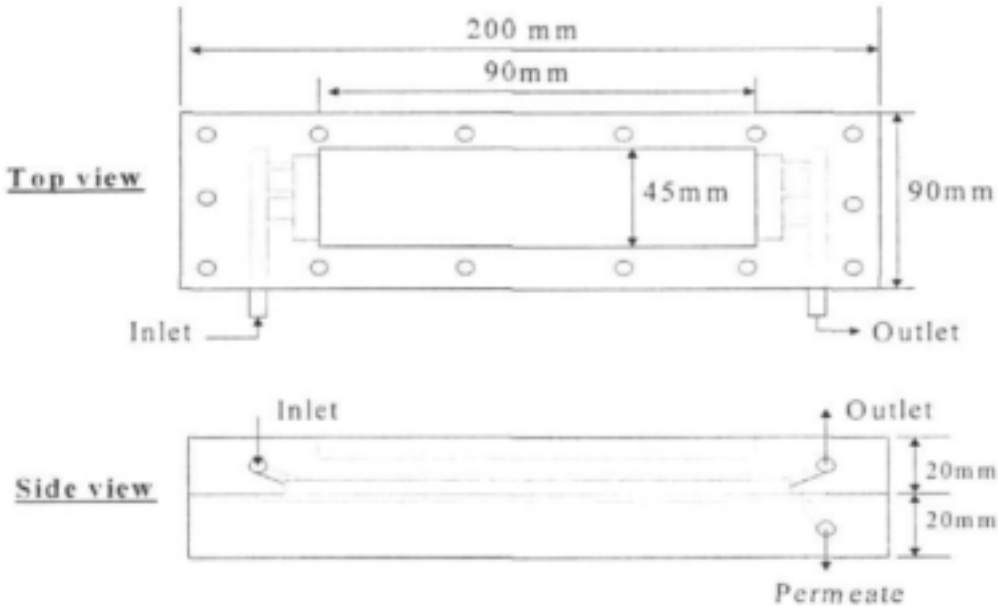

Fig. 3-2. Test cell for MF.

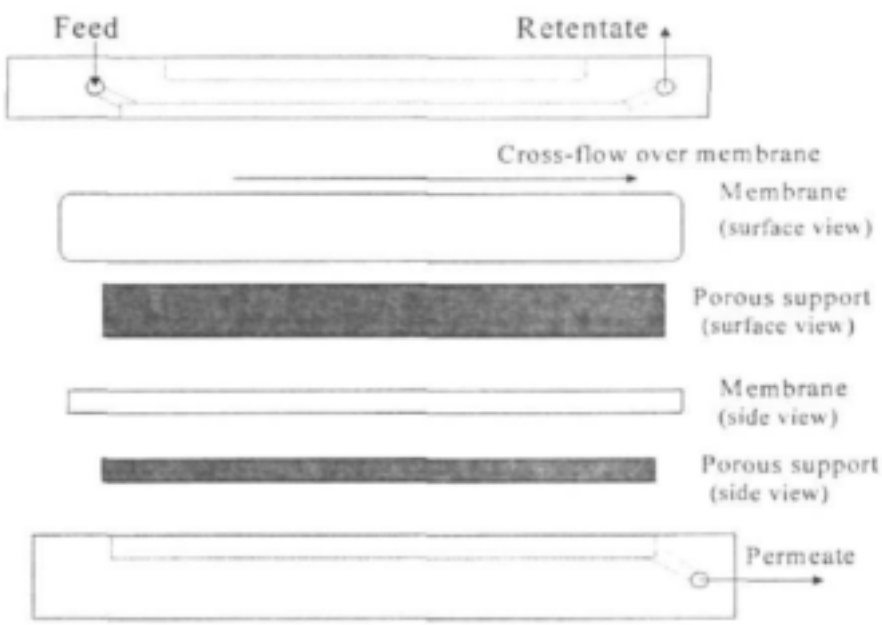

Fig. 3-3. Placement of membrane in cell

3.2.3. *Experimental cell reflections*

Ultrasonic measurement uses sound waves to measure the location of a moving or stationary interface and can provide information on the physical characteristics of the media through which the waves travel [Lynnworth, 1989; Ensminger, 1998; PANAMETRICS, 2000]. Ultrasonic, nondestructive testing introduces high frequency sound waves into a test object to obtain information about the object without significantly altering or damaging it. Two basic quantities are measured in ultrasonic testing; they are the time of flight or the length of time taken for the sound to travel through the sample, and the amplitude of the received signal. Based on velocity and round trip time of flight through the material, the material thickness can be calculated as follows:

$$\Delta S = \tfrac{1}{2} c \Delta t \qquad (3\text{-}1)$$

ΔS = material thickness; c = material sound velocity; Δt = time of flight

Measurements of the relative changes in signal amplitude can be used for sizing flaws or measuring the attenuation of a material. The relative change in signal amplitude is commonly used in ultrasonic testing.

Fig. 3-4 is a cross-sectional view of a typical flat-sheet cell that was used in the UTDR experiments. A membrane was placed between two poly-methyl methacrylate (Perspex) plates. A transducer was externally mounted in contact with the top plate. The feed solution flowed over the face of the membrane. The permeate was withdrawn from the bottom side. Now, suppose a fouling layer with thickness Δs is present on the membrane surface and the reflected echoes A, B and C are generated from the various interfaces within the cell. The corresponding time-domain response is shown in Fig. 3-5. The top plate/feed solution interface is represented by echo A and the initial feed solution/membrane interface by B. In general, once fouling is initiated on the membrane surface, the acoustic impedance difference and the topographical characteristics at the feed solution/membrane interface will change, resulting in a change in the amplitude of echo B. Further, if the fouling layer is thick enough to be measured by the ultrasonic signal, i.e. it falls within the spatial resolution capabilities of the system, a new echo C will be formed as a consequence

of the new feed/fouling interface. If the difference in arrival times, Δt, between echoes B and C is measured, the thickness of the fouling layer, ΔS, can be determined by equation (3-1). Thus, the detection of the interface echoes allows fouling to be monitored in real-time.

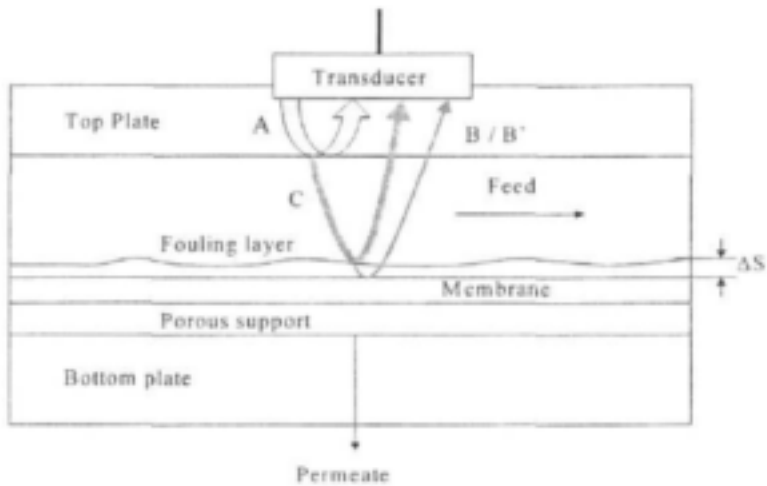

Fig. 3-4. Schematic representation of the principle of UTDR measurements.

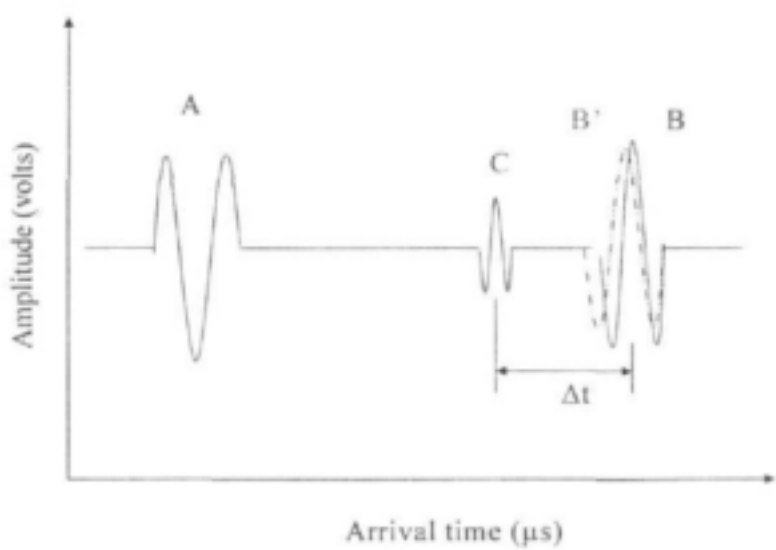

Fig. 3-5. Corresponding time-domain response for set-up in Fig. 3-4.

3.2.4. MF fouling experiments

Each experiment commenced with pure water being circulated through the system at the desired flow rate and applied pressure, for two hours, to compress the membrane and to build up a stable flow field. Once steady state was attained (the compaction of the membrane stops and the distance to B becomes constant), the feed was switched to the paper mill effluent solution to initiate the fouling phase in which particle polarisation and fouling occurred. This phase was allowed to continue until the ultrasonic response and permeate flux had stabilised. The overall objective of the experiments was to obtain quantitative information on the ultrasonic response of fouling behaviour within a reasonable time scale. The fouling experiments were carried out at axial velocities of 1.0±0.01 cm/s (Re=35.7±0.4) and 4.2±0.05 cm/s (Re=150±1.5), applied pressure 100±5 kPa and temperature 24±1°C. All runs were made in the laminar flow regime with Re < 400. The total operating time for the fouling experiments was about 8-16 h, depending upon the specific axial velocity employed.

3.2.5. Cleaning experiments in MF

After the membranes were fouled with paper effluent they were cleaned by three methods, in turn, namely: ultrasound, forward flushing and ultrasound together with forward flushing, for cleaning durations of 20 min each. The feed solution was changed from effluent to water at the same operating conditions as used during the fouling phase in order to compare the cleaning efficiencies of these three methods. Forward flushing was performed by opening valve V1 and closing valve V2 (Fig. 3-1). The cross-flow filtration cell was immersed in a water bath maintained at a temperature of 24±1°C during ultrasonic cleaning. The cell was irradiated with a horn ultrasonic cleaner (Medal W-375, Ultrasonics INC.), with a frequency of 20 kHz and a power of 375 W (Fig. 3-6). Ultrasound associated with forward flushing was performed with intermittent forward flushing, with a flow rate of 40-50 cm/s during ultrasonic irradiation. To investigate the cleaning efficiency of each cleaning method, the cleaned membrane was used to filter pure water under the same operating condition as used during the fouling phase.

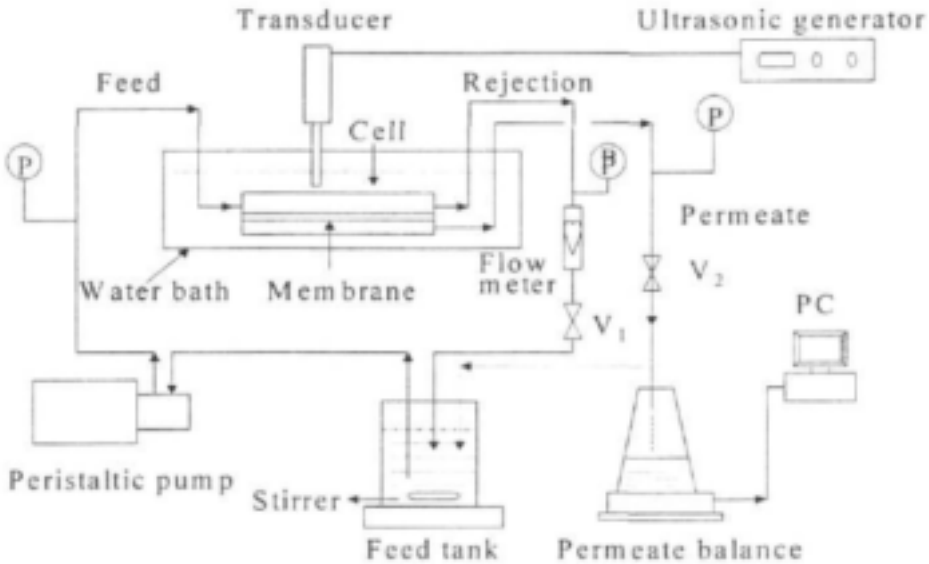

Fig. 3-6. Experimental set-up for ultrasonic cleaning in crossflow MF.

3.2.6. Morphological characterisation of the fouling layer

A morphological study of the fouled membrane samples, by scanning electron microscopy (SEM), was deemed necessary in order to establish a correlation between the measurement of UTDR and the coverage of the fouling layer on the membrane surface. This was done with a LEO S440 SEM. Samples were viewed at 10 kV and 20 mm working distance.

Although the SEM analyses resulted in high-resolution images, which provided important insight into the morphological growth of a fouling layer, results were still limited by the fact that the sampling areas were very small (relative to the overall size of the membrane), as was the part of membrane that was scanned by the transducer.

This was overcome by preparing the samples in two stages. First, a piece of membrane was removed directly underneath the area the transducer was scanning. The sample was then analyzed under an optical microscope for general features and trends, and a representative area was identified for SEM analysis. By doing so, a representative sample was always taken.

3.3 Results and discussion

This section presents the results of experiments carried out in the development of UTDR by using the experimental methodology described in Section 3.2. The data generated during real-time measurement of membrane fouling include the permeation rate, system pressure and ultrasonic responses from the membrane surface as digitised waveforms. Each set of ultrasonic data generated consisted of 500 data points. This is quite a substantial amount of data that made files very large and frustratingly slow to handle. For the sake of easy handling, only the membrane echo, and the fouling echo (if present), were thus used in the discussions that follow.

3.3.1. Fouling experiments

If fouling occurs on the membrane surface, changes in the reflected signal can be expected due to modifications in the morphology of the membrane-solution interface. A new interface signal will be observed in the time-domain if the fouling layer thickness approaches a critical value relative to the resolution of the ultrasonic measurement system.

Experiment with paper mill effluent at axial velocities of 1.0 and 4.2 cm/s

The applied pressure was controlled at 100 kPa and permeate measurements were taken every 5 min. A gradual decrease in permeate flow was detected and after 6 or 18 hours the experiment was stopped (Fig. 3-7). Ultrasonic echoes were taken every 10 min or 30 min. Ultrasonic signal responses in the fouling experiments are shown in Figs. 3-8 and 3-9.

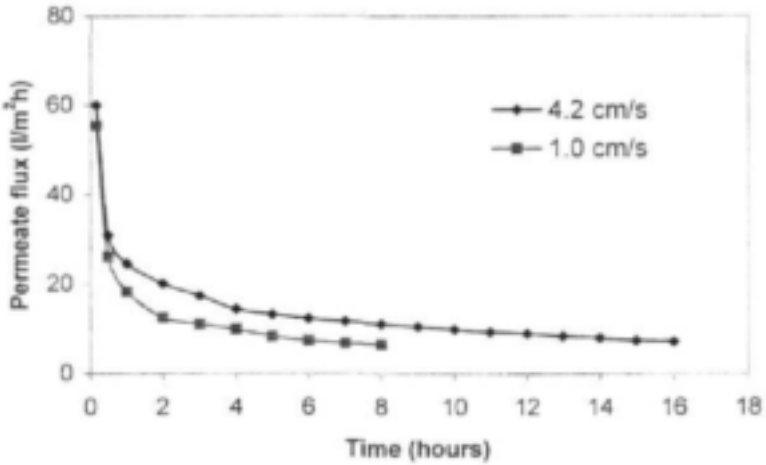

Fig. 3-7 Permeate flux vs. time during paper mill effluent fouling experiments at axial velocities of 1.0 and 4.2 cm/s.

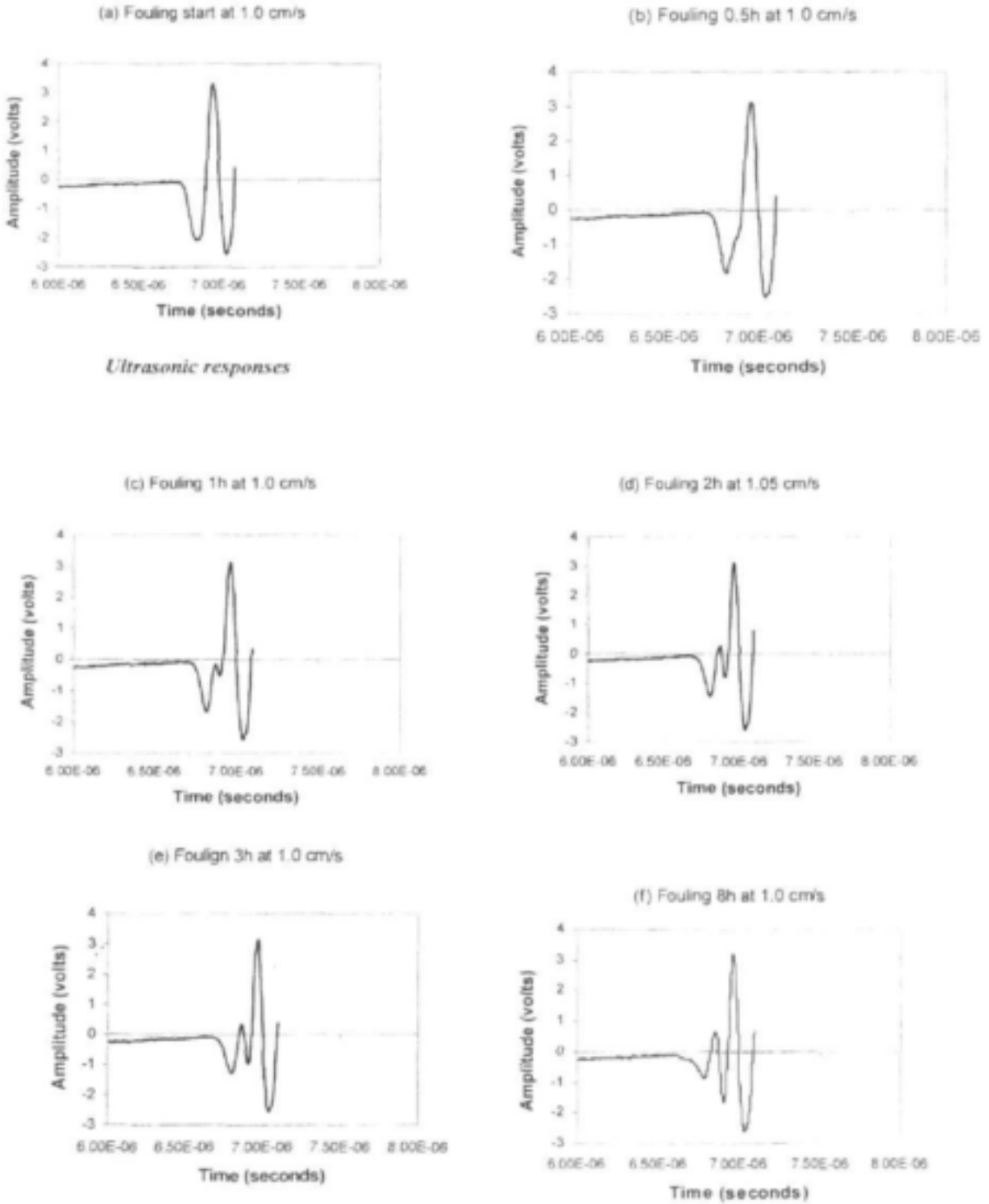

Fig. 3-8. Ultrasonic signal responses in the fouling experiment by paper mill effluent at axial velocity of 1.0 cm/s, after 0 (start), 0.5, 1, 2, 3 and 8 h of operation.

At the commencement of fouling an instantaneous and rapid decline in the flux was observed, followed by a more gradual decline after 2 h of operation (Fig. 3-7). The instantaneous flux decline results primarily from concentration and particle polarization, and the formation of a cake layer near or on the membrane surface, while the gradual decline is presumed to occur as a result of the slow growth and consolidation of the fouling layer. Fig. 3-7 also shows that decreases in permeate flux were faster at an axial velocity of 1.0 cm/s than they were at 4.2 cm/s. It may be that high shear rates, generated at the membrane surface, tend to shear off deposited material, and thus reduce the hydraulic resistance of the fouling layer [Cheryan, 1998].

Consistent with above observation, the corresponding ultrasonic signal response displayed rapid amplitude changes as fouling proceeded at an axial velocity of 1.0 cm/s (Fig. 3-8). At the commencement of fouling, the large peak represents the clean nylon membrane. After 1 h of operation, a second echo of ultrasonic response was obtained before the main membrane echo. The formation of the second echo is a result of the change in acoustic impedance between the bulk solution and the membrane. If the fouling layer is thick enough to be measured by the ultrasonic signal, that is, it falls within the spatial resolution capabilities of the system, a new echo will be formed as a consequence of the bulk solution/fouling interface [Mairal and Greenberg et al., 1999]. Further growth of the cake layer will result in a denser fouling layer being formed and a larger change in acoustic impedance between the membrane and the layer is expected. This would be detected as a sharper reflection. Thus, an echo with greater amplitude is seen in Fig. 3-8 at 2, 3 and 8 h of fouling operation.

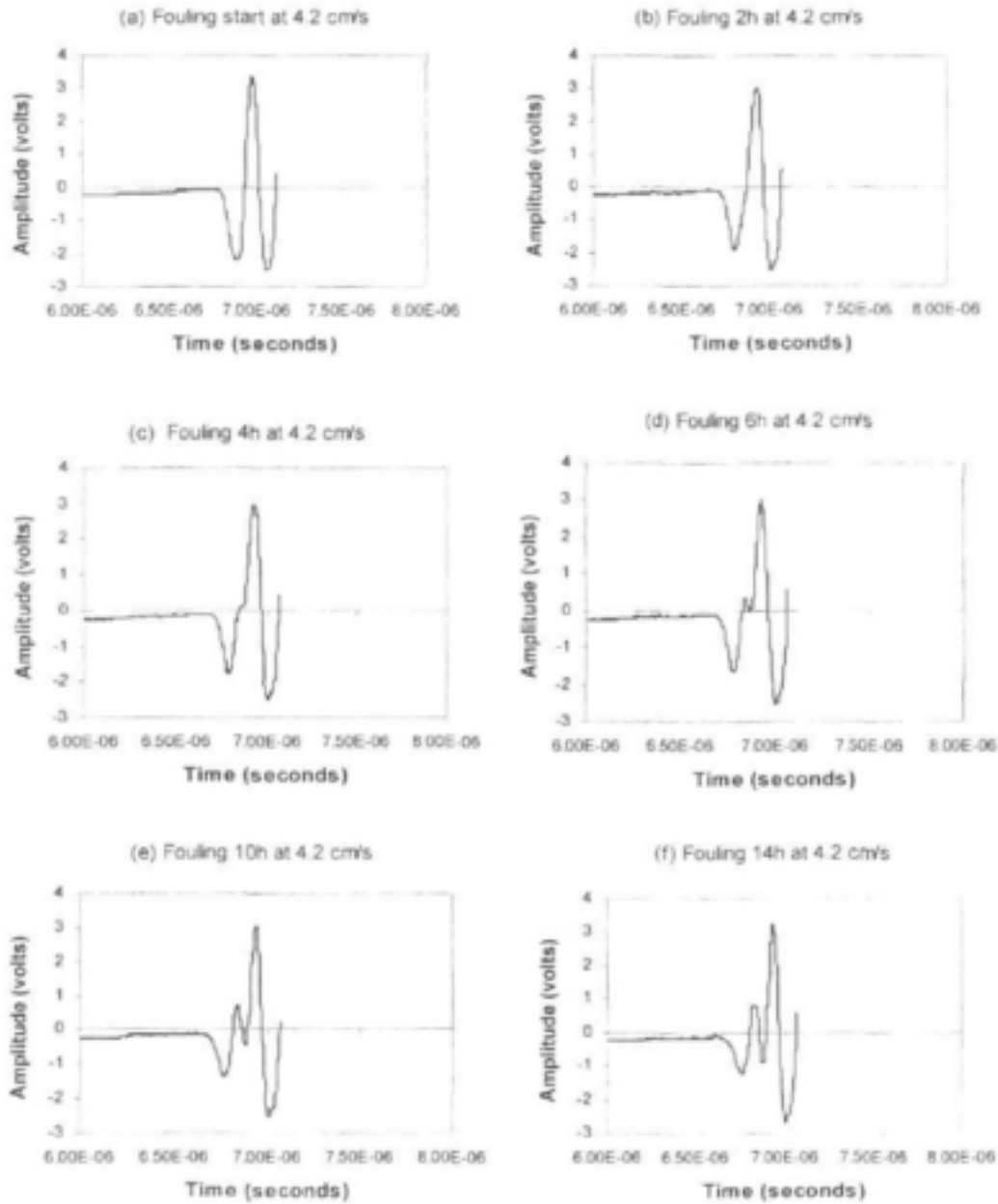

Fig. 3-9. Ultrasonic signal responses in the MF paper mill effluent fouling experiment at an axial velocity of 4.2 cm/s, after 0 (start), 2, 4, 6, 10 and 14 h of operation.

Fig. 3-9 shows ultrasonic signal responses in the fouling experiment at the axial velocity of 4.2 cm/s, after 0 (start), 2, 4, 6, 10 and 14 h of operation. By comparison with results recorded at the axial velocity of 1.0 cm/s (Fig. 3-8), it was found that the fouling echo at the axial velocity of 4.2 cm/s appeared later than that at 1.0 cm/s. After 6 h of fouling operation at 4.2 cm/s, a second echo of ultrasonic response appeared before the membrane peak (Fig. 3-9). A shaper reflection of fouling layer emerged after 10-14 h fouling at 4.2 cm/s. However, a larger peak of the fouling echo arose only after 3 h of fouling operation at 1.0 cm/s (Fig. 3-8). The fouling echo appeared and grew quickly at lower axial velocity because of the lower shear rate. This indicates that the UTDR technique is able to detect the fouling echo appearance and growth during fouling processes at different axial velocities.

In order to confirm the UTDR measurement and membrane coverage, fouled membranes were taken for SEM analysis after fouling periods of 1 and 6 h at 1.0 cm/s, and 4 and 16 h at 4.2 cm/s (Fig. 3-10). The SEM micrographs of the membrane surface after 1h of fouling operation at 1.0 cm/s confirmed complete membrane coverage with the fouling layer (Fig. 3-10a). More and larger particles were left on the membrane surface after 16 h of fouling operation at 4.2 cm/s (Fig. 3-10d). Inductively-coupled plasma analysis showed that the main chemical composition of the fouling layer was the breakdown products of lignin or lignosulphonates [Domingo, 2001].

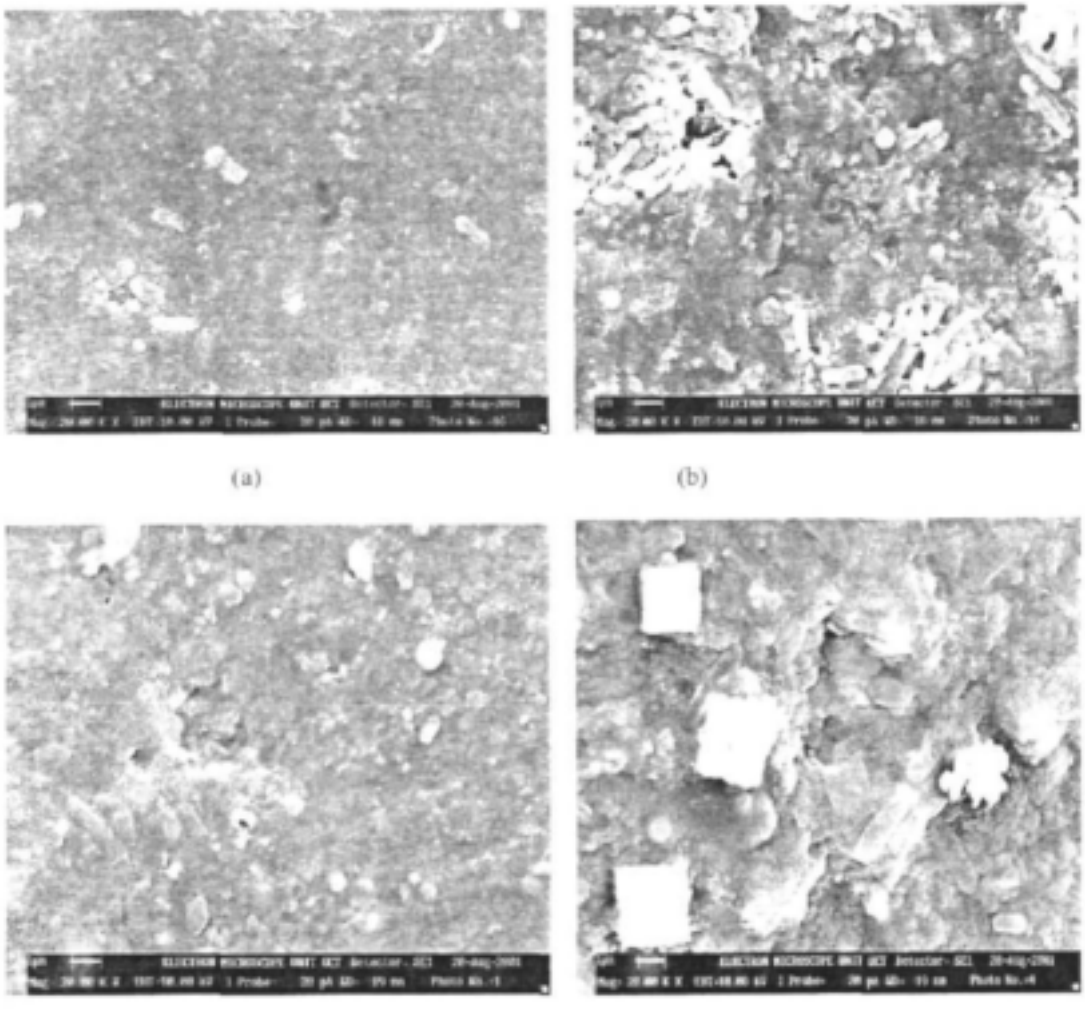

Fig. 3-10. Microscopic images of the Nylon membrane surface during the paper mill effluent fouling experiments: after fouling periods of 1 h (a) and 8 h (b) at 1.0 cm/s, 4h (c) and 16 h at 4.2 cm/s; magnification: X 20,000.

The time-domain movement of the second/fouling echo was observed as a result of an increase in the fouling layer thickness. The UTDR technique is in fact measuring fouling layer thickness. If the difference in arrival times between membrane and fouling layer echoes, Δt, is measured, then the thickness of the fouling layer, ΔS, can be determined from the equation 3-1.

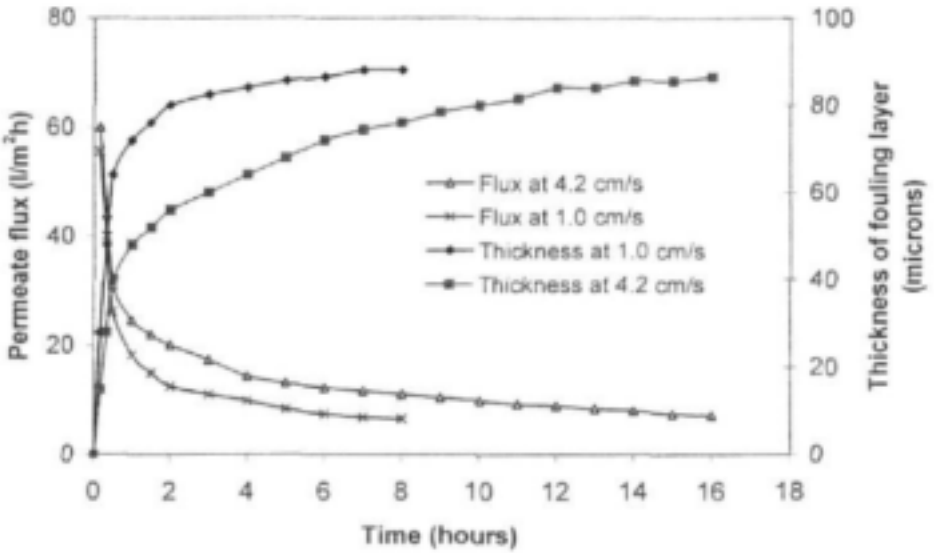

Fig. 3-11. Thickness of fouling layer and permeate flux vs. time during fouling phases by paper effluent, at axial velocities of 1.0 and 4.2 cm/s.

The detection of the interface echoes allows fouling to be monitored in real-time. Fig. 3-11 (subtraction done) illustrates the relationship between the thickness of the fouling layer, permeate flux and fouling time at the axial velocities of 1.0 and 4.2 cm/s. The thickness obtained by UTDR represents fouling layers. Fig. 3-11 shows the fouling initiation and growth as fouling proceeds. The thickness of the fouling layer increased rapidly at the beginning of fouling because of cake layer formation. The thickness of the fouling layer at 1 h fouling was 48 and 72 μm at 4.2 and 1.0 cm/s, respectively. After 1 h fouling, the thickness continued to increase slowly as fouling proceeded. The reverse holds for ultrasonic amplitude decline and flux decline behaviour. Furthermore, Fig. 3-11 also shows that the thickness of the fouling layer increased more rapidly at the axial velocity of 1.0 cm/s than at 4.2 cm/s. The thickness

of the fouling layer was 88 μm after 8 h of fouling at 1.0 cm/s, and after 16 h of fouling at 4.2 cm/s.

3.3.2. Cleaning experiments

Before commencing with the cleaning experiments, the feed solution was changed from effluent to pure water at 100 kPa and an axial velocity of 4.2 cm/s, in order to compare the cleaning efficiencies of the three methods mentioned. During the pure-water phase, although the relative amplitude continued to decrease because of changing the bulk solution from effluent to pure- water (see Fig. 3-13), an increase in permeate flux and a decrease in the fouling echo, in comparison with 18 h fouling echo, were observed (see Figs 3-12 and 3-14). This suggests that the UTDR technique is able to detect subtle changes in the cake layer on the membrane surface.

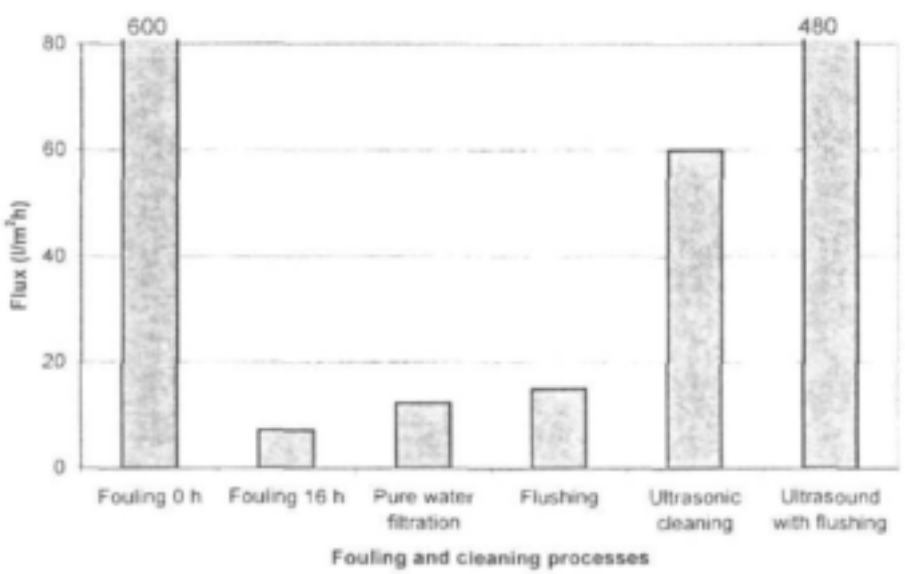

Fig. 3-12 Changes of permeate flux during fouling and cleaning processes (at 4.2 cm/s and 100 kPa): fouling 16 h; pure water; crossflushing; ultrasonic cleaning and ultrasound associated with crossflushing.

(start of fouling at 0h)

The next series of membrane cleaning experiments was intended to examine the suitability of the UTDR technique for fouling removal strategies and the ability of the UTDR technique to evaluate the efficiencies of the three cleaning methods under study, namely: ultrasound, crossflushing and ultrasound associated with crossflushing.

As mentioned earlier (Section 3.2.5), three different cleaning methods, each applied for 20 min, were used to treat the membrane fouled by effluent. The cleaning solution was pure water. The cleaned membrane was used to filter pure water after each cleaning process in order to capture the changes in ultrasonic signal responses on the membrane surface and the data of the permeate flux of the cleaned membrane. Figs. 3-12 and 3-13 show the results of fouling and these cleaning experiments in terms of the changes in permeate flux and relative amplitude, respectively. Fig. 3-14 shows the changes in fouling echo and recovery of ultrasonic signal response during fouling and cleaning processes.

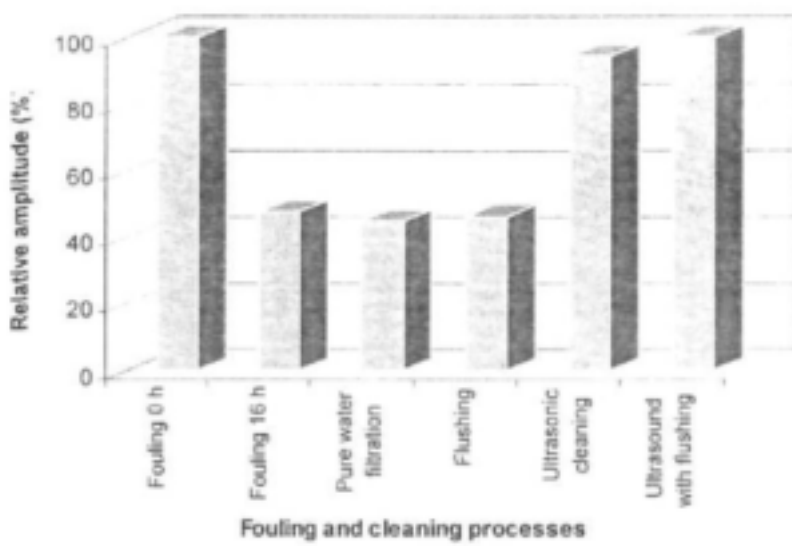

Fig. 3-13 Changes in relative amplitude during fouling and cleaning processes (at 4.2 cm/s and 100 kPa): fouling 16 h; pure water; crossflushing; ultrasonic cleaning and ultrasound associated with crossflushing.

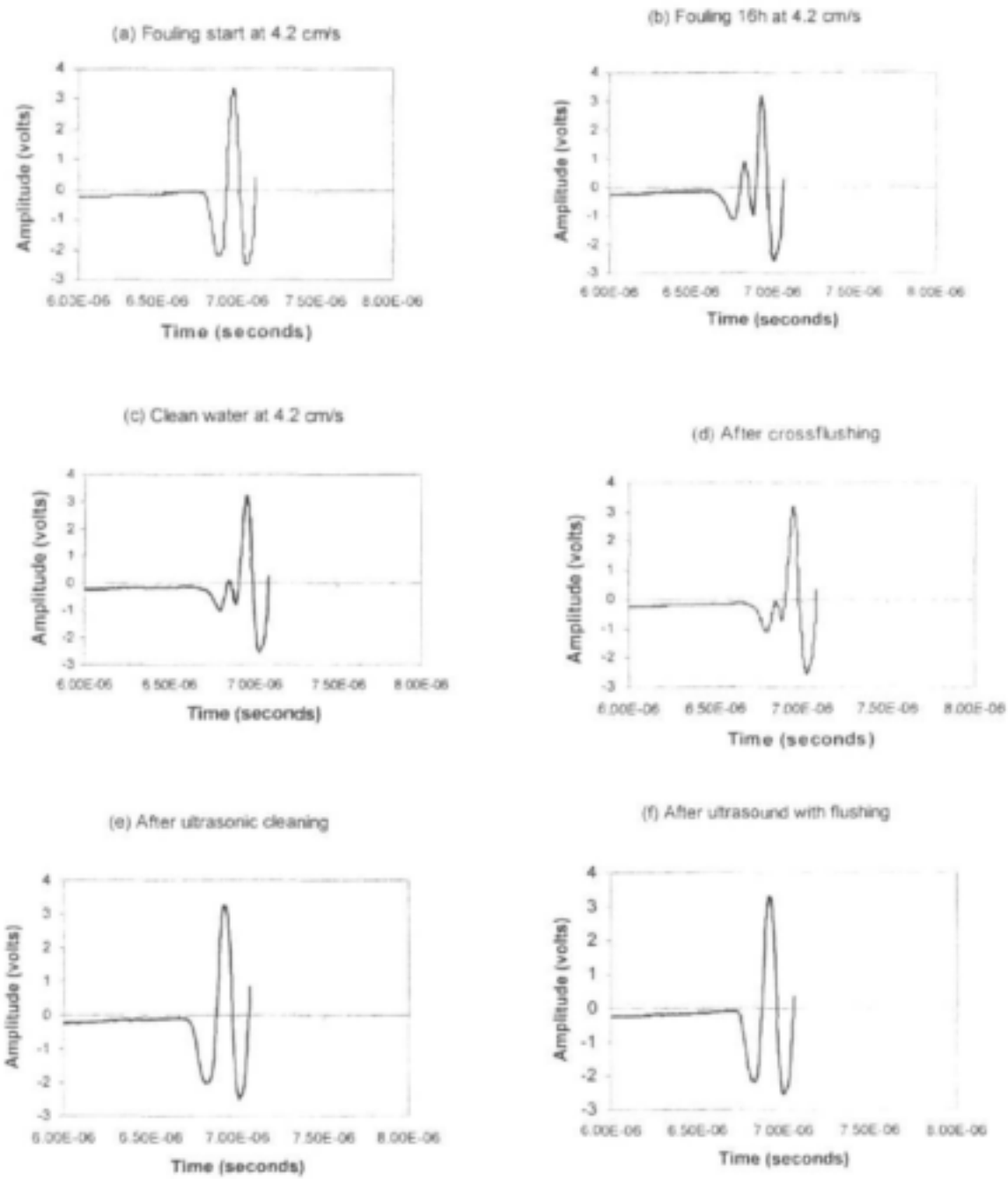

Fig. 3-14. Ultrasonic signal responses during the fouling and cleaning experiment at axial velocity of 4.2 cm/s and 100 kPa, at 0 (start) and 16 h fouling; pure water after 16 h fouling; after crossflushing; after ultrasonic cleaning; and ultrasound associated with crossflushing.

Crossflushing slightly increased the water permeate flux and relative amplitudes in Figs 3-12 and 3-13, respectively. This suggests that crossflushing can reduce the reversible fouling cake layer by reversing the pressure differential across the membrane. The cake layer deposited on the membrane is expected to become re-suspended and swept away by tangential- or cross-flow [Redkar and Davis, 1995]. Fig. 3-14 shows a change in the fouling echo after flushing. The peak of the fouling echo decreased because the density of fouling layer was reduced after flushing. Therefore, the UTDR technique is able to explore the presence and the removal of the cake layer in real-time. In addition, it was found that the paper effluent fouling on the nylon membrane is difficult to clean by flushing alone. SEM analysis revealed that there were still large particles present on the membrane surface after flushing (Fig. 3-15a). Hence, membrane fouling is caused by the adsorption of foulant both on and inside the membrane. Additional cleaning methods are needed.

Figs. 3-12 and 3-13 show that the water permeate flux and relative ultrasonic amplitude increased significantly after ultrasonic cleaning. This suggested that ultrasonic treatment could effectively disperse the fouling layer on the membrane because of the cavitation phenomenon and acoustic streaming [Zhu and Liu, 2000]. Collapse of the cavities formed acoustically has sufficient energy to remove the foulant from the membrane (Fig. 3-15b). The disappearance of the second echo indicated the removal of the fouling layer in Fig. 3-14. In Fig. 3-13 the relative amplitude after ultrasonic cleaning was about 90%, signifying that there was still some fouling on the membrane (Fig. 3-15). Furthermore, the permeate flux of 32.2 l $m^{-2}h^{-1}$ obtained after ultrasonic cleaning was still lower than 600 l $m^{-2}h^{-1}$, the original water flux. Hence, ultrasound associated with crossflushing was applied in an effort to remove the membrane fouling. Results in Fig. 3-12 show that the water permeate flux of 480 l $m^{-2}h^{-1}$, after ultrasound associated with flushing, was close to the original water flux. This method of ultrasound associated with flushing was able to enhance the permeate flux 40 times, but there was some fouling. The ultrasonic signal response is shown in Figs 3-13 and 3-14. 96% relative amplitude indicated that the fouled membrane was well cleaned by ultrasound associated with flushing. This is because ultrasonic cavitation results in hydraulic pressure impulses on the deposited fouling layer by impinging actions, similar to the water-hammer effect [Perusich and Alkire, 1991]. Acoustic streaming jets give rise to an enhanced convection and

mixing, in terms of a series of micro-vortices, near the membrane surface. The crossflushing produces a high tangential or cross-flow rate (40-50 cm/s) on fouling layers. Thus, ultrasound associated with flushing was the most effective of the cleaning methods; this method cleaned the fouled membranes almost completely.

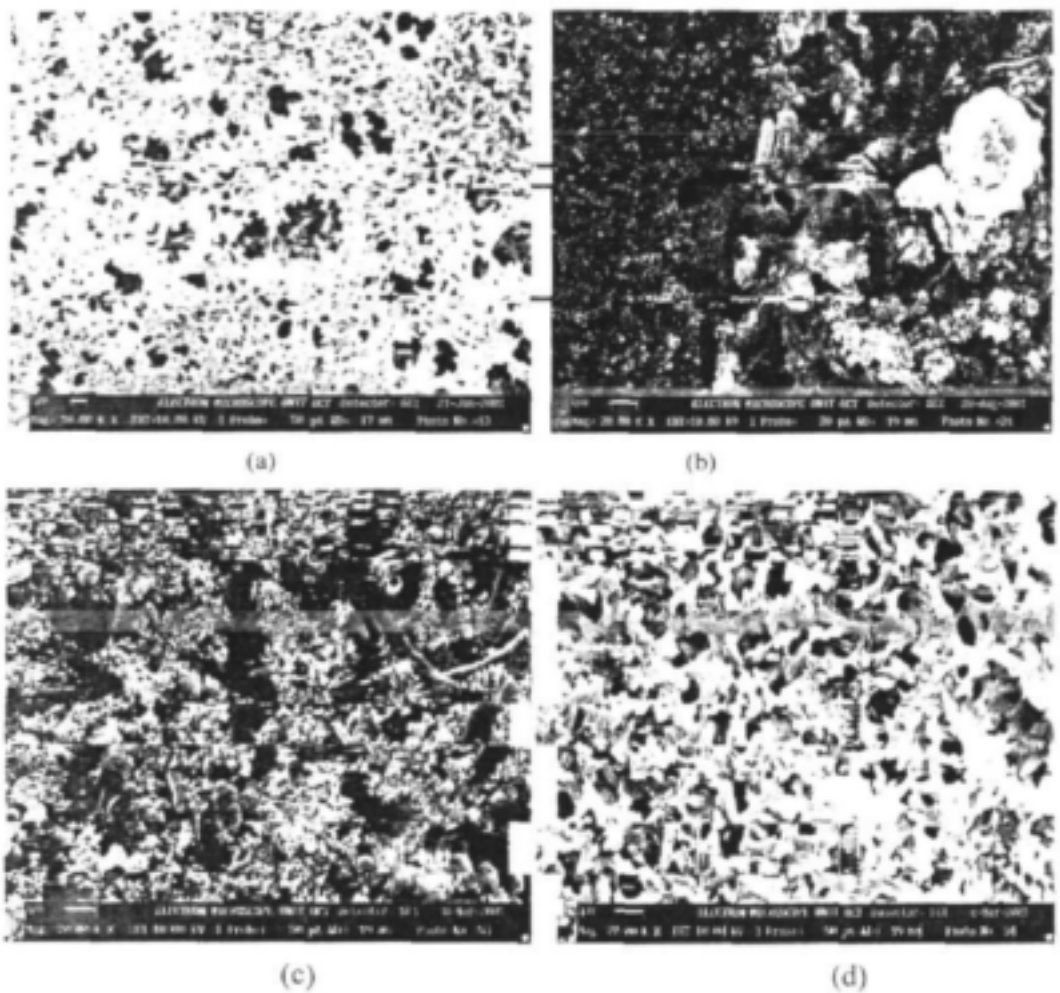

Fig. 3-15. Microscopic images: (a) clean nylon membrane; the cleaned Nylon *membrane surface, after cleaning by* (b) crossflushing; (c) ultrasonic cleaning; (d) ultrasound with crossflushing; magnification: X 20,000.

Morphological analysis of the cleaned membrane shown in Fig. 3-15c showed that the pore structure appeared again after ultrasound with crossflushing. These results demonstrate that the UTDR technique can monitor removal of the fouling layer and

membrane cleaning and that it is suitable to study the effectiveness of various cleaning techniques.

3.4. Summary

This section of research described the first application of the UTDR technique to the non-invasive, in-situ, continuous visualization of fouling and defouling in flat-sheet MF nylon membranes. Results show that the UTDR technique can effectively detect fouling-layer initiation and growth on, and its removal from, the membrane in real-time. The acoustic signal response has a good correspondence with flux-decline behavior.

The UTDR technique is also capable of detecting subtle changes such as the presence and/or absence of a cake layer on the membrane surface and distinguishing between two modes of growth at axial velocities of 1.0 and 4.2 cm/s. More specifically, the formation of a second echo in the time domain demonstrates that the UTDR technique can be used to quantify the thickness of a fouling layer on the membrane surface.

In cleaning experiments, results show that ultrasound associated with crossflushing is the most effective cleaning method, since this method cleaned the fouled membranes almost completely. It is better than either the flushing or ultrasonic cleaning (without flow) methods. This method is able to enhance the permeate flux 40 times. The fact that the UTDR technique monitors changes on the membrane surface makes it very suitable to study membrane cleaning and to determine the effectiveness of various cleaning techniques.

Results of SEM analyses of the fouled and cleaned membrane surfaces support UTDR visualisation results.

4. Ultrasonic measurement of organic fouling in UF

4.1. Introduction

Ultrafiltration (UF) is used for product recovery and pollution control in fields such as the food and dairy industries, pharmaceutical industry, textile industry, chemical industry, metallurgy, paper industry and leather industry [Lonsdale, 1982; Jonsson and Tragardh, 1990; Cheryan, 1998]. UF has become an increasingly important separation process, but membrane fouling is still a major problem in UF membrane separations.

Membrane fouling is a very complicated phenomenon due to the wide variety of foulants encountered in practice. Although fouling cannot be completely reduced, a significant amount of research has been conducted to understand the dynamics of the fouling process so that preventative methods can be developed. The development of a non-destructive technique to monitor the presence and growth of a fouling layer on a membrane surface in real time, under realistic operating conditions, is of great importance. A non-destructive technique cannot only characterize and distinguish the various phenomena underlying the flux decline, but can also aid in elucidating the exact mechanism and nature of fouling-layer growth. The development and utilization of a suitable non-destructive technique for the on-line monitoring of fouling in industrial and laboratory applications would enable the effectiveness of fouling remediation and cleaning strategies to be quantified.

It is known that ultrasonic measurement is extensively used in high-resolution flaw detection, thin material thickness gauging, medical research, and materials characterization to measure sound velocity and attenuation. The technique uses sound waves to measure the location of a moving or stationary interface and can provide information on the physical characteristics of the media through which the waves travel [Ensminger, 1998]. Recently, substantial progress has been made in application of UTDR to membrane and fouling research (see Section 3.2.3).

In this section, efforts to further understand the UTDR technique for the non-destructive investigation of fouling in a UF system, so as to further evaluate the capabilities of the UTDR technique and its applicability in different membrane separation systems, are described. Paper mill effluent from a wastewater treatment plant was again used as feed solution.. Results of this study showed some new findings. The UTDR technique can also be used to monitor organic fouling deposition and removal in ultrafiltration (UF), although the results of ultrasonic response signals obtained in this study with a UF system are more complicated than those obtained in MF [Section 3.3]. This is because of the asymmetric polysulfone (PS) membrane with polyester backing used in this UF system.

4.2. Experimental

4.2.1. UF system and UTDR measurement system

The effluent from a wastewater treatment plant of Mondi Kraft Mills, Mondi Ltd, South Africa was used as the feed solution. The wastewater treatment plant comprised the following processes: pretreatment, dissolved air flotation (DAF), MF and UF. Samples were taken from the MF product. The characteristics of the effluent are summarized in Table 4-1.

Flat-sheet polysulfone (PS)/polyester composite membranes with a molecular mass cut-off (MMCO) of about 35 kD (prepared by Ed Jacobs at the Polymer Institute, University of Stellenbosch) were used in all the fouling experiments. In order to monitor the onset and advancement of fouling on a membrane surface, a flatbed filter cell 200 mm long and 100 mm wide was designed and used in this study (Figs. 3-2 and 3-3). A PS membrane was placed between two Perspex plates.

A schematic representation of a UF experimental system and a UTDR measurement system used was shown in Fig. 3-1 (see Section 3.2.1). The UF system allows for the accurate control of inlet pressure, retentate flow rate and temperature. The ultrasonic measurement system consists of a 10 MHz ultrasonic transducer (Panametrics V111), a pulsar-receiver (Panametrics 5058PR) and a digital oscilloscope (HP Model 54602B). A

transducer that emits signals to and receives them from the various layers within the flatbed cell was externally mounted so as to be in contact with the top plate of the test cell. An oscilloscope connected to the pulsar-receiver captured and displayed the data as amplitude changes on its front panel. This data was stored on a computer's hard drive. Commercially available, food-grade salad oil was used to couple the transducer to the top plate surface.

Table 4-1

Characteristics of paper mill effluent (MF product)[a]

Items	Value	Items	Value
pH	5.33	Sulphate, SO_4, mg/l	1232
Conductivity, μS/cm	315	Fluoride, F, mg/l	0.2
Suspended solids (SS), mg/l	720	Silica as Si, mg/l	5.8
Total dissolved solids, mg/l	4545	Chloride, Cl, mg/l	103
Chemical oxygen demand	4090	Soap, oil & grease, mg/l	2.8
Biochemical oxygen demand	900	Potassium, K, mg/l	24
Aluminum as Al, mg/l	12.6	Iron as Fe, mg/l	3
Calcium, Ca, mg/l	122	Sodium, Na, mg/l	1270
Total Iron, Fe, mg/l	3.3	Magnesium, Mg, mg/l	16.2
Total dissolved iron, mg/l	3.3	Potassium as K, mg/l	30

[a]The data from Mondi Piet Retief, Mondi Ltd, South Africa.

4.2.2. Experimental procedure and fouling experiments

In each UF experiment, continuous stirring in the feed tank was provided for. The permeate flux was measured on a balance, connected to a PC. During the experiments both the retentate and permeate were recycled to the feed tank after flux measurements. Each experiment commenced with the circulation of pure water through the system at the desired flow rate and applied pressure, for 0.5 h, to compress the membrane and to build up a stable flow field. Once steady state was attained, the feed was switched to the

effluent solution to initiate the fouling phase during which concentration polarization and fouling occurred. This phase was allowed to continue until the ultrasonic response and permeate flux had stabilized.

Cross-flow filtration was investigated. The fouling experiment was carried out at a linear flow rate of 2.1 ± 0.02 cm/s (Re=532 ± 5.3), applied pressure 185 ± 5 kPa and temperature 20 ± 1°C. The total operating time for the fouling experiments was 20 h.

4.2.3. Cleaning experiments

Before commencing with the cleaning experiments, the feed solution was changed from effluent to pure water at 185 kPa and an axial velocity of 2.1 cm/s, in order to obtain the pure water flux (PWF) of a fouled membrane. The fouled membrane was cleaned by three methods, in turn, namely: forward flushing, ultrasonic cleaning and ultrasound together with forward flushing, for cleaning times of 20 min each. The feed solution was changed from effluent to water at the same operating conditions as used in the fouling phase in order to compare the cleaning efficiencies of these three methods. In Fig. 3-1, forward flushing was performed with valve V2 closed. Valve V1 was opened only after the transmembrane pressure differential over the membrane subsided and reached zero, under the pre-determined flushing velocity. The cross-flow filtration cell was immersed in a water bath at temperature 20±1°C during ultrasonic cleaning. The cell was irradiated with a horn ultrasonic cleaner (Medal W-375, Ultrasonics INC.) with a frequency of 20 kHz and a power of 375 w.

Ultrasound associated with forward flushing was performed with intermittent forward flushing, at linear flow rate of between 40 and 50 cm/s, during ultrasonic irradiation. To investigate the cleaning efficiency of each cleaning method, the cleaned membrane was used to filter pure water under the same operating condition as used during the fouling phase. The UTDR measuring system captured the changes in ultrasonic signal responses after each different cleaning method.

4.3. Experimental results

4.3.1. Hydrostatic pressure experiment

A hydrostatic pressure experiment with pure water was first carried out to investigate the resolution capabilities of the UTDR technique. The hydrostatic pressures ranged from 0 to 220 kPa. Fig. 4-1 shows ultrasonic response signals of a clean PS membrane at hydrostatic pressures of 0 and 160 kPa during the hydrostatic pressure experiment. Results of a typical hydrostatic pressure experiment are shown in Fig. 4-2.

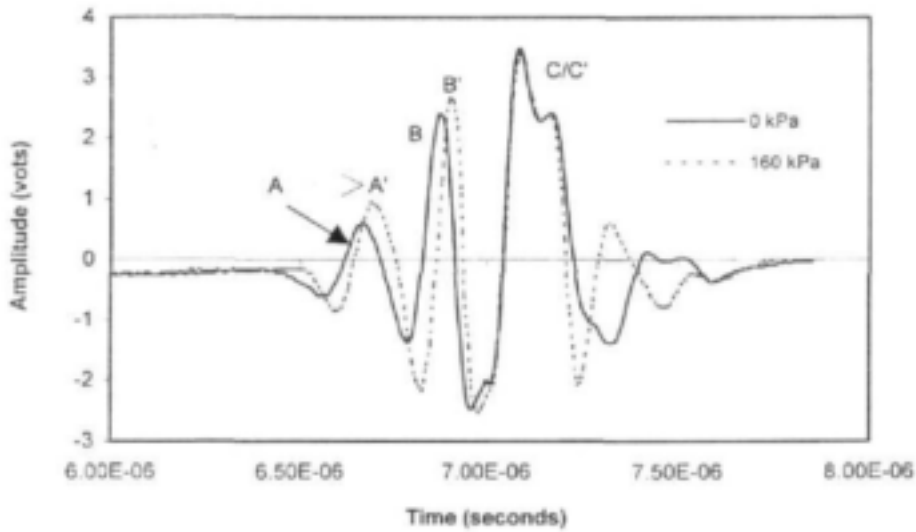

Fig. 4-1. Ultrasonic response signals of a composite PS membrane at hydrostatic pressures of 0 and 160 kPa during a hydrostatic pressure experiment with pure-water. (The primary reflections are identified as A, B, and C which correspond to: feed (water)/polysulfone (PS) layer, PS layer/polyester backing, and polyester backing/porous metallic support interfaces. The reflections A', B' and C' occurred at a hydrostatic pressure of 160 kPa.)

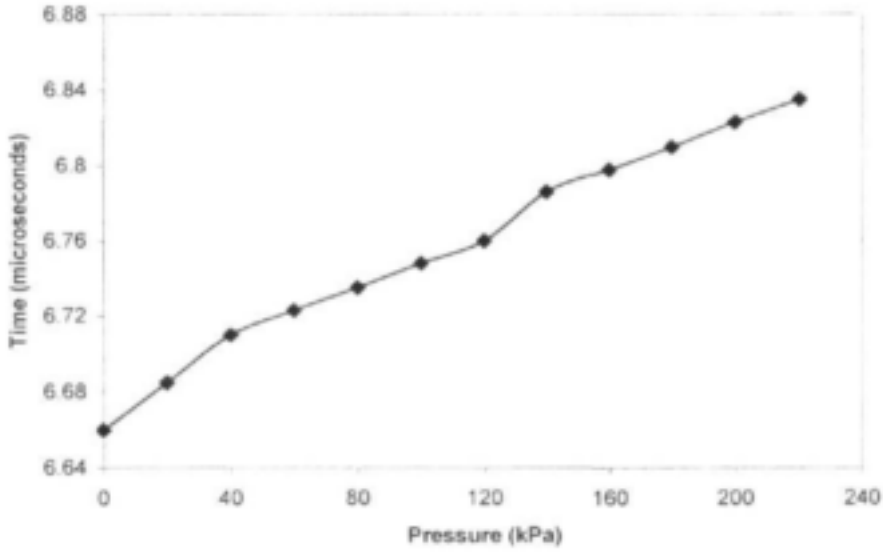

Fig. 4-2. Time delay of PS membrane echo signal versus hydrostatic pressure during pure-water filtration.

4.3.2. Fouling experiment

As has been mentioned, once steady state was attained after 0.5 h pure water filtration, the feed was switched to paper mill effluent to initiate the fouling experiment in which concentration polarization and fouling occurred. Crossflow fouling experiments were carried out a linear flow rate of 2.1 ± 0.02 cm/s (Re=532 ± 5.3), applied pressure 185 ± 5 kPa and temperature 20 ± 1°C. This phase was allowed to continue until the ultrasonic response and permeate-flux had stabilized. Fouling operation was stopped and restarted at 9 h. Fig. 4-3 shows permeate flux vs. operating time. Results of ultrasonic response signals after 0 (start), 2, 9, 9.5, 14 and 20 h of operation during the crossflow fouling experiment are shown in Fig. 4-4.

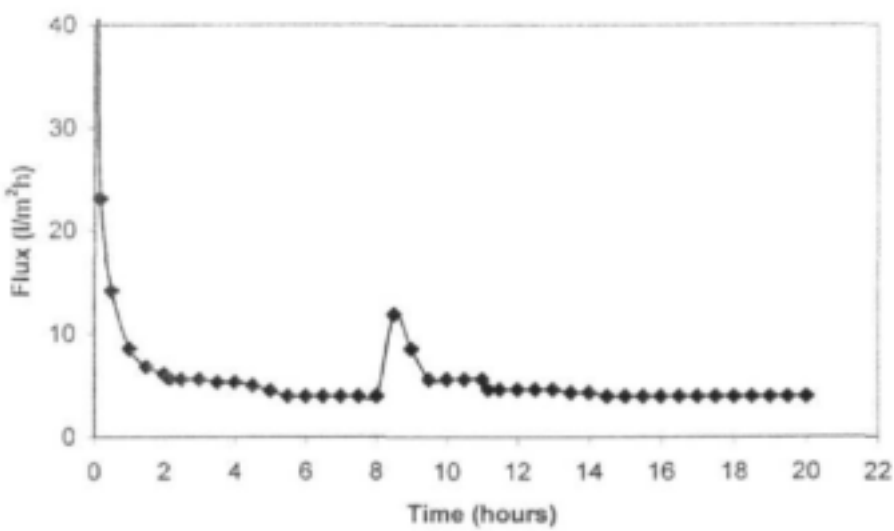

Fig. 4-3. Permeate-flux vs. time in paper mill effluent fouling experiment at flow rate 2.1 cm/s and pressure 185 kPa (stop and restart at 9 h of operation).

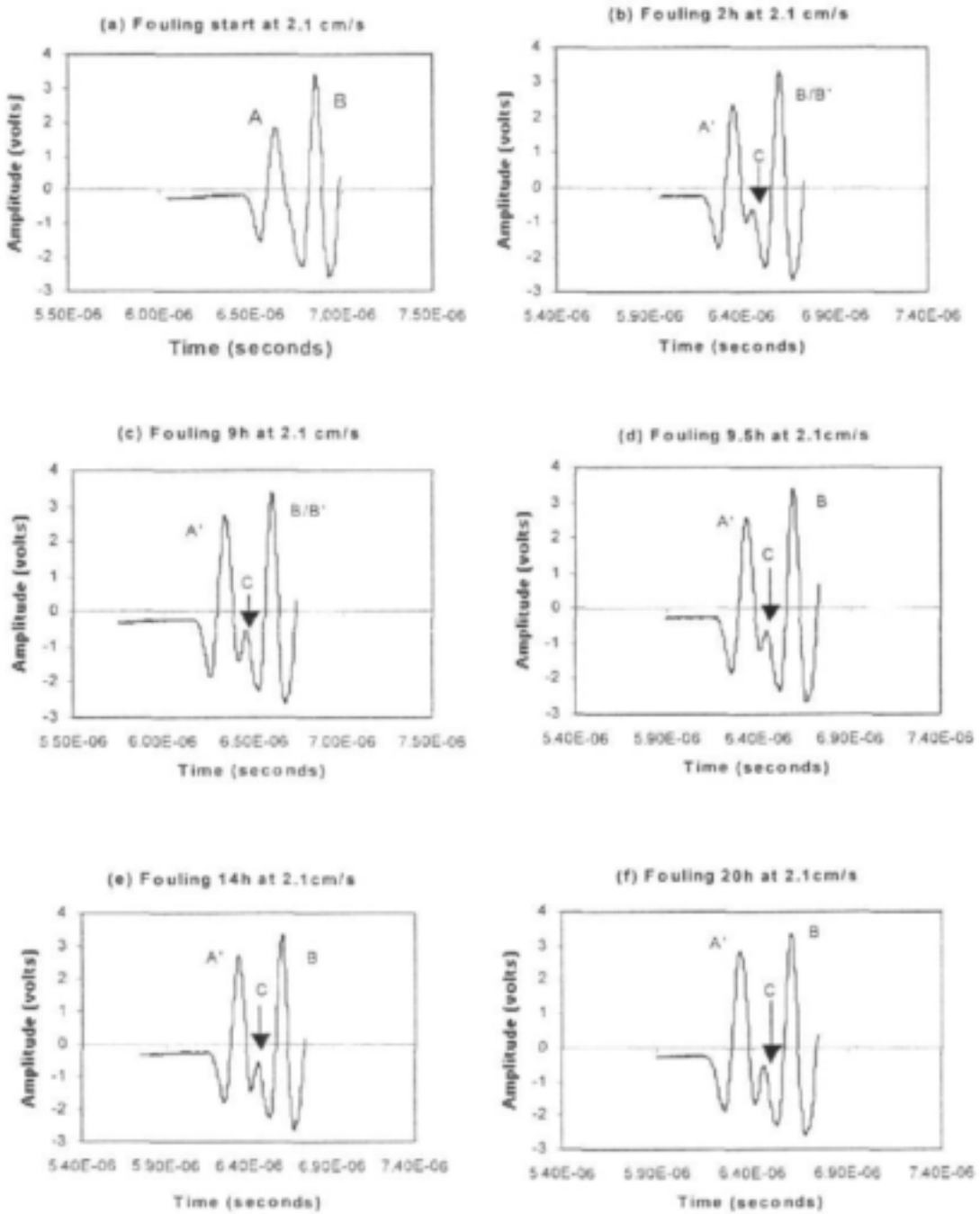

Fig. 4-4. Ultrasonic signal responses after (a) 0 (start), (b) 2 h, (c) 9 h, (d) 9.5 h, (e) 14 h and (f) 20 h of operation in the fouling experiment (185 kPa, 2.1 cm/s) carried out with paper mill effluent. The reflection signals A, B, C and A' are generated from feed (water)/PS (PS_1/PS_2) layer, PS layer/PE backing, PS_2 layer/PE backing and feed/fouling layer (combined PS_1) interfaces. Stop and restart at 9 h of operation.

4.3.3. Cleaning experiments

The next series of membrane cleaning experiments was intended to examine the suitability of the UTDR technique to defoul the membrane and the ability of the UTDR technique to evaluate the efficiencies of the three cleaning methods (forward flushing, ultrasonic cleaning, and ultrasound together with forward flushing, respectively, for cleaning times of 20 min each). The cleaned membrane was used to filter pure water after each cleaning process in order to capture the changes in ultrasonic signal responses on the membrane surface and the data of the pure water flux of the cleaned membrane. Pure water flux recovery of the cleaned membrane obtained by different cleaning methods is shown in Fig. 4-5. Fig. 4-6 shows the results of ultrasonic response signals during the cleaning experiments.

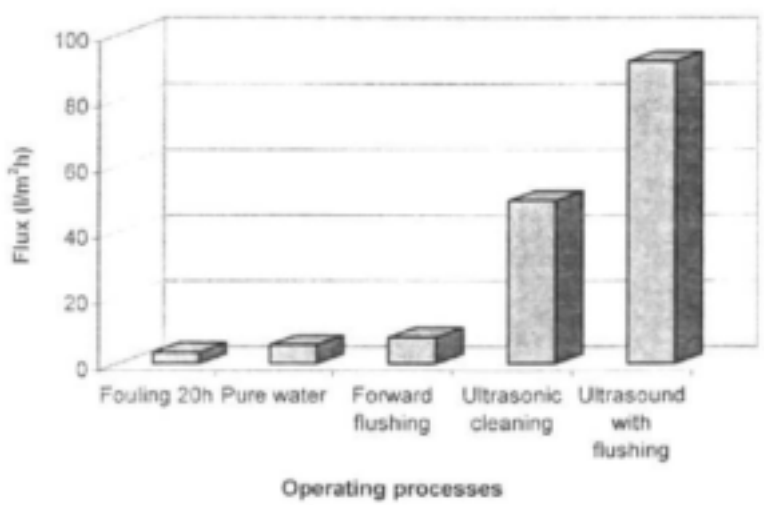

Fig. 4-5. Changes of permeate flux during fouling and cleaning processes (at 2.1 cm/s and 185 kPa): fouling 20 h; pure water; forward flushing; ultrasonic cleaning and ultrasound associated with forward flushing.

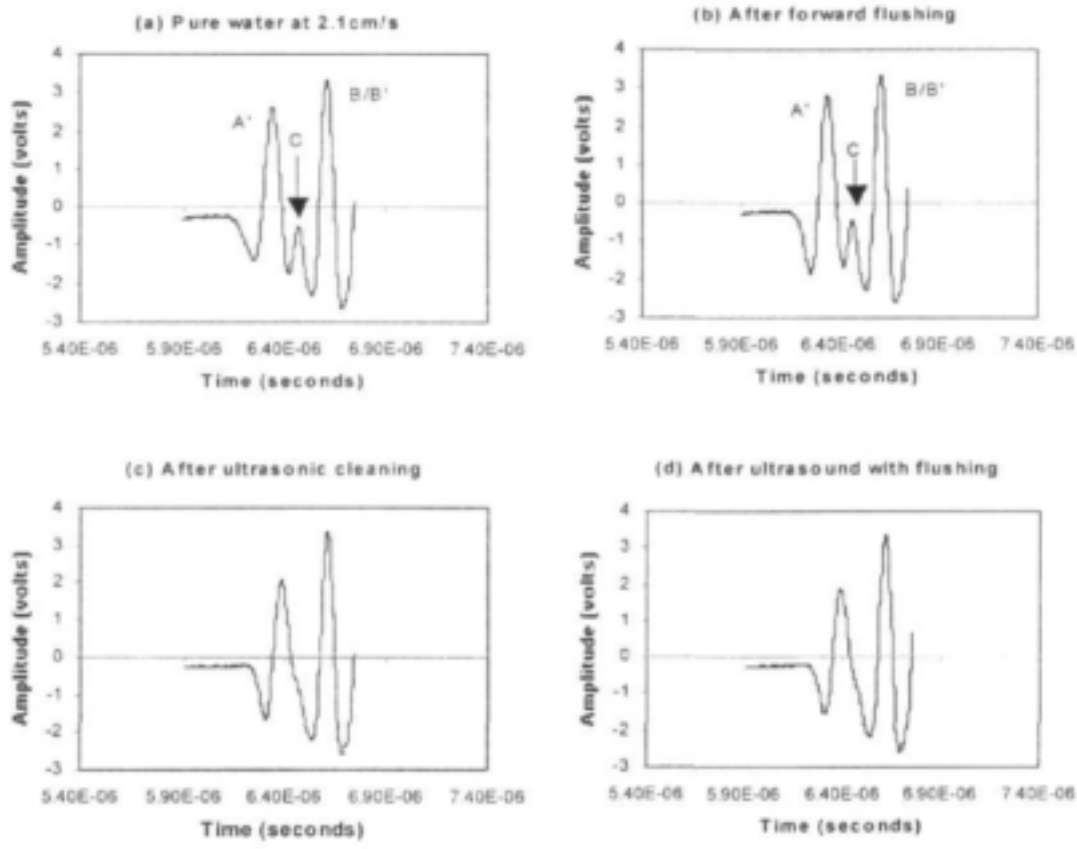

Fig. 4-6. Ultrasonic signal responses after (a) pure water filtration after 20 hours of operation in fouling experiment; (b) forward flushing; (c) ultrasonic cleaning; (d) ultrasound with forward flushing. The reflection signals A', B and C are generated from feed (pure water)/fouling layer (combined PS_1), PS_2 layer/polyester backing and a dense PS_1 layer/a porous PS_2 layer interfaces.

4.4. Interpretation of results

4.4.1. Hydrostatic pressure experiments

As shown in Fig. 4-1, ultrasonic response signals during the hydrostatic pressure experiment revealed a polysulfone (PS) composite membrane that is composed of two PS layers and a polyester backing layer. The reflected signals A, B and C were generated from the feed solution (water)/PS surface, PS layer/ polyester backing layer and polyester backing layer/metallic porous support interfaces. As the hydrostatic pressure increased, the membrane moved farther from the transducer, as shown in Fig. 4-1. The membrane echo signals A and B shifted into signals A' and B' when the hydrostatic pressure increased from 0 to 160 kPa. Fig. 4-1 also shows that sharper reflection signals A' and B' occurred under a hydrostatic pressure of 160 kPa. This indicates that the PS membrane was compacting, causing changes in acoustic impedance under a higher hydrostatic pressure. These phenomena, especially membrane densification, will be further investigated in a future project.

Results of a typical hydrostatic pressure experiment (Fig. 4-2) show that a near linear relationship exists between the hydrostatic pressure and the delay time of the membrane signal (signal A to A' as reference signal). This corresponds to a change in spacing between the top plate and the membrane. The space between the top plate and the membrane widens as the hydrostatic pressure increases, and the delay time of membrane signal is increased. Results of the hydrostatic pressure experiments proved that the resolution of the system was sensitive enough to detect the presence of a fouling layer.

4.4.2. Fouling experiments

As shown in Fig. 4-3, at the beginning of fouling a rapid decline in the flux was observed, followed by a more gradual decline after 2 h of operation. The flux decline resulted primarily from slow growth of the fouling layer on the membrane surface. Consistent with this observation, the corresponding ultrasonic signal responses exhibited rapid amplitude changes as fouling proceeded (Fig. 4-4). Fig. 4-4 shows an increase in

amplitude of echo signal A' as fouling proceeds. A new signal C between signals A and B appeared after 2 h of operation (Fig. 4-4 (b)) and gradually grew as fouling proceeded (Fig. 4-4 (c-f)). These results differed completely from those achieved in earlier research carried out by Mairal [Mairal and Greenberg et al., 1999 and 2000] – no fouling signal was obtained - because of different separation systems. In our study we got an echo of the fouling layer, and growth and movement of the signal.

In order to gain more insight into the process of ultrasonic testing of membranes and membrane fouling, and to better understand the processes related to the deposition of fouling layers, a predictive mathematical modeling program - Ultrasonic Reflections, was developed under the new project [Li, Sanderson and Hallbauer, 2002].

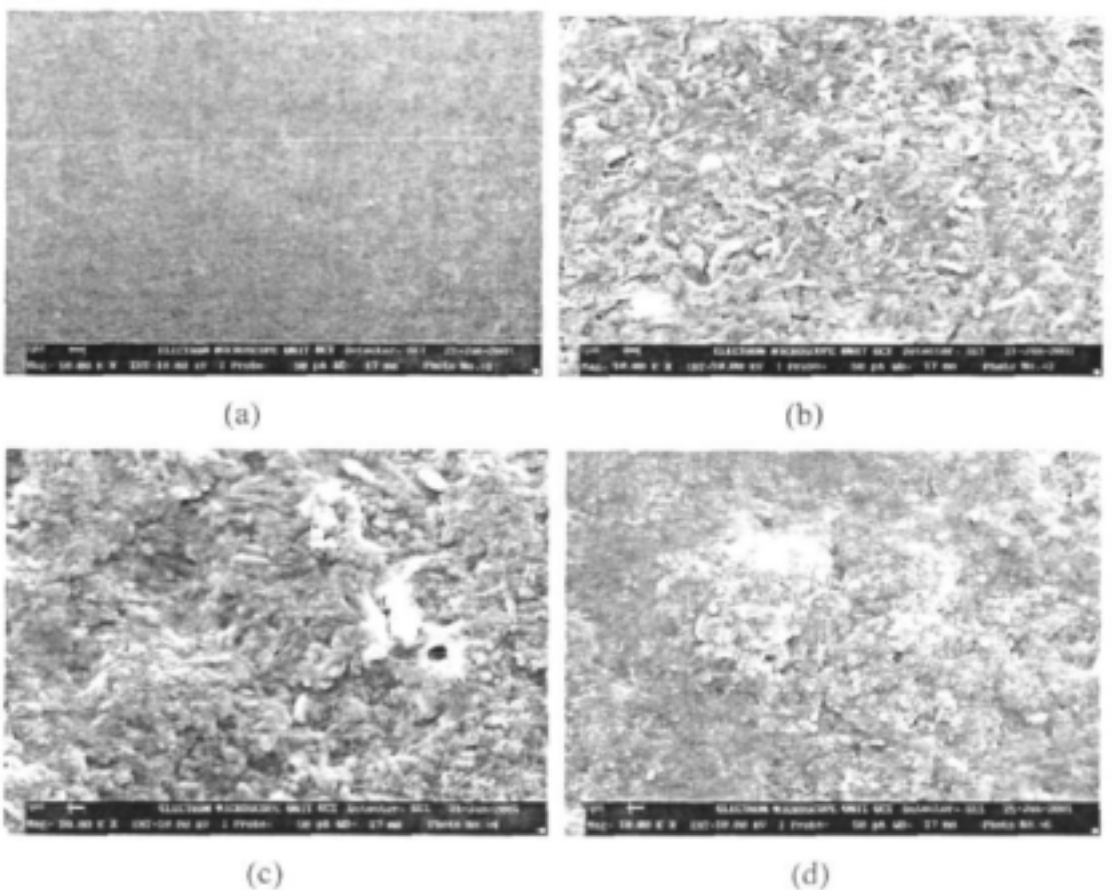

Fig. 4-7. Microscopic images of (a) a clean membrane and a fouled PS membrane by paper mill effluent after fouling times of (b) 0.5 h, (c) 2 h and (d) 20 h; magnification: X 20,000.

In order to study membrane coverage, two experiments were carried out under exactly the same fouling conditions, and stopped after specific times. Membrane samples were taken for SEM analysis after 0.5, 2 and 20 hours of operation. Results are shown in Fig. 4-7. Morphological characterization of the fouled membrane revealed complete membrane coverage with the fouling layers after 0.5 (Fig. 4-7 b) and 2 hours (Fig. 4-7 c) of fouling operation. There were more and denser fouling layers on the membrane surface after 20 hours of fouling operation (Fig. 4-7 (d)). This suggests that the sharper echo peak was reflected from the fouled membrane surface with a denser fouling layer (Fig. 4-4 (f)). This indicates that morphological observations of membrane coverage are in agreement with non-invasive, in situ, ultrasonic measurements.

Another basic quantity measured in non-destructive ultrasonic testing is the time of flight or the amount of time taken for the sound to travel through the sample. In other words, the UTDR technique can quantify the thickness of a fouling layer (on a membrane surface) by comparing time-domain signals as shown in Fig. 4-4. The thickness of a fouling layer on a membrane surface can be calculated by Equation (3-1) (the sound velocity in the fouling layer is 1550 m/s, estimated according to modelling).

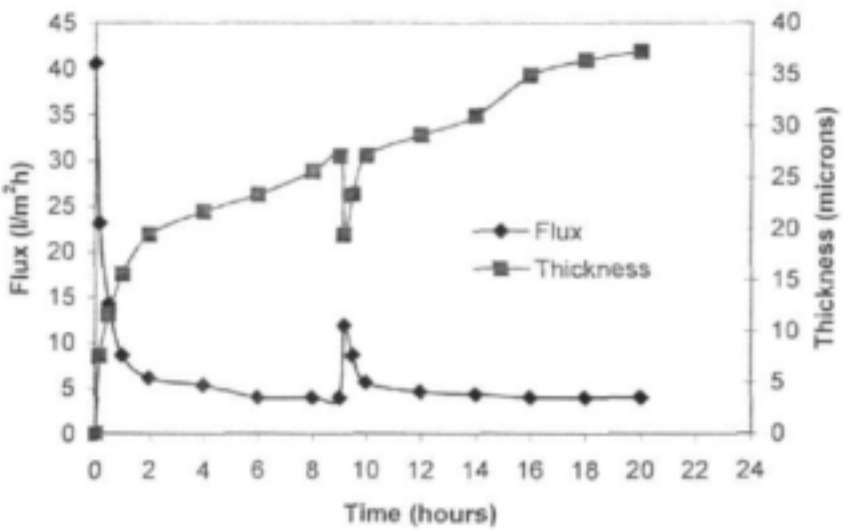

Fig. 4-8. Thickness of fouling layer vs. operation time during fouling experiment by paper mill effluent at axial velocity of 2.1 cm/s and operating pressure 185 kPa.

Fig. 4-8 illustrates changes in thickness of a fouling layer during fouling operation at an axial velocity of 12.5 cm/s. The thickness of the fouling layer increased rapidly at the beginning of fouling because of concentration polarization and fouling layer formation, followed by a slow increase due to gradual growth of the fouling layer. The thickness of the fouling layer after 2 and 20 h of fouling operation was 19.4 and 37.2 μm.

Something particularly interesting is seen to occur at 9 h in Fig. 4-8. At this point there was a significant decline in the thickness of the fouling layer, followed by an increase in thickness. These changes in thickness coincided with a stop and restart of the fouling operation (at 9 h). Interrupting the fouling experiment resulted in flow destabilization and relaxation of the fouling layer. Changes in flow and shear rates upon re-commencement of the fouling experiment resulted in a decrease in the fouling layer thickness or partial dissolution of the fouling layer and reduction of its density. These factors resulted in a rapid decline in the thickness as the fouling layer conformation on the membrane surface was altered. The changes in ultrasonic signals can also be observed by comparing Fig. 4-4 (c) and (d). Indeed, the flux increase observed in Fig. 4-3 corresponded to the substantial amplitude change. The results obtained from this study suggest that the combination of flux determination and UTDR measurements can provide a much clearer view of the fouling behavior of a membrane than flux decline alone can.

4.4.3. Interpretation of cleaning experiments

Before commencing with the cleaning experiments, the feed solution was changed from effluent to pure water at 185 kPa and an axial velocity of 2.1 cm/s, in order to determine pure water flux of the fouled membrane. This was used to compare the cleaning efficiencies of the three methods. Figs. 4-5 and 4-6 show the results of fouling and the cleaning processes in terms of the changes in permeate flux and ultrasonic response amplitudes.

An increase in permeate flux (Fig. 4-5) and a decrease in the amplitude of the ultrasonic response signal of a fouling layer, in comparison to a 20 h fouling echo signal in Fig. 4-4 (f) and to a fouling echo signal in pure water (Fig. 4-6 (a)), were observed because of the switch-over from effluent to pure water during the pure water phase. This change resulted in the reduction of concentration polarization on the membrane surface. This suggests that subtle changes on the membrane surface can be detected by the UTDR technique.

Flushing slightly increased the pure water flux (Fig. 4-5). This suggests that forward flushing can reduce membrane fouling. The deposited fouling layer on the membrane surface is expected to become re-suspended and swept away by tangential- or cross-flow [Redkar and Davis, 1995]. The peak of the fouling echo signal decreased because the density of the fouling layer was reduced after forward flushing (Fig. 4-6). Therefore, the UTDR technique is able to explore the presence and the removal of the fouling layer in real-time. In addition, it was found that the paper effluent fouling on the PS membrane was difficult to clean using only forward flushing. SEM analysis revealed that there was still a dense fouling layer on the membrane surface after forward flushing, although many pores produced by forward flushing appeared on the fouling layer (Fig. 4-10a). Hence, membrane fouling is caused by the adsorption of foulant both on and inside the membrane. Membrane fouling was only partially irreversible and additional cleaning methods were needed.

Fig. 4-5 shows that the pure water flux increased from 7.92 l/m^{2}h after forward flushing to 49.5 l/m^{2}h after ultrasonic cleaning. There was a significant decrease in the ultrasonic amplitude of the differential signal, from 3.0 V after forward flushing to 0.125 V after ultrasonic irradiation (Fig. 4-9). This suggests that ultrasonic treatment can effectively disrupt the fouling layer on the membrane because of the cavitation phenomenon and acoustic steaming [Mason and Lorimer, 1988]. The disappearance of the echo signal C indicated that the fouling layer was removed by ultrasonic irradiation (Fig. 4-6). However, Figs. 4-13 (c) and 4-14 show that the signal amplitude after ultrasonic cleaning is 0.125 volts, signifying that there is still some fouling on the membrane (Fig. 4-10 b). Furthermore, the permeate flux of 49.5 l/m^{2}h obtained after ultrasonic cleaning was still

lower than 190 l/m^{2}h, the original pure water flux. Hence, ultrasound associated with forward flushing was applied in an effort to clean the membrane. The pure water flux of the membrane cleaned by ultrasound associated with flushing increased to 92 l/m^{2}h (Fig. 4-5). Although it is still lower that the original pure water flux, the ultrasonic signal response in Fig 4-6 shows that the differential signal disappeared after ultrasound with forward flushing. It indicated that the fouled membrane was largely cleaned by ultrasound associated with flushing. Morphological analysis of the cleaned membrane showed that there was no fouling layer was present on the membrane surface (Fig. 4-10 c). This is because the forward flushing produces a high tangential or cross-flow rate (40-50 cm/s) on fouling layers. Thus, ultrasound associated with flushing was the most effective of the cleaning methods. These results demonstrate that the UTDR technique can monitor the removal of the fouling layer. It is suitable to study the effectiveness of various cleaning techniques.

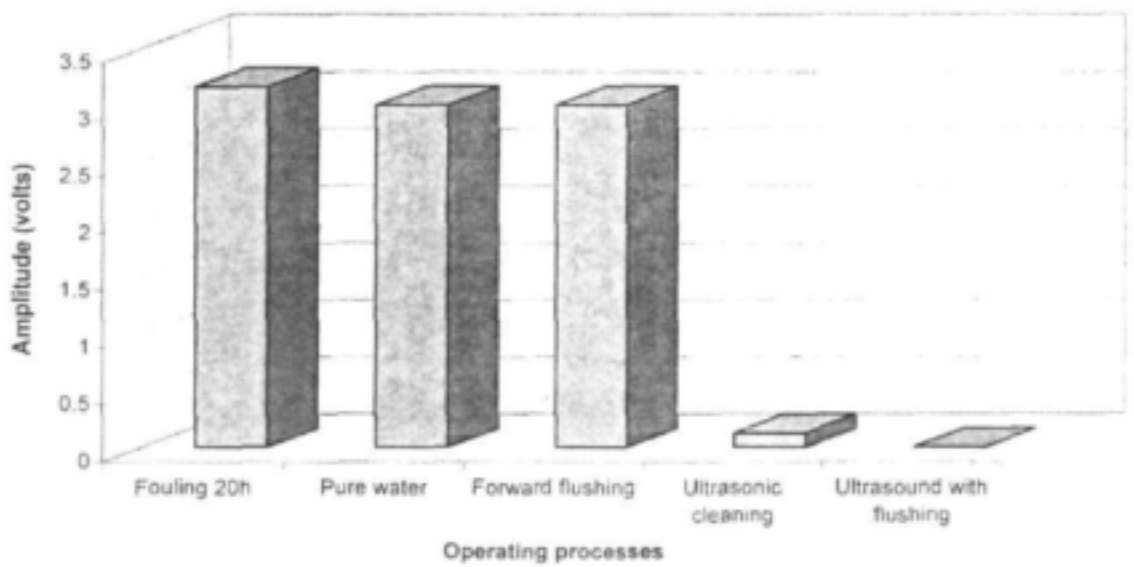

Fig. 4-9. Changes in ultrasonic signal amplitude during fouling and cleaning processes: fouling 20 h, pure water, forward flushing, ultrasonic cleaning and ultrasound with forward flushing.

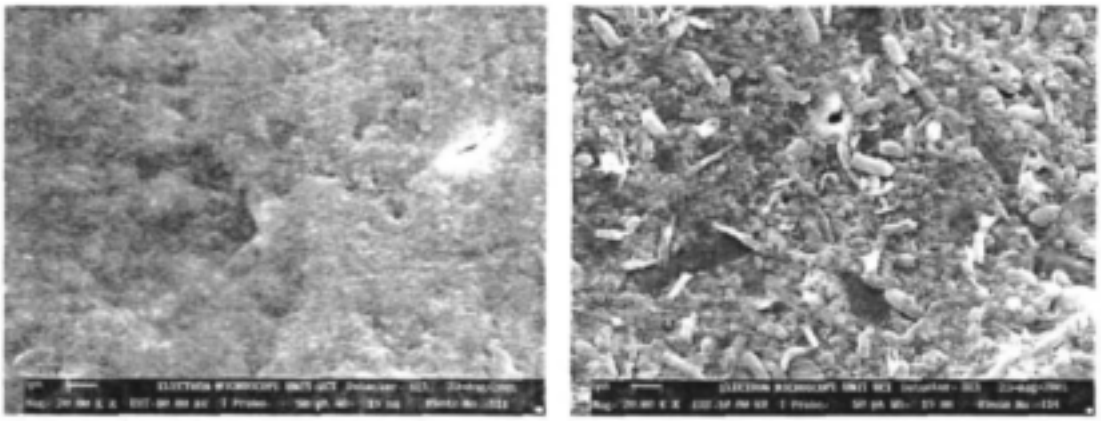

(a) (b)

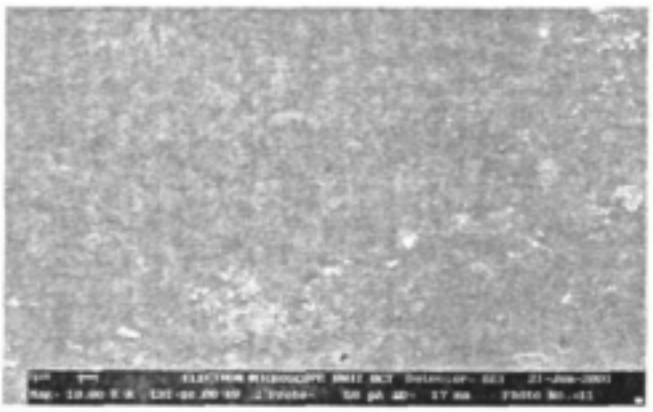

(c)

Fig. 4-10. Microscopic images of the cleaned PS membrane surface: after cleaning by (a) forward flushing; (b) ultrasonic cleaning; (c) ultrasound with forward flushing; magnification: 20,000.

In b), foulant is loosened but not removed.

In c), the loosened bits of foulant are removed.

4.5 Summary

Results of the hydrostatic pressure experiments prove that the ultrasonic measurement system is sensitive enough to detect membrane compaction and movement in the time domain with hydrostatic pressure.

The ultrasonic UTDR technique can effectively detect fouling-layer initiation and growth on, and its removal from, a UF membrane in real-time. The structure of an asymmetric composite PS membrane was detected by UTDR.

The UTDR technique is also capable of detecting subtle changes in cake layer formation on the membrane surface, and the stop and recommencement of ultrafiltration.

The formation of a second (fouling layer) echo signal in the time domain demonstrated that the UTDR technique can be used to quantify the thickness of a fouling layer on the membrane surface.

In cleaning experiments, results show that ultrasound associated with forward flushing is an effective cleaning method. The fact that the UTDR technique monitors changes on a membrane surface makes it very suitable to study membrane cleaning and determine the effectiveness of various cleaning techniques.

Results of the outcome of UTDR are in good agreement with SEM and flux analyses.

5 Ultrasonic measurement of inorganic fouling in RO

5.1. Introduction

One of the main difficulties encountered in desalination by reverse osmosis (RO) is the decline in permeate flux with time. It is known that the general cause for this flux decline is membrane fouling. In the treatment of saline waters by RO, sparingly soluble salts such as calcium sulphate ($CaSO_4$) can be deposited on a membrane when its concentration builds up beyond its solubility limit in the concentration polarisation layer. This precipitation leads to a serious decline in the permeate flux. There is considerable practical interest in understanding the mechanism by which precipitation causes flux decline.

A significant amount of research has been conducted to better understand the dynamics of the fouling process in RO membranes so that preventative steps can be developed [Belfort et al., 1979; Matthiasson et al., 1980; Brunelle, 1980; Potts et al., 1981]. In the literature, several models describe membrane fouling caused by salt deposition or colloidal coagulation [Fane, 1986; Fountoukidis et al., 1989; Logan et al., 1985; Gilron and Hasson, 1987; Borden et al., 1987; Vilker et al., 1981]. Fane [1986] claimed the permeate production rate to be related to the amount of free membrane area in heterogeneous UF membranes. This model predicts that there will be a linear relation between the fractional flux decline and the nominal surface density of the deposit. This model assumed a deposit structure consisting of n cylindrical growth sites per unit area, of constant height, density and growing radius.

Gilron and Hasson [1987] further studied calcium sulphate fouling of RO membranes and developed a new model – the surface blockage model. They proposed that flux decline is due to blockage of the membrane surface by lateral growth of the deposit rather than the hydraulic resistance of a cake building up at the membrane surface. This model predicts that there is a relatively open deposit structure, with large areas of the membrane being free of deposit. As more salt precipitates on the membrane surface, the deposit grows out laterally to cover a larger area of the membrane. In this case, the deposit can be seen at as having a constant thickness but a differential porosity.

Although progress has been made in the understanding and modelling of fouling phenomena, these models are based on an assumption that the calcium salts form crystals on the membrane surface when supersaturation occurs in the concentration polarisation layer. Little has been reported in the literature describing an in-situ technique or method to visualize the actual state of inorganic deposition on the RO membranes. Although numerous non-invasive scientific tools and techniques, such as an optical shadowgraph technique, a radio-isotope technique, a video camera, a high-speed camera, a laser triangulometer and micro-video photography have been used in the study of membrane fouling [Mackley and Sherman, 1992; Wakeman, 1994; Altmann and Ripperger, 1997; Li et al, 1998; Kools et al., 1998], these techniques have been used to investigate cake growth and layer formation during microfiltratoin (MF) (particle size > 3 μm). Further, use of an optical probe requires an optical window. Use of this procedure in commercial, high-pressure membrane modules is not practical. Optical probes only provide information on the outermost part of the fouling layer.

Recently, substantial progress has been made in the application of ultrasonic testing to membranes and fouling research [Peterson et al., 1998; Reinsch et al., 2000; Bond et al, 2000; Mairal et al., 1999 and 2000; Koen, 2000; Li et al., 2002]. Specifically, Mairal et al. [1999 and 2000] employed non-invasive ultrasonic time-domain reflectometry (UTDR) for the real-time characterisation of calcium sulphate fouling on RO membranes. Using six ultrasonic transducers and a high performance pulsar-receiver, they were able to monitor the membrane compaction and fouling in real time and gain insight into the dynamics of fouling growth. The results show good correspondence between the decline in the ultrasonic signal amplitude and the development of a fouling layer [Mairal and Greenberg et al., 2000]. One advantage of UTDR is that it does not require optical windows.

In this section the use of UTDR to investigate calcium carbonate deposition and removal in flat-sheet RO membrane modules will be described. Results show that an echo of a fouling layer appeared and grew on the membrane surface as fouling proceeded. Furthermore, UTDR was also successfully employed to monitor membrane cleaning. Flux measurements and SEM analyses corroborated the UTDR

results. Overall, the results confirmed the effectiveness of the UTDR technique to visualize particle deposition on and removal from membrane surfaces.

5.2. Experimental

5.2.1. Desalination system and experimental design

The selection of an appropriate membrane separation system involves the choice of a separation process, a feed solution containing one or more potential foulants, a membrane, a separation module and an associated flow system.

Fig. 5-1 is a schematic representation of the RO desalination system and UTDR measuring system. The assembly consisted of: a 40-liter feed tank for storage and supply of the fouling solution, a high-pressure positive displacement pump for pressurisation of the feed solution, a rectangular test cell (240 mm length and 100mm width), a cooling system on the feed tank, analogue pressure gauges and valves, and a by-pass line parallel to the test cell. The by-pass line is necessary to vary both the flow rate and the pressure inside the cell, separately. Pressure was controlled by means of the back-pressure valve on the outlet line of the cell. The cross-flow membrane system had one feed stream entering the system, one concentrate stream (brine) and one permeate stream (purified water) leaving the system. These three streams were circulated back to the feed tank in the experimental set-up. Feed flow to the cell was measured with a flow meter and manually controlled with a valve. Permeate was measured manually with a stopwatch and volumetric flask.

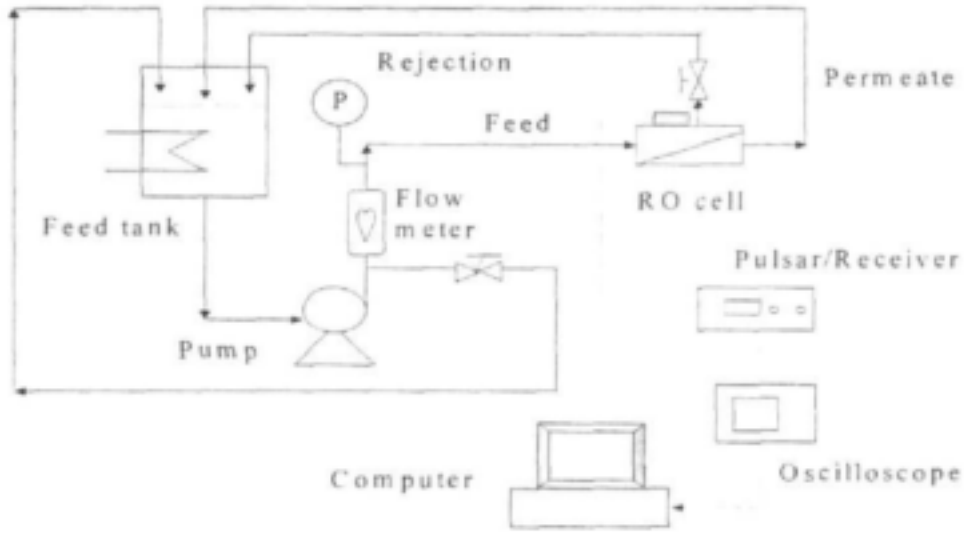

Fig. 5-1. RO experimental set-up and UTDR measurement system.

Hydranautics ESPA3 polyamide membranes were used in all of the fouling experiments. Membranes were cut from manufacturer-supplied long rolls, 1 m wide and several meters long. All experiments were carried out in 2 - 2.5 MPa operating pressure range, with flow rates varying between 0 and 100 ml/min. Feed concentrations varied between 0.5 and 2 g/l, while the temperature was controlled at 25 ± 1 °C.

The ultrasonic measurement system consisted of a 7.5 MHz ultrasonic transducer (Panametrics V111), a pulsar-receiver (Panametrics 5058PR) and a 150 MHz digital oscilloscope (HP Model 54602B) with sweep speeds from 5s/div to 2ns/div and 1mv/div sensitivity. The wave record in this study was half of wave record (1/2 sinus waveform/signal). Commercially available, food-grade honey was used to couple the transducer to the top plate surface.

5.2.2. Fouling experiments

The fouling experiments were carried out using a 2 g/l calcium carbonate solution (pH = 8.40). Cross-flow as well as dead-end modes of operation were investigated. All cross-flow experiments were carried out in the laminar flow region with axial velocities between 0 and 1.1 cm/s. Each experiment consisted of three phases. First,

the membrane was soaked in pure water for at least 24 h prior to the start of the experiment. Then the membrane was placed inside the cell and exposed to clean water at the desired operating conditions of the experiment. Once steady state with respect to the permeate flux and the ultrasonic signal was achieved, the feed was switched to the fouling solution to initiate the third phase, in which changes in the measured variables occurred due to concentration polarisation and fouling. The pure-water phase ensured that the processes such as membrane compaction and adsorption of trace organic ions on the membrane surface stabilised before initiation of the fouling phase, thereby facilitating an unambiguous interpretation of UTDR and flux behaviour. The experiments were allowed to continue until the ultrasonic response and permeate flux had stabilised. The test cell was then opened and the fouled membrane samples were collected for morphological analyses.

5.2.3. Cleaning experiments

The potential ability of the UTDR technique to detect the presence of a fouling layer may also make it suitable to monitor the removal of a fouling layer. Cleaning experiments were therefore carried out to demonstrate the potential of the UTDR technique for such an application. The membranes were first fouled to steady-state levels, as described in the previous section, after which clean water was introduced to clean the membranes. Experiments were carried out at the same operating pressures as those used during the fouling phase. At the end of the cleaning experiments, membrane samples were removed for morphological characterisation.

5.2.4. Morphological characterisation of the fouling layer

The purpose of the morphological study of the fouled membrane samples using scanning electron microscopy (SEM) was deemed necessary in order to establish a correlation between the measurement of UTDR and the presence of a fouling layer. The samples were analysed in a Topcon ABT50 SEM machine. The operating conditions were: accelerating voltage 25 kV, working distance 8 mm and stage tilt angle 0°.

The samples were prepared in two stages. First, a piece of membrane was removed from underneath the transducer scanning area. The sample was then analysed under

an optical microscope for general features and trends, and a representative area was identified for SEM analysis.

5.3. Results and discussion

5.3.1. Crossflow experiments

As has been mentioned, once steady state was attained after pure-water filtration, the feed was switched to a 2 g/l calcium carbonate ($CaCO_3$) solution, to initiate the fouling experiment. Cross-flow fouling experiments were carried out at 2.2 MPa and a crossflow velocity of.1 cm/s. The permeate flux of a 7 h fouling experiment is summarised in Fig. 5-2.

Permeate flux declines as fouling proceeds (Fig. 5-2). The flux decline results primarily from concentration polarisation and the slow growth of the fouling layer. Consistent with this observation, the corresponding ultrasonic signal responses exhibit rapid amplitude changes as fouling proceeds (Figs. 5-3 and 5-4). The large peak represents the membrane. The broadness of the peak could be a function of the composite structure of the desalination membrane, having a denser face and a more porous and compressible substrate. The formation of the second echo, representing a response signal of a fouling layer, (Fig. 5-3) was observed within the first hour of operation. The fouling layer on the membrane surface had a different acoustic impedance to that of the bulk solution. The cause of appearance of the second echo is as a result of the changes in acoustic impedance between the bulk solution and the membrane. If the fouling layer is thick enough to be measured by the ultrasonic signal, that is, it falls within the spatial resolution capabilities of the system, a new echo will be formed as a consequence of the bulk solution/fouling interface.

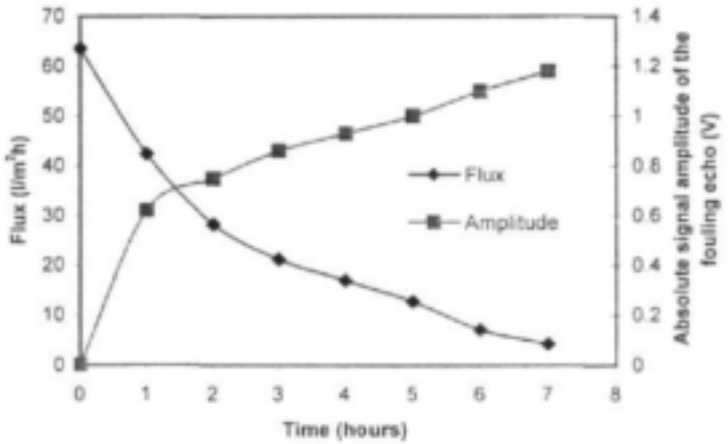

Fig. 5-2. Permeate flow and absolute signal amplitude of the fouling layer echo versus time for calcium carbonate fouling experiment with 1.1 cm/s cross-flow.

As fouling layer growth progressed, more fouling layers formed, until the entire membrane was covered with a uniform fouling layer. If more fouling covers the membrane surface, a denser fouling layer is formed and a larger acoustic impedance change between the bulk solution and the membrane is expected. This would be detected as a sharper reflection. Thus, an echo with greater amplitude is observed at 2, 3, 5 and 7 h of fouling operation in Figs. 5-3 and 5-4. These changes in the absolute signal amplitude of the fouling echo with time are illustrated in Fig. 5-2 (the absolute signal amplitude of a fouling echo = a signal amplitude of a fouling echo at testing time minus that at fouling start). The absolute amplitude of the fouling layer after 2 and 3 h of fouling operation was 0.75 and 0.86 volts respectively (Fig. 5-3). The absolute signal amplitude of the fouling echo was 1.18 volts after 7 h of fouling operation (Fig. 5-2). The difference in arrival time between the fouling and membrane echoes was 19 and 20 ns after 2 and 3 hours of fouling (Fig. 5-3). The movement of the fouling layer echo in the time-domain resulted from an increase in the thickness of the fouling layer.

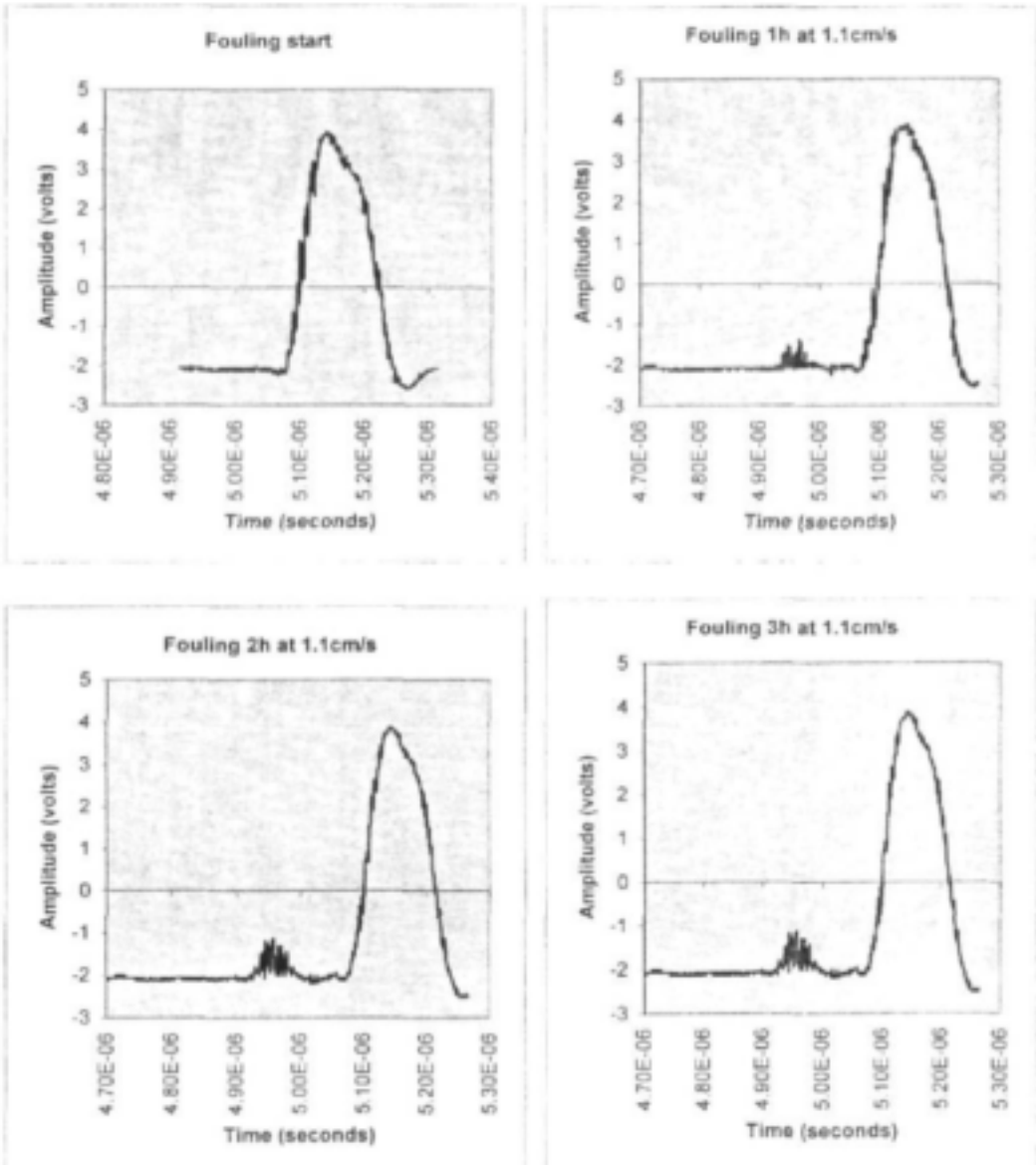

Fig. 5-3. Ultrasonic responses at the start and after 1, 2 and 3 hours of operation with 2 g/l $CaCO_3$ fouling experiments at 1.1 cm/s crossflow.

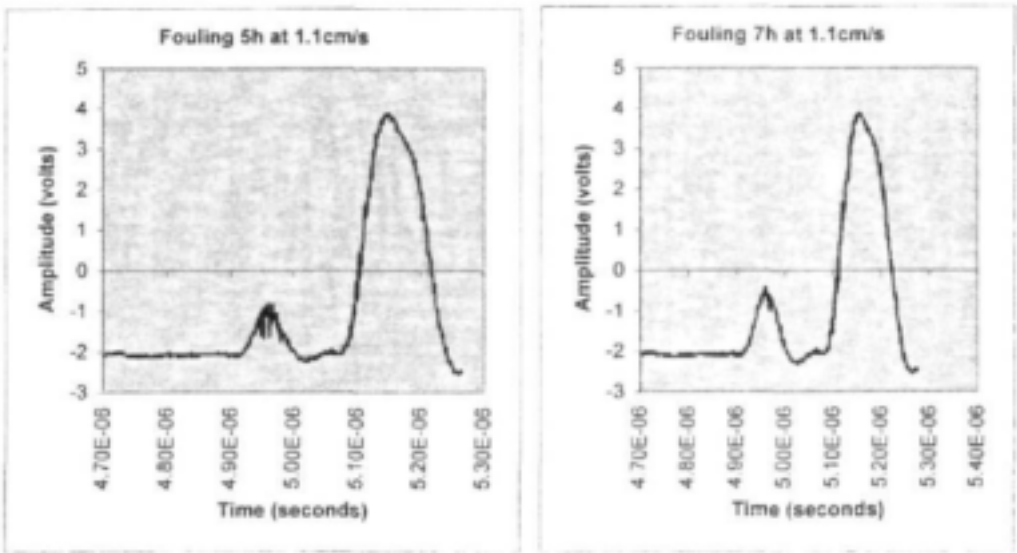

Fig. 5-4. Ultrasonic responses after 5 and 7 hours of operation for the cross-flow fouling experiment with 2 g/l $CaCO_3$ at 1.1 cm/s cross-flow.

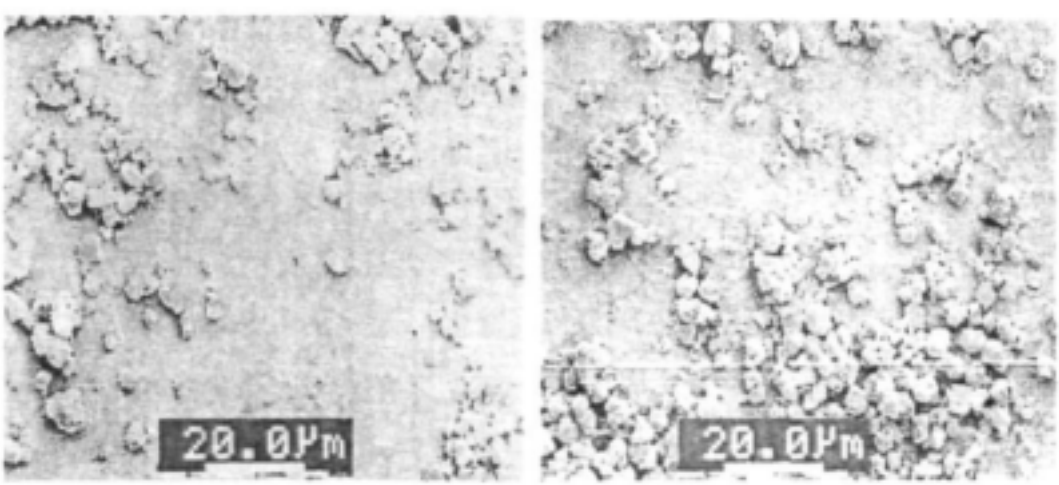

1 hour 2 hours

Fig. 5-5. SEM images: the membrane surfaces after 1 and 2 hours of operation with 2 g/l $CaCO_3$ feed solution at flow rate 1.1 cm/s and pressure 2.2 MPa.

In order to study membrane coverage, four experiments were carried out under exactly the same fouling conditions, and stopped after specific periods. Membrane samples were taken for SEM analysis after 1 hour, 2 hours, 3 hours and 7 hours of operation. Results are shown in Figs. 5-5 and 5-6. Morphological characterisation of the membrane after 7 hours revealed complete membrane coverage with calcium

carbonate. $CaCO_3$ deposits, which may change into the more stable calcite from a meta-stable aragonite [Kronenberg, 1998].

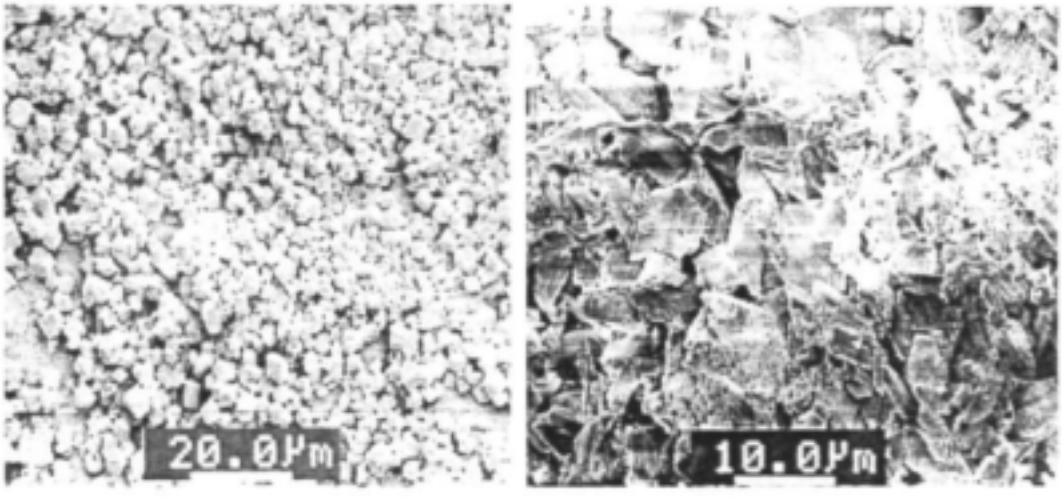

Fig. 5-6. Representative SEM images: the membrane surfaces after 3 and 7 hours of operation on a 2 g/l $CaCO_3$ feed solution at flow rate 1.1 cm/s and pressure 2.2 MPa.

The UTDR technique was in fact measuring fouling layer thickness, which could be calculated by Eq. (3-1). The thickness of the fouling layer was 165 μm after 7 h of fouling (the velocity of the ultrasonic wave in the fouling layer was 1650 m/s). Although the fouling layer thickness measurement by UTDR is not an accurate indication of the fouling layer thickness, the echo signal of the fouling layer can indicate the state and progress of the fouling layer on the membrane surface and provide an early warning to adjust system-operating parameters.

5.3.2 Dead-end experiments

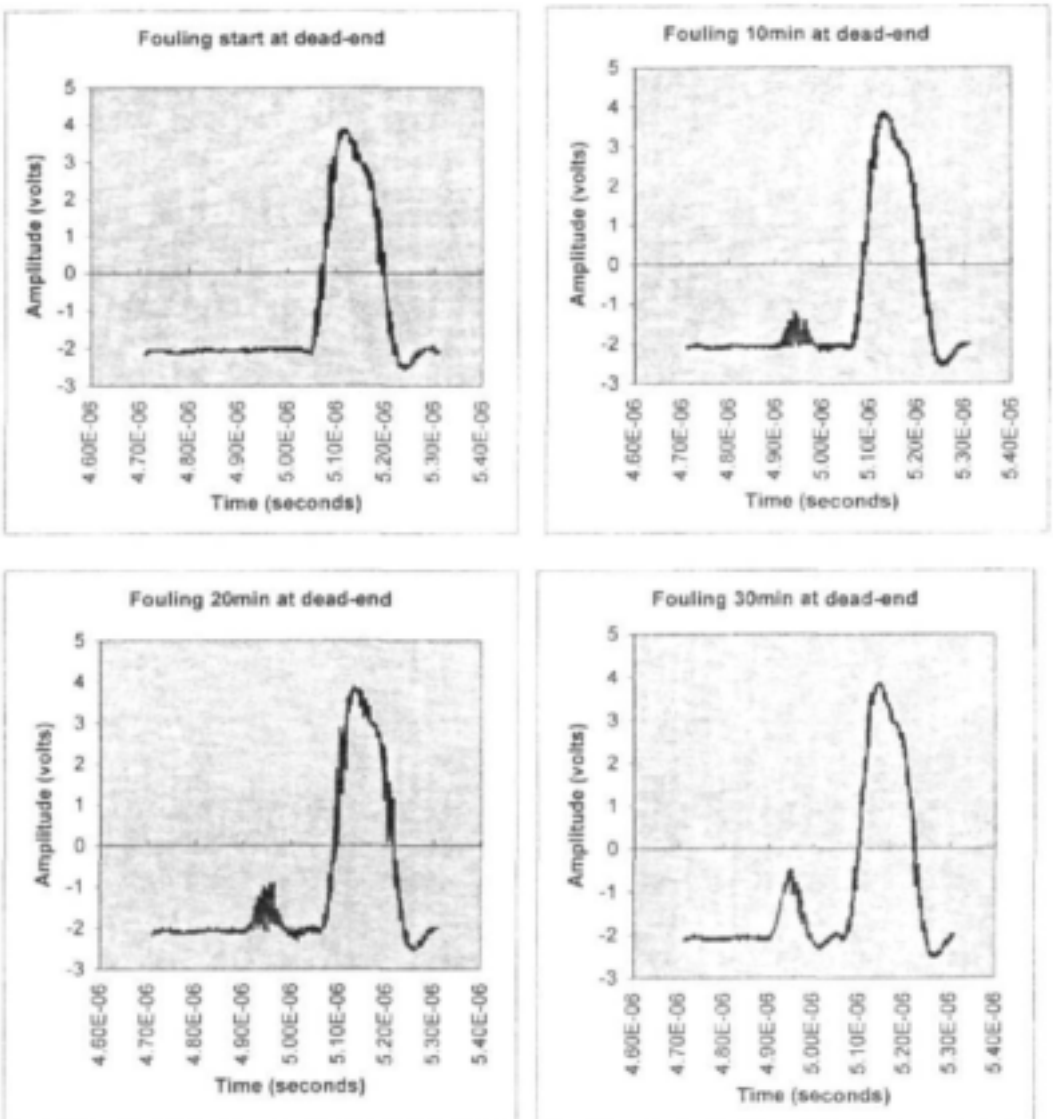

Fig. 5-7. Ultrasonic responses at the start and after 10, 20 and 30 min of operation with 2 g/l $CaCO_3$ in a dead-end experiment.

Dead-end experiments were carried out with 2 g/l calcium carbonate at 2.2 MPa. Results showed that the most significant changes took place within a very short time. Permeation rate values dropped to very low levels within 20 minutes and permeate measurements could no longer be performed accurately. The formation of a second echo in the time domain was almost immediately noticeable in the ultrasonic response (Fig. 5-7). This is because there is lack of turbulence and flow rate during dead-end

experiments. Turbulence, whether produced by stirring, pumping, or moving the membrane, has an effect on flux in the mass transfer-controlled region. Agitation and mixing of the fluid near the membrane surface can control the effects of concentration polarization and reduce the hydraulic resistance and thickness of fouling layer [Cheryan, 1998]. Morphological analysis of the fouled membranes revealed complete coverage of the surfaces in 30 min of dead-end operation (Fig. 5-8). The UTDR fouling layer thickness was calculated as *165 μm after 30 min of fouling operation in* the dead-end experiment (the velocity of the ultrasonic wave in the fouling layer was calculated as 1 650 m/s).

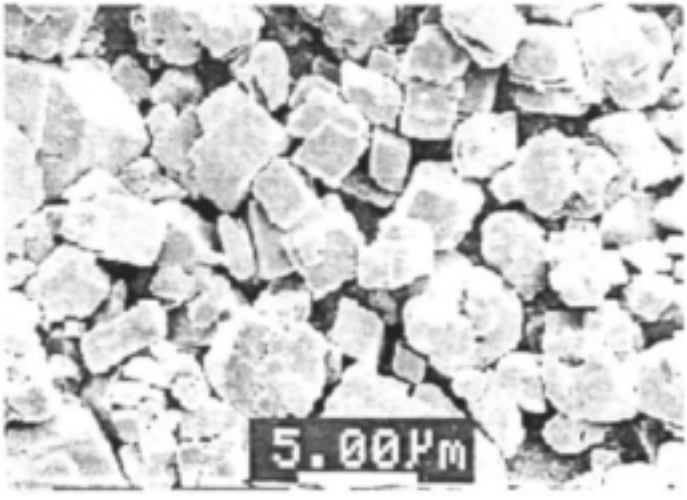

Fig. 5-8. Representative SEM images: the membrane surfaces after 30 min of operation with 2 g/l $CaCO_3$ in dead-end experiments.

5.3.3. Cleaning experiments

To investigate the possibility of using the UTDR technique to monitor fouling removal in real time, several experiments were carried out. The experimental procedure was to foul a membrane to steady state levels, after which it was cleaned with pure water. Both the fouling and cleaning phases were carried out at the same operating pressure of 2.2 MPa and cross-flow velocity of 1.1 cm/s. After a membrane was fouled with 2g/l calcium carbonate feed solution, it was cleaned again with water. Fig. 5-9 shows the fouling results. The second/fouling echo with a sharp reflection,

before the main membrane echo, appeared after 9 h of fouling operation. It also indicated that a denser fouling layer was formed on the membrane surface.

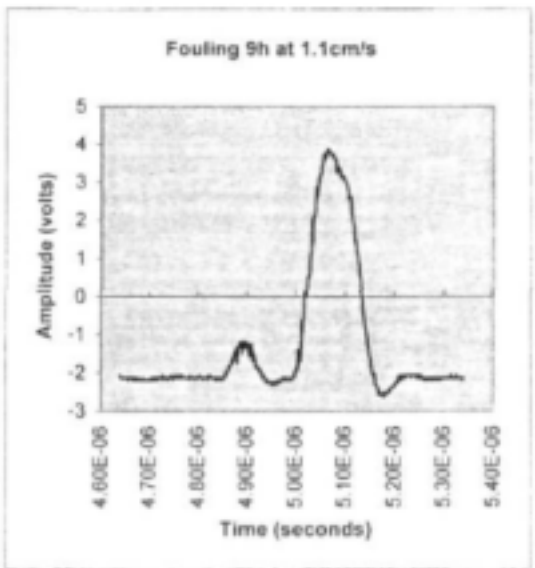

Fig. 5-9. Ultrasonic response of membrane after 9 hours of fouling with $CaCO_3$ at pressure 2 MPa and 1.1cm/s linear flow.

The cleaning process was conducted under the same pressure and cross-flow conditions as the fouling process. Fig. 5-10 shows changes in permeate flux during the cleaning process. Although permeate flow increased during the 3h cleaning experiment, because of reduction of the concentration polarisation and partial dissolution of the fouling layer and reduction of its density, the original flux of a clean membrane was never obtained. It indicated that there was still some fouling on the membrane.

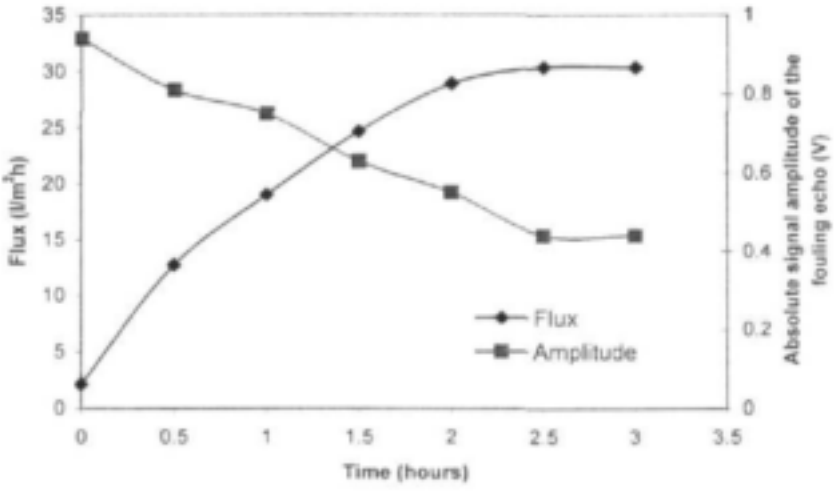

Fig. 5-10. Permeate flow and absolute signal amplitude of the fouling layer echo versus vs. time for the cleaning phase of the cleaning experiment.

Corresponding ultrasonic responses during the cleaning phase are presented in Figs. 5-11 and 5-12. The absolute signal amplitude of the fouling layer with time is illustrated in Fig. 5-10. In Fig. 5-11 it was found that the peak of the second/fouling echo decreased at the start of the cleaning phase, in comparison to the ultrasonic signal response after 9 hours of fouling with calcium carbonate (Fig. 5-9). This is because the change in the bulk solution from calcium carbonate solution to pure water resulted in the reduction of concentration polarization on the membrane surface. Changes in flow and shear rates upon commencement of the cleaning experiment resulted in a decrease in the fouling layer density. This suggests that the UTDR technique is able to detect subtle changes on the membrane surface. In Fig. 5-11, the peak of the second echo gradually declined as cleaning proceeded, because of partial dissolution of the fouling layer and reduction of its thickness. The absolute signal amplitude of the fouling echo is 0.81 and 0.63 volts after 0.5 and 1.5 hours of cleaning (Fig. 5-10). It is shown in Fig. 5-11 that the peak after 1.5 hours of cleaning is gentler than that after 0.5 hours of cleaning. This suggests that the density of the fouling layer after 1.5 hours of cleaning is lower than that after 0.5 hours of cleaning. This phenomenon is explained by modeling the fouling layer deposition using ultrasonic transfer signals and reflections. (This study will be described in a forthcoming article.)

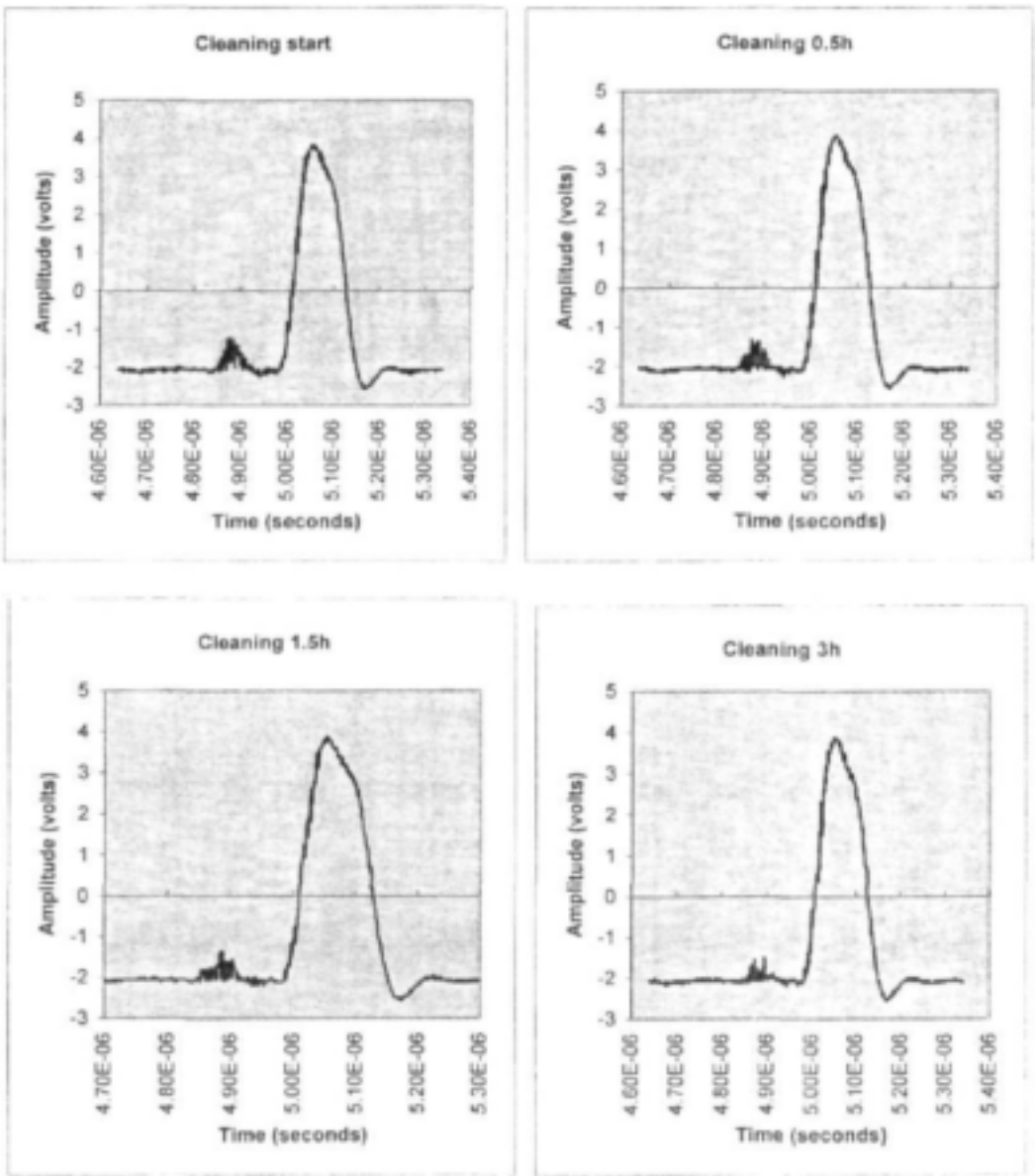

Fig. 5-11. Ultrasonic responses at the start and after 0.5, 1.5 and 3 hours of operation for the cleaning phase of the cleaning experiment.

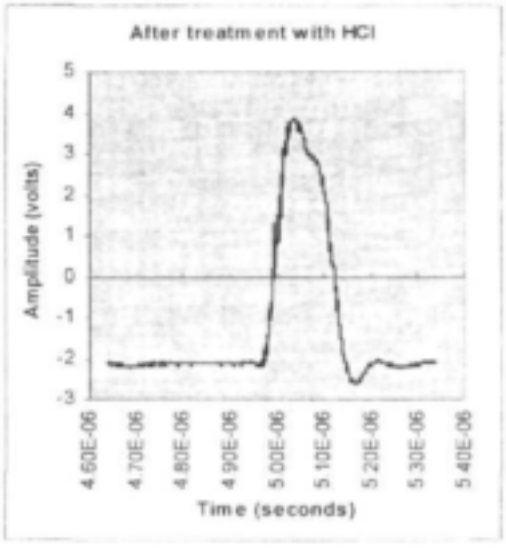

Fig. 5-12. Ultrasonic responses after treatment with hydrochloric acid, for the cleaning phase of the cleaning experiment.

After 3 h cleaning operation, the second echo was still observable (the absolute amplitude of the fouling layer was 0.44 volts in Fig. 5-10). This demonstrated that it is difficult to clean the fouled membrane with water alone. In fact, morphological analysis of the membrane after the cleaning phase with pure water revealed that some fouling was still visible on the membrane surface (Fig. 5-13 a). Additional cleaning methods were needed. Results of ultrasonic responses after treatment with hydrochloric acid (HCl) are shown in Fig. 5-12.

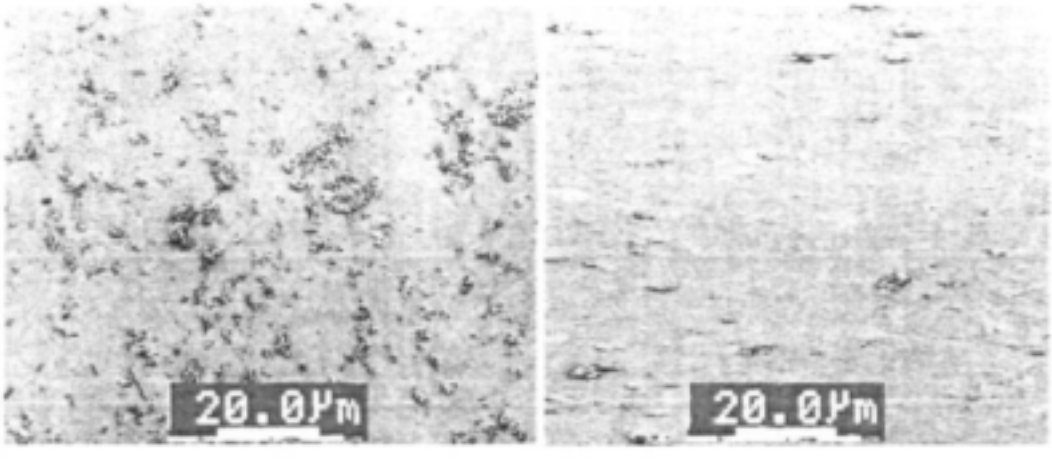

(a) (b)

Fig. 5-13. SEM images of a membrane surface: (a) after 3 hours of cleaning with water; (b) after 30 min treatment with dilute HCl.

The disappearance of the second echo clearly indicated the removal of the fouling layer from the membrane. Morphological analysis of the membrane by SEM showed the same results. After treatment with diluted HCl, the membrane was almost clean (Fig. 5-13 b).

5.4. Summary

The results of this study showed that an ultrasonic testing technique is able to visualize inorganic fouling of RO membranes non-destructively, in situ, and under actual operating conditions in a flat-sheet, high-pressure test cell.

The ultrasonic technique can monitor subtle changes on a membrane surface due to the growth of calcium carbonate fouling. More specifically, a fouling echo obtained in the time domain indicates the actual state of the fouling layer on the membrane surface.

An increase in the amplitude of the fouling echo results from the build-up of the fouling layer. Moreover, the movement of the fouling echo in the time-domain is seen, due to an increase in the thickness of the fouling layer. The ultrasonic testing technique is capable of distinguishing between dead-end and crossflow modes of fouling growth.

The fact that the UTDR technique can monitor the removal of a fouling layer and membrane cleaning makes it a very suitable tool to study the effectiveness of various cleaning techniques.

6 Conclusions and recommendations for future research

6.1 Conclusions

- The acoustic response signals provided a good measurement of fouling-layer growth on membranes in flat-sheet membrane separation systems. The UTDR technique was sensitive to changes occurring on the membrane surface.

- The ultrasonic technique could effectively detect fouling-layer initiation, its growth on and removal from the membranes tested, in real time. Further, the UTDR technique was able to distinguish between a series of growth modes. Data also showed the formation and growth of a fouling layer echo as fouling proceeded. Hence, the UTDR technique can be used to quantify the thickness of a fouling layer on a flat sheet membrane surface.

- The UTDR technique was successfully used to monitor membrane cleaning and to evaluate the cleaning effectiveness of various cleaning methods.

- Results of cleaning experiments showed that ultrasound associated with flushing was, of the cleaning methods used, the most effective method.

- UTDR results corroborated flux measurements and SEM analyses. Overall, the results confirmed the effectiveness off the UTRD technique to visualise fouling deposition on and its removal from membrane surfaces.

Numerous publications have emanated from this work (from both the present project 930 and a follow-up project 1166) and consideration is currently being given to patenting a surveillance apparatus for monitoring membrane fouling. These achievements will be expanded on in the following project #1166.

6.2 Recommendations

This preliminary investigation has formed the sound basis for a second project (#1166) on the visualisation of the effects of electro-magnetic turbulence defouling techniques in different membrane units. (This project is currently in progress.)
Membrane units should include: UF tubular and capillary membrane modules. Spiral-would modules could also be considered.

Specific recommendations are:

- Develop UTDR to measure mainly organic fouling in UF tubular and capillary membrane modules.
- Develop UTDR to visualise fouling and cleaning in a multi-layer module.
- Advance the UTDR to evaluate the cleaning efficiencies of different cleaning methods in tubular membrane modules.
- Develop ultrasonic reflection modelling to understand the signal reflection of a fouling layer on a membrane surface. (Preliminary work in this area has already been very successful.)
- Develop a more sensitive analysis of ultrasonic data to isolate fouling effects from all other reflections.
- Develop a technique and a unit to apply the UTDR technique obtained, to commercial separation plants at a low to moderate cost, but to give improved fouling monitoring and control.

References

Abdel-Jawad, M., S. Ebrahim, F. Al-Atram, S. Al-Shammar, Pretreatment of the municipal wastewater feed for reverse osmosis plants, Desalination 109 (1997) 211-223.

Al-Malack, M.H., G.K. Anderson, Formation of dynamic membranes with crossflow microfiltration, J. Membr. Sci. 112 (1996) 287-296.

Altmann, J., R. Ripperger, Particle deposition and layer formation during crossflow microfiltration, J. Membr. Sci. 124 (1997) 119-128.

Bacchin, P., P. Aimar and V. Sanchez, AIChE J, 41 (1995) 368.

Baker, J.S., S.J. Judd, S.A. Parson, Antiscale magnetic pretreatment of reverse osmosis feed water, Desalination 110 (1997) 151-165.

Band, M., M. Gutman, V. Faerman, E. Korngold, J. Kost, P.J. Plath, V. Gantar, Influence of specially modulated ultrasound on the water desalination process with ion-exchange hollow fibres, Desalination 109 (1997) 303-313.

Belfort G. and B. Marx, Artifical particulate of hyperfiltration membranes – analysis and protection from fouling, Desalination 28 (1979) 13-30.

Belfort, G. and R.W. Altena, Desalination 47 (1983) 105.

Belfort, G., J Membr. Sci. 40 (1989) 123.

Belfort, G., R.H. Davis and A.L. Zydney, J Membr. Sci. 96 (1994) 1.

Bierck, B. R. and R.I. Dick, In-situ examination of effects of pressure differential on compressible cake filtration, Water Sci. and Technol. 22 (12) (1990) 125-133.

Bierck, B.R., S.A. Wells and R.I. Dick, Compressible cake filtation: monitoring cake formation and shrinkage using synchrotron X-rays, J Water Pollution Control 60 (5) (1988) 645-653.

Bond, L.J., A.R. Greenberg, A.P. Mairal, G. Loest, J.H. Brewster, W.B. Krantz, in: D.O. Thompson, D.E. Chimenti (Eds.), Review of progress in quantitative non-destructive evaluation, vol. 14, Plenum Press, New York, 1995, pp. 1167-1173.

Bond, L.J., G.Y. Chai, A.R. Greenberg, W.B. Krantz, US Patent No. 6161435, 2000

Borden, J., J. Gilron and D. Hasson, Analysis of RO flux decline due to membrane surface blockage, Desalination 66 (1987) 257-269.

Brunelle M.T., Colloida; fouling of reverse osmosis membranes, Desalination 32 (1980) 127-135.

Burch, G., Practical experiments with circulating sponge balls on UF membranes with paper mill effluent, 4th WISA-MTD Symposium-Membranes: Science & Engineering, Stellenbosch, South Africa, 26-27 March 2001.

Butt, F.H., F. Rahman and U. Baduruthamal, Desalination 101 (1995) 219

Carter, J.W. and G. Hoyland, Fifth Inernat. Symp Fresh Water from Sea 4 (1976) 21.

Chai, X., Takaomi Kobayashi, Nobuyuki Fujii, Ultrasound-associated cleaning of polymeric membranes for water treatment, Separation and Purification Technology 15 (1999) 139-146.

Chakravorty, B., A. Layson, Ideal feed pretreatment for reverse osmosis by continuous microfiltration, Desalination 110 (1997) 143-149.

Cheryan, M., Ultrafiltration and microfiltration handbook, Technomic Publishing Company, Inc., Lancaster, 1998.

Davis, R.H., in Membranes Handbook, W.S.W. Ho and K.K. Sirkar (eds.), Chapman and Hall, New York, 1992.

Domingo, G.S., Cleaning and pre-treatment techniques for UF membranes fouled by pulp and paper effluent, M.Sc thesis, University of Stellenbosch, South Africa, 2001.

Domingo, GS, EP Jacobs, P Swart, Characterization of foulants present in effluents emanating from the Piet Retief Mondi Kraft paper mill, 4th WISA-MTD Symposium-Membranes: Science & Engineering, Stellenbosch, South Africa, 26-27 March 2001.

Dudley, L.Y. and E.G. Darton, Desalination 105 (1996) 135.

Dudley, L.Y., E.G. Darton, Pretreatment procedures to control biogrowth and scale formation in membrane systems, Desalination 110 (1997) 11-20.

Ensminger, D., Ultrasonics, Marcel Dekker, New York, 1988.

Fane, A.G. and C.J.D. Fell, Desalination 62 (1987) 117.

Fane, A.G., Ultrafiltration: factors influencing flux and rejection, In: Filtration and Separation (Edited by R.J. Wakeman), Vol. 4, Elsevier, Amsterdam, 1986, p.101.

Ford, R.D., Introduction to Acoustics, Elsevier, Armsterdam, 1970.

Fountoukidis, E., Z.B. Marouls and D. Marinos-Kouris, Modeling of Calcium sulphate fouling of reverse osmosis membranes, Desalination 72 (1989) 294-318.

Frederick, J.R., Ultrasonic Engineering, John Wiley and Sons, New York, 1965.

Gilron, J. and D. Hasson, Calcium sulphate fouling of reverse osmosis membranes: flux decline mechanism, Chem. Eng. Sci. 42 (1987) 2351-2360.

Ginn, M., G.L. Cobb, L.E. Broxton and K.R. McNeely, Method of filtering for mineral slurries, Minerals Engineering 10 (1997) 654.

Glater, J., J L York and K. S. Campbell, Scale formation and prevention (Chapter 10), In: Principles of Desalination Part B (Edited by K S Spiegler and A D K Laird), Academic Press, New York, 1980, pp. 627-678.

Haerle, A.G. and R.A. Haber, Real-time monitoring of cake thickness during slip casting, J Mater. Sci. 28 (1993) 5679-5683.

Hamachi, M., M. Mietton-Peuchot, Experimental investigations of cake characteristics in crossflow microfiltration, Chem. Eng. Sci. 54 (1999) 4023-4030.

Harvey, R., US Patent No. 3,206,397, 1965.

Hodgson, P. H., V.I. Pillay, A.G. Fane, Visual study of crossflow microfiltration with inorganic membranes: resistance of biomass and particulate cake, Proceedings of the Sixth World Filtration Congress, Nagoya, 1993, pp. 607-610.

Howell, J.A., V. Sanchez and R. W. Field, Membranes in bioprocessing: theory and applications, Blackie Academic & Professional (published), Glasgow, 1993.

Hung, C-C. and C. Tien, Desalination 18 (1976) 173.

Huotari, H. M., G. Tragardh and I.H. Huisman. Crossflow membrane filtration enhanced by an external DC electric field: a review, Chem. Eng. Research and Design 77(1999) 461-468.

Hurvey, R., US Patent No. 3206397 (1965)

Hutchins, D.A. and H.D. Mair, Ultrasonic monitoring of slip-cast ceramics, J. Mater. Sci. Lett. 8 (1989) 1185-1187.

Jaffar, A.E., The application of a novel chemical treatment program to mitigate scaling and fouling in reverse osmosis units, Desalination 96(1994) 71-79.

Jiraratannon, R., A Chanachai, A study of fouling in the ultrafiltration of passion fruit juice, J Membr. Sci. 111 (1996) 39-48.

Jonsson Ann-sofi, Gun Tragardh. Ultrafiltration applications, Desalination 77 (1990) 135-179.

Jönsson, G. and C.E. Boesen, in: Synthetic Membrane Processes, G. Belfort, ed., Academic Press, Orlando, 1984, pp. 101-130.

Kennedy, M., S.M. Kim, I. Muteryo, L. Broens and J Schippers. Intermittent crossflushing of hollow fiber ultrafiltration system, Desalination 118 (1998) 175-188.

Koen, L.J., Ultrasonic time-domain reflectometry as a real-time non-destructive visualization technique of concentration polarization and fouling on reverse osmosis membranes, M.Sc. thesis, University of Stellenbosch, South Africa, 2000.

Khulbe, K.C., T. Matsuura, S. Singh, G. Lamarche, S.H. Noh, Study on fouling of ultrafiltration membrane by electron spin resonance, J. Membr. Sci. 167 (2000) 263-273.

Kimura, S. and S-I. Nakao, Fouling of cellulose acetate tubular reverse osmosis modules treating the industial water in Tokyo, 17 (1975) 267-275.

Kools, W.F.C., S. Konagurthu, A.R. Greenberg, L.J. Bond, W.B. Krantz, Th. Van den Boomgaard, H. Strathmann, Use of ultrasonic time-domain reflectometry for real-time measurement of thickness changes during evaporative casting of polymer films, J. Appl. Polm. Sci. 69 (1998) 2013-2019.

Kost, J. and R. Langer, Ultrasound enhancement of membrane permeability, US Patent No. 4,7802,212, 1988.

Kronenberg, K.J., Magnetic water treatment de-mystified, http:/www.gcea.com/treatment, 1998.

La Heij, E. J., P.J.A.M. Kerkhof Kopinga, L. Pel, Determining porosity profiles during filtration and expression of sewage sludge by NMR imaging, AIChE J. 42 (4) (1996) 953-959.

Laborie, S., C. Cabassud, L. Durand-Bourlier, J.M. Laine, Flux enhancement by a continuous tangential gas flow in ultrafiltration hollow fibres for drinking water production: effects of slug flow on cake structure, Filtration & Separation, Oct. 1997, p886-891.

Lenart, I. and D. Auslander, Ultrasonic, 9 (1980) 216.

Lentdch, S., P. Aimar and J.L. Orozco. Enhanced separation of albumin-poly(ethylene glycol) by combination of ultrafiltration and electrophoresis, J Membr. Sci. 80 (1993) 221-232.

Li, H., A.G. Fane, H.G.L. Coster, S. Vigneswaran, Direct observation of particle deposition on the membrane surface during crossflow microfiltration, J. Membr. Sci. 149 (1998) 83-97.

Li, H., E. Ohdaria and M. Ide, Effect of ultrasonic irradiation on permeability of dialysis membrane, Jpn. J. Appl. Phys. 35 (5B) (1995) 3225.

Li, Jianxin; RD Sanderson, EP Jacobs, Non-invasive visualization of the fouling of microfiltration membranes by ultrasonic time-domain reflectometry, J. Membrane Science, 201 (2002) 17-29.

Loeb, S. and S. Sourirajan, Adv. Chem. Ser, 38 (1962) 117.

Logan, D.P., and S. Kimura, Control of gypsum scale on reverse osmosis membranes, Desalination, 54 (1985) 321-331.

Lonsdale, H.K., The growth of membrane technology, J Membr. Sci. 10 (1982) 81-181.

Lonsdale, H.K.; in: Desalination by Reverse Osmosis, U. Merten, ed, MIT press, Cambridge, 1966, pp. 93-160.

Lu, W.M.; K.L. Tung, C.S. Pan, K.J. Hwang, Crossflow microfiltration of mono-dispersed deformable particle suspension, J. Membr. Sci. in press, 2001.

Lynnworth, L.C., Ultrasonic measurement for process control theory, techniques, applications, Academic Press, San Diego, 1989.

Maartens, A., P. Swart, E.P. Jacobs, Feed water pretreatment: methods to reduce membrane fouling by natural organic matter, J Membr. Sci. 163 (1999) 51-62.

Mackley, M.R., Sherman N.E., Cross-flow cake filtration mechanisms and kinetics, Chem. Eng. Sci. 47 (1992) 3067-3084.

Mairal, A.P., Greenberg A.R., William B. Krantz, Investigation of membrane fouling and cleaning using ultrasonic time-domain reflectometry, Desalination 130 (2000) 45-60.

Mairal, A.P., Greenberg A.R., Krantz W. B., Leonard J. Bond, Real-time measurement of inorganic fouling of RO desalination membranes using ultrasonic time-domain reflectometry, J. Membr. Sci. 159 (1999)185-196.

Marshall, A.D., P.A. Munro and G. Träagårdh, Desalination 91 (1993) 65.

Mason, T. J, J. P Lorimer, Sonochemistry: theory, applications and uses of ultrasound in chemistry, Ellis Horwood, Chichester, 1989 pp. 29.

Mason, Timothy J. and J Phillip Lorimer, Sonochemistry: theory, applications and uses of ultrasound in Chemistry, Ellos Horwood Ltd, Chichester, 1988, pp. 1-17.

Matthiasson E. and B. Sivik, Concentration polarization and fouling, Desalination 35 (1980) 59-103.

McDonogh, R.M., H. Bauser, H. Stroh, H. Chmiel, Concentration polarization and adsorption effects in crossflow ultrafiltration of proteins, Desalination 79 (1990) 217-231.

McDonogh, R.M., H. Bauser, H. Stroh, U. Grauschoph, Experimental in situ measurement of concentration polarization during ultra- and micro-filtration of bovine serum albumin and dextran blue solutions, J. Membr. Sci. 104 (1995) 51-63.

Michaels, A.S., Chem. Eng Prog., 64 (1968) 31.

Mores, W.D. and R.H. Davis, Direct visual observation of yeast deposition and removal during microfiltation, J. Membr. Sci. 189 (2001) 217-230.

Mukherjee, D., A. Kulkarni and W.N. Gill. Chemical treatment for improved performance of reverse osmosis membranes, Desalination 104 (1996) 239-249.

Mulder, M., Basic principles of membrane technology, Kluwer Academic Pubulishers, The Netherlands, 1991.

Muralidhara, H.S., Enhance separations with electricity, Chemtech. May 1994, 36-41.

Nilsson, J.L., J Membr. Sci. 52 (1990) 121.

Noble, R.D. and S.A. Stern, Membrane separations technology principles and applications, Elsevier Science B.V., Amsterdam, 1995.

Nourtila-Jokinen, J. and M. Nystrom, Comparison of membrane separation processes in the international purification of paper mill water, J Membr. Sci. 119 (1996) 99-115.

Okazaki, M and S. Kimura, J Chem. Eng Japan, 17 (1984) 145

Oppenheim, S.F., G.R. Buettner, J.S. Dordick, V.G.J. Rodgers, Applying electron paramagnetic resonance spectroscopy to the study of fouling in protein ultrafiltration, J. Membr. Sci. 96 (1994) 289-297.

PANAMETRICS, INC., Technical notes, 2000.

Parnham, C.S. and R.H. Davis. Protein recovery from bacterial cell debris using crossflow microfiltration with backpulsing, J Membr. Sci. 118 (1996) 259-268.

Perusich, S.A., R.C. Alkire. Ultrasonically induced cavitation studies of electrochemical passivity and transport mechanisms. I. Theoretical. J. Electrochem. Soc. 138 (3) (1991) 700-707.

Peterson, R.A., A.R. Greenberg, L.J. Bond, W.B. Krantz, Use of ultrasonic TDR for real-time noninvasive measurement of compressive strain during membrane compaction, Desalination 116 (1998) 115-122.

Pontie, M., X. Chasseray, D. Lemordant, The streaming potential method for the characterization of ultrafiltration organic membranes and the control of cleaning treatments characterization, J Membr. Sci. 129 (1997) 125-133.

Potts, D.E., R.C. Ahlert and S.S. Wang, A critical review of fouling of reverse osmosis membranes, Desalination 36 (1981) 235-264.

Price, G.J., (Ed.). Current Trends in Sonochemistry, Royal Society of Chemistry, Cambridge, 1992, p1-7.

Rautenbach, R. and R. Albrecht, Membrane Processes, John Wiley & Sons, England, 1989.

Redkar, S., V. Kuberkar and R.H. Davis. Modeling of concentration polarization and depolarization with high-frequency backpulsing, J Membr. Sci. 121 (1996) 229-242.

Redkar, S.G. and R.H. Davis. Enhancement of crossflow microfiltration performance using high frequency reverse filtration, AIChE J. 41 (1995) 501-508.

Reinsch, V.E., A.R. Greenberg, S.S. Kelley, R. Peterson, L.J. Bond, A new technique for the simultaneous, real-time measurement of membrane compaction and performance during exposure to high-pressure gas, J. Membr. Sci. 171 (2000) 217-228.

Schippers, J.C.; J. Verdouw, The modified fouling index: a method of determining the fouling characteristics of water, Desalination 32 (1980) 137-148.

Schippers, J.C.; J.H. Hanemaaijer, C.A. Smolders and A. Kostense, Desalination 38 (1981) 339.

Schmidt, E. and F. Löffeler, Preparation of dust cakes for microscopic examination, Power Technol. 60 (1990) 173.

Schwinge, J., D. Wiley and A.G. Fane, Flux improvements with a new spacer geometry for ultrafiltration, World Chem Eng Congress, Melbourne (2001).

Sheppard, J.D., D.G. Thomas, and K.C. Channabasappa, Desalinaiton 11 (1972) 385.

Shimichi, W., Japan Patent No. 07,31974, 1995.

Sokolov, S., Elek-Nachr-Tek, 6 (1929) 451

Strathmann, H., J Membr. Sci. 9 (1981) 121.

Tanny, G.B.; D. Hauk and U. Meuin, Biotechnical applications of a pleated cross-flow microfiltration module, Desalination 41 (1982) 299-312.

Tarleton, E.S. and R.J. Wakeman, Electro-acoustic crossflow microfiltration, Filtr. & Sep. 29 (9-10) (1992) 425-432.

Tiller, F.M., N.B. Hsyung, D.Z. Cong, Role of porosity in filtration: XII filtration with sedimentation, AIChE J. 41 (5) (1995) 1153.

Treffry-Goatley, K., M.I. Buchan, G.E. Renchen and C.A. Buckley, The dewatering of sludges using a tubular filter press, Desalination 67 (1987) 467-479.

Tung, K.L., S. Wang, W.M. Lu, C.H. Pan, In situ measurement of cake thickness distribution by a photointerrupt sensor, J. Membr. Sci. 190 (2001) 57-67.

Vilker, V.L., C.K. Colton, K.A. Smith, Concentration polarization in protein ultrafiltration, Part 1: An optical shadowgraph technique for measuring concentration profiles near a solution-membrane interface, AIChE. J. 27 (1981) 632-637.

Vyas, H.K.; A.J. Mawson, R.J. Bennett, A.D. Marshall, A new method for estimating cake height and porosity during crossflow filtration of particulate suspersions, J. Membr. Sci. 176 (2000) 113-119.

Wakeman, R.J. and E.S. Tarleton. An experimental study of electroacoustic crossflow microfiltration, Chem. Eng. Research & Design, 69(1991) 386-397.

Wakeman, R.J., Visualization of cake formation in crossflow microfiltration, Trans. *IChemE, Part A 72 (1994) 530-540.*

Wandelt, B.; P. Schmitz, D. Houi, Investigation of transient phenomena in crossflow microfiltation of colloidal suspersions using NMR cicro-imaging, in: Proceedings of the 6th World Filtration Congress, Nagoya, Japan, 1992, pp. 601-606.

Weast, Robert C., Handbook of Chemistry and Physics, Chemical Rubber Co., Cleveland, Ohio, 1970.

Yao, S., M. Costello, A.G. Fane, J.M. Pope, Non-invasive observation of flow profiles and polarization layers in hollow fibre membrane filtration modules using NMR micro-imaging, J. Membr. Sci. 99 (1995) 207-216.

Zhu, Chao, Guangliang Liu. Modeling of ultrasonic enhancement on membrane distillation, J Membr. Sci. 176 (2000) 31-34.

Other related WRC reports available:

Development and implementation of biological cleaning techniques for ultrafiltration and reverse osmosis membranes fouled by organic substances

P Swart, A Maartens, J Engelbrecht, Z Allie and EP Jacobs

The project aimed to investigate and ameliorate the fouling of polysulphone ultrafiltration membranes used in the treatment of Cape brown waters, pulp and paper effluent, and abattoir effluent. The water and effluents were characterised and enzymes and other cleaning methods investigated for the cleaning of fouled membranes. In respect of the brown water and pulp and paper effluents, surface active and fouling prevention agents were evaluated and successfully applied. In the case of ultrafiltration membranes fouled in abattoir effluent, it was found that a blend of lipase and protease enzymes was effective as a cleaning agent to restore the membrane flux.

Report Number: 660/1/99 **ISBN: 1 86845 449 5**

Development of characterising and cleaning techniques to classify foulants and to remove them from ultra- and microfiltration membranes by biochemical means

P Swart, A Maartens, AC Swart & EP Jacobs

The main objectives of this research project were the identification and classification of membrane foulants occurring in abattoir, wool-scouring and other industrial effluents. Two further aims were the development of methods for the biological removal of such foulants from membrane surfaces and the cloning and large-scale preparation of specialised enzymes to degrade specific foulants.
Proteins and lipids were found to be the main foulants in abattoir effluents, whilst proteins and waxes were predominant foulants in wool-scouring effluents. Lipases and esterases were successful enzymes for the removal of foulants from abattoir and wool-scouring effluents, respectively, and restored the fluxes in fouled membranes.
These promising results indicated that enzyme-based biological cleaning regimes hold great promise for the restoration of fouled ultrafiltration membranes.

Report Number: 531/1/96 **ISBN: 1 86845 209 3**

TO ORDER: Contact **Rina** or **Judas** - Telephone No: 012 330 0340
Fax Number: 012 331 2565
E-mail: publications@wrc.org.za

Water Research Commission
Private Bag X03, Gezina, 0031, South Africa
Tel: +27 12 330 0340, Fax: +27 12 331 2565
Web: http://www.wrc.org.za

1868459497

Designed by The Kashan group K-2102 (www.kashangroup.com)